UNIVERSITÀ DI PARMA

# UNIVERSITA' DEGLI STUDI DI PARMA

DOTTORATO DI RICERCA IN
***BIOTECNOLOGIE E BIOSCIENZE***

CICLO XXXVII

# Biotechnology for Sustainability: Nanobiotechnological Approaches to Improve Plant Resilience

**Coordinatore:**
Chiar.ma Prof.ssa Elena Maestri

**Tutore:**
Chiar.ma Prof.ssa Elena Maestri

**Supervisore:**
Chiar.mo Prof. Nelson Marmiroli

**Co-Tutori:**
Dott.ssa Caterina Agrimonti
Dott. Luca Pagano

**Dottorando:** Ilenia Iosa

Anni Accademici 2021/2022 – 2023/2024

# Summary

# Abstract

Agriculture is severely suffering due to the escalating incidence of abiotic stresses, exacerbated by global warming, which has been leading to reduced agricultural yields and extensive economic losses. Despite its longstanding presence over the centuries, salinity pollution is a very current issue that has not been solved and still endangers agricultural productivity worldwide, threatening food supply and human well-being. Nowadays, soil salinization phenomena are affecting increasingly large areas around the world, forcing plants into a state of osmotic, ionic, and oxidative stress. In Italy, particularly well-known is the case of the Po Valley. During the summer of 2022 a prolonged period of drought resulted in a drastic loss of water flow in the Po River basin, followed by the conspicuous infiltration of seawater for about 40km inland, concerning extensive cultivated areas. Nano-biotechnology offers promising and eco-friendly solutions that can support the transition to a more sustainable and resilient agri-food system. Nanomaterials (NMs) and microbial-based biostimulants, in fact, hold the potential to foster plant development and protection by decreasing agrochemicals exploitation and restoring soil health and fertility. Plant biostimulants can be based on the use of plant growth-promoting rhizobacteria (PGPR) as single species or as microbial consortia (MCs). In either case, traceability procedures are required to improve their performance in field trials. To assess the shelf life of PGPR inoculated into the soil is important to determine which elements contribute to their effectiveness and their interactions with plants and indigenous soil microbiota. The present work developed a real-time PCR (qtPCR) method to specifically detect and quantify bacteria of a microbial consortium (MC_C) designed by Tabacchioni et al. (2021) and comprising five PGPR species: *Burkholderia ambifaria*, *Bacillus amyloliquefaciens*, *Azotobacter chroococcum*, *Pseudomonas fluorescens*, and *Rahnella aquatilis*. Through a review of scientific literature and *in silico* sequence analyses a set of primer pairs was found to tag three out of the five bacterial species (*B. ambifaria*, *B. amyloliquefaciens* and *R. aquatilis*). MC_C was administered to the soil of two wheat varieties, *Triticum durum* (cv. Svevo) and *Triticum aestivum* (cv. Bramante), alone or in combination with biochar and the mycorrhizal fungus *Rhizophagus intraradices*. Over the duration of the experimental field trial, rhizospheric soil samples were collected at different times to be tested via the qtPCR assay. The results obtained proved the successful colonization of bacteria with a maximum of growth reached between 15 and 20 days after the application into the soil. The analyses also evidenced that biochar positively influenced PGPR growth. In conclusion, qtPCR was once more an effective method to trace the fate of supplied bacterial species in the consortium when used as a cargo system for their delivery. Microbial-based biostimulants are not the unique novel products that can strengthen plant defense systems against biotic and abiotic stresses. In recent years, also nanomaterials have

become increasingly attractive for agricultural applications due to the specific properties closely dependent on their nanoscale size. The research work in collaboration with the Connecticut Agricultural Experiment Station (CAES, New Haven, CT, USA) aimed to investigate the morphological, physiological and molecular effects due to the combination of microbial-based biostimulants and nanomaterials on plants of agronomic interest exposed to salt stress. At first, silicon dioxide ($SiO_2$) and chitosan-tripolyphosphate (Ch/TPP) nanoparticles (NPs) were selected, based on their well-known properties in alleviating symptoms of abiotic stresses, to be tested in a greenhouse explorative experiment on cherry tomato plants (*Solanum lycopersicum* L.) with a commercial microbial-based product (Micro-$H_2O$**)** comprised of *Bacillus subtilis* and *Bacillus amyloliquefaciens.* The microbial consortium and $SiO_2$ NPs have been purchased for research purposes, meanwhile Ch/TPP NPs were produced in-house following the protocol by Pontes et al. (2021) and characterized prior to use. The analysis of the morphological parameters and the determination of chlorophyll and carotenoids content evidenced the positive contribution of $SiO_2$ NPs, alone or combined with PGPR, in enhancing development and photosynthetic efficiency of the plants. Cherry tomato plants were also tested under saline irrigation, even though data collected require further investigations before drawing any conclusions about the efficacy of the treatments. Therefore, silicon dioxide nanoparticles, considered under optimal growth conditions more effective than chitosan-tripolyphosphate nanoparticles, were selected to be used in a second greenhouse experiment. For this purpose, $SiO_2$ NPs have been administered alone or combined with Micro-$H_2O$ to soybean plants (*Glycine max* L.) subjected to salt stress for a total duration of three weeks. The morphological data collected confirmed the influence of $SiO_2$ NPs in modulating the architecture of the root system under salt stress conditions. Ameliorating nutrients and water uptake, silica positively affected the development of roots and leaves of plants. In accordance with the scientific literature, under salt stress conditions silica nanoparticles were also found to relieve the stress sensed by plants limiting sodium internalization and rising calcium content into the roots. PGPR favored instead the accumulation of potassium and regulated the uptake of other nutrients such as the boron involved in seeds and flowers production. The association $SiO_2$ NPs-*Bacillus* strains enhanced stress defense in soybean plants, restoring the plant photosynthetic activity compromised under saline irrigation. In conclusion, the coupled nano-biotechnological approaches proved to be effective in enhancing plant health under salt stress conditions. Although further investigations are needed to better elucidate the physiological and molecular plant response to nanomaterials and PGPR, the experimental outcomes gathered so far highlighted the real potential of these approaches for agricultural applications.

# 1. State of the Art

## 1.1 The Future of Food and Agriculture

Agriculture is severely suffering under the effects of global warming that threatens water, food and feed safety consequently impacting on human and animal health, not to mention the disastrous consequences for crop productivity and for the nutritional quality of the produce (Duchenne-Moutien & Neetoo, 2021; Fiodor et al., 2021). Among the challenges of the current agricultural system is the requirement to boost agricultural production by 28 % over the next decade, to meet the food demand of a sharply increasing world population whose size is estimated to reach 9.3 billion people by 2050 (FAO, 2014; Benitez-Alfonso et al., 2023). Balancing between the increasing rate of production and the minimization of the negative environmental impacts requires an urgent transition to more sustainable agricultural practices. This transformation could ensure adequate profitability and social and economic equity, while decreasing greenhouse gases (GHGs) emissions, preserving natural ecosystems and protecting natural resources (FAO, 2014; Rockström et al., 2017). To achieve this goal, considerable resources are being invested in researching eco-friendly strategies for the improvement of agricultural applications. Innovative nanobiotechnological approaches can contribute to the realization of this task, holding the potential to foster resilience and sustainability in the agricultural sector (Du et al., 2022; Khan et al., 2023).

The rate of anthropogenic GHGs emissions has increased over the past century, contributing substantially to the warming of the atmosphere, landmasses and oceans. As stated by the Intergovernmental Panel on Climate Change (IPCC), the earth's surface temperature was 1.09°C higher during the first decade of the 21st century (2011-2020) than in the pre-industrial period (1850-1900), with regional variations across land (+1.59°C) and ocean (+0.88°C). Climate change has already caused irreversible damage to ecosystems, threatening food and water security (IPCC, 2023).

Undertaking urgent mitigation and adaptation actions is a key step in limiting and slowing the exacerbation of the current climate situation. Lacking strengthened policies for zero carbon dioxide ($CO_2$) emissions and mitigation of other GHGs, especially methane ($CH_4$), the situation is projected to get worse and the average temperature to rise 2.8°C by 2100 (IPCC, 2023) (**Figure 1.1**). Among the various effects of global warming, we find the distortion of climatic factors such as temperature, relative humidity, UV rays, and precipitation (Maggiore et al., 2020; Duchenne-Moutien & Neetoo, 2021) (**Figure 1.2**). The shift in their patterns could influence the normal risk rate of extreme weather events resulting in altered intensity, frequency and duration on a regional or on a global scale (Huber et al., 2011; Diffenbaugh et al., 2017; Heino et al., 2023;). The 2019 IPCC Special Report on Climate

Change and Land, reported that warming has led to an intensification of drought phenomena in several areas across the world, comprising Mediterranean, north-eastern Asia, west Asia, large part of Africa and parts of South America. On the other hand, over the last decades, the frequency of heavy precipitation appears to be higher on the global scale (IPCC, 2019).

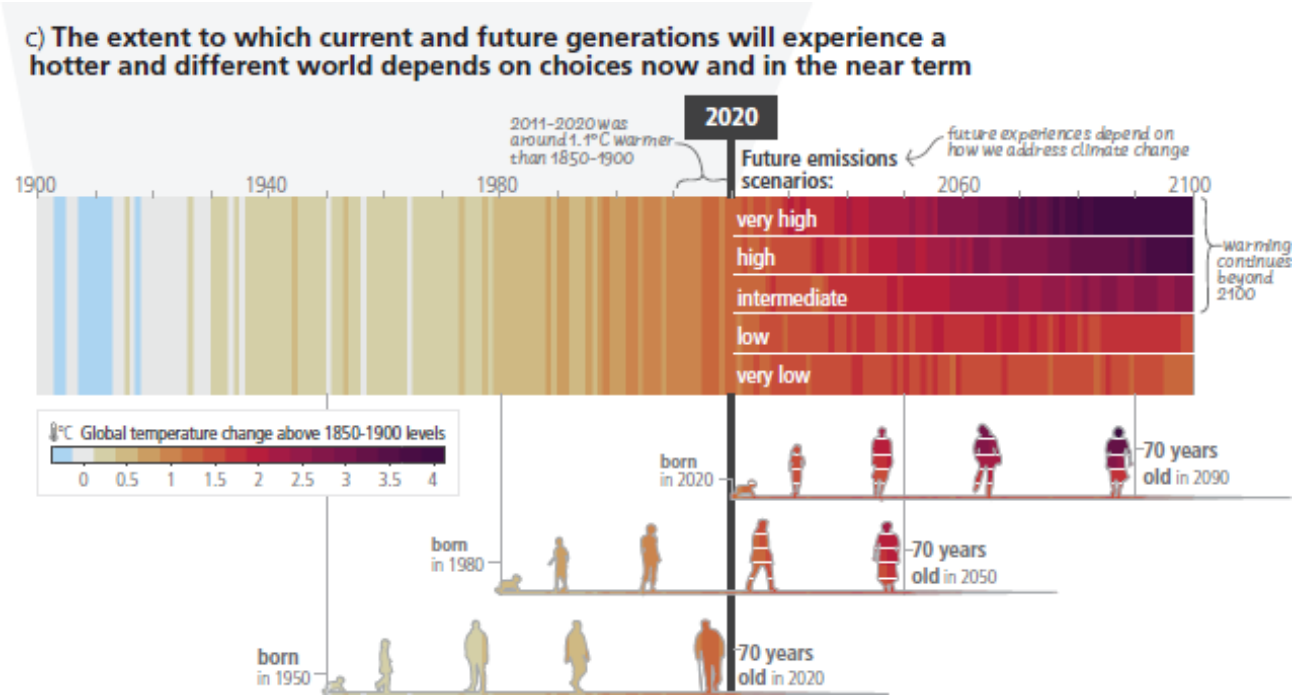


**Figure 1.1.** The image depicts the world's rising surface temperature over the period from 1900 to 2020, with a forecast to 2100. Changes in climate over the lifetime of three generations (born in 1950, 1980 and 2020) are also illustrated. The climate strips represent different GHGs emission scenarios, from very low to very high values, illustrating long-term trends induced by anthropogenic and natural impacts. The generational icons are colored according to the global surface temperature for each year and the segments within the icons from 2020 to 2021 indicate the possible future cases. The picture is taken from Figure SPM.1 of the United Nations Intergovernmental Panel on Climate Change (IPCC), AR6 Synthesis Report with partial elaboration.

In the last couple of decades alone, violent episodes of torrential rainfall struck many European countries (i.e. France, northern Italy and Switzerland in 2000, long the lower Danube in 2006, in Germany and France in 2016) as well as the United States (i.e. Nebraska, South Dakota, Iowa and Mississippi) resulting in massive inundations that have had major negative economical and human health-related impacts (Kron et al., 2019; Ebi et al., 2020). The episodes mentioned above represent just some examples of a climatic situation that is already endangering human well-being and that is expected by some forecasts to reach an increase in average global precipitation of 5-15% by the end of the century (Duchenne-Moutien & Neetoo, 2021). Global warming is also menacing soil quality and fertility, through the reduction of soil moisture content (**Figure 1.2**). In turn, this phenomenon aggravates desertification and land degradation processes in many regions, especially arid regions, low-lying coastal and permafrost areas and river deltas (IPCC, 2019). Land deterioration processes

include the soil salinization phenomena, which nowadays are severely affecting the physico-chemical and biological characteristics of the soil (Tang et al., 2024).

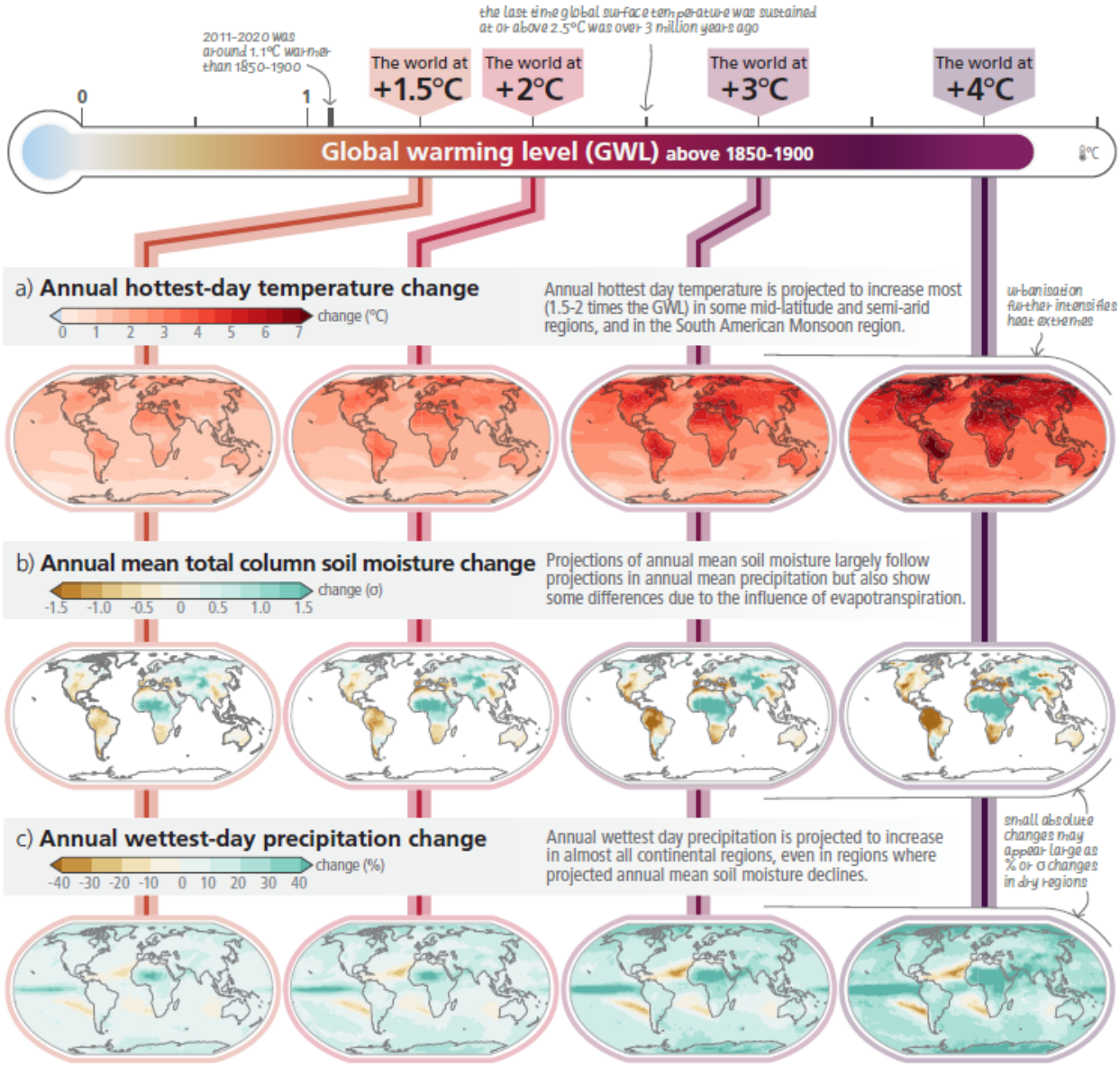


**Figure 1.2.** The image shows the predicted changes in maximum annual daily temperature, average annual soil column moisture, and maximum annual daily precipitation under different possible global warming scenarios (1.5°C, 2°C, 3°C, 4°C relative to the pre-industrial period 1850-1900). Maximum annual change in daily temperature (°C) **(a)**; average annual change in total soil column moisture (standard deviation) **(b)**; maximum annual daily precipitation (%) **(c)**. In **(a)** and **(b)** large positive relative changes in dry regions may coincide with small absolute variations. In panel **(b)**, the unit is the standard deviation of the interannual variability of soil moisture content over the period 1850-1900, commonly used to characterize drought severity.

## 1.2 The Issue of Soil Salinization

Salinity pollution is a tale almost as old as agriculture itself. In fact, today we know that some of the very first farming societies in the world, Sumer and Akkad, already suffered from issues related to human-driven salinity pollution in their agricultural lands due to their irrigation practices. About six thousand years ago in the Tigris-Euphrates floodplain in Mesopotamia, the Sumerian system of sustained irrigation induced a slow build-up of salt in the soil. Over the centuries this salt accumulation in the soil caused a steady but noticeable decrease in agricultural crop yield, that the Sumerian scribes themselves noticed. Interestingly, even though these ancient farmers tried mitigation efforts, the salinization of soil in this region at this time is thought to have contributed significantly to the decline of the great Mesopotamian civilizations (El-Ashry et al., 1985).

Despite its longstanding presence over the centuries, salinity pollution is a very current issue that has not been solved and still endangers agricultural productivity worldwide, threatening food supply and human well-being (Ilangumaran & Smith, 2017; Tang et al., 2024). This phenomenon can compromise soil integrity, fertility and biodiversity. Soil salinization negatively impacts plant health, exposing soil itself to wind-and-water driven erosion and leading to a disruption of the biological functioning of its colonizing microorganisms (Hassani et al., 2021). The soil surface affected by high salinity events is expanding worldwide and includes, based on recent studies, 20% of cultivated areas and 33% of irrigated lands (Uyettandele et al., 2015; Abdelraheem et al., 2019). Soil depletion, ion-toxicity, and nutrient imbalance induced by high saline concentrations drastically reduce plant development and productivity with a projected large economic loss of 27.3 billion annually (Giannelli et al., 2023; Shrivastava & Kumar, 2015).

In general, excessive accumulation of soluble salts in the soil is known to depend on the concomitance of natural (primary) and anthropogenic (secondary) processes (Fiodor et al., 2021).

Primary salinization mainly results from wet or dry deposition of oceanic salts via precipitation and wind and from the erosion of rock materials, whereas only a small contribution is provided by the movement of salts dissolved in the shallow groundwater to the soil surface zone (Hassani et al., 2021). The influence of human activities on salt deposition processes, known as secondary salinization, is due to the utilization of saline or brackish irrigation water and to the over-exploitation of fertilizers and groundwater aquifers (Fiodor et al., 2021; Hassani et al., 2021).

There are several studies highlighting the correlation between the fluctuation of climatic factors induced by global warming and the alteration of soluble salt accumulation dynamics in the soil. In arid and semi-arid regions, for example, the increase in average temperature and the high evaporation

rate of irrigation water can promote the salt accumulation in the more superficial soil layers, particularly where the internal drainage capacity into the subsoil is reduced (Eswar et al., 2021; Omuto et al., 2020). In coastal regions, on the other hand, the major driving force of salinization phenomena is represented by the sea level rise (Chun et al., 2018). The average sea level rise recorded from 1901 to the present is about 0.29m and by the end of the current century, it is predicted to surge in about 70% of all the coastal regions of the world. This factor can influence storm surges by causing saltwater infiltrations into groundwater aquifers (Eswar et al., 2021). Italy itself in the summer of 2022 was subjected to a prolonged period of drought that devastated the Northeast, particularly the Po Valley. The drastic loss of water flow in the Po River basin was followed by the conspicuous infiltration of seawater, for about 40km inland, affecting extensive cultivated areas (Straffelini & Tarolli, 2023).

## 1.3 Salinity Stress: from a Plant perspective

If the salt accumulation in the soil exceeds a certain threshold, reaching an electrical conductivity (EC) value of 4dS/m, the same soil is considered saline (Khalid et al., 2022; Naseri et al., 2022). Among all salts, sodium chloride is the most common as well as the most soluble (Giannelli et al., 2023). In general, plants display variable degrees of tolerance and use different mechanisms of adaptation and regulation. Once accumulated in the soil, sodium ions ($Na^+$) can be translocated in the tissues causing osmotic and ion toxicity to plants (Ayaz et al., 2022; Fu & Yang, 2023). For example, halophytes are species of plants that have adapted to survive high salt concentrations developing mechanisms such as extrusion and leaf deposition (Bose et al., 2017; Van Zelm et al., 2020).

However, sodium is not the only toxic element to plants. The accumulation of chlorine ions ($Cl^-$) can also be damaging to plant physiology, especially in the case of the most sensitive ones. Such is the case for a plant crop of high agricultural importance in today's economy, the soybean (*Glycine max L.*) (Ilangumaran & Smith, 2017).

Salt accumulation causes a depletion in soil water potential and in water availability for plants, which is reflected in a water deficit or osmotic stress situation for plants. Osmotic stress can trigger reduction in turgor, as well as induce stomata closure to prevent water loss and transpiration. The closure of stomata affects the amount of $CO_2$ available, while reducing the catalysis efficiency of the enzymes responsible for fixation and disrupting photosynthetic activities (Chaves et al., 2009; Ilangumaran & Smith, 2017; H. Zhou et al., 2024). The accumulation of sodium ions can also alter the balance between pH and electropotential changes in thylakoid membranes, disrupting the $H^+$-motive force that enables energy production in chloroplasts (Bose et al., 2017). Plants react to osmotic

stress by closing their stomata, helping to limit ions translocation to the shoot. Due to sodium ions accumulation, plant growth is slowed (Fiodor et al., 2021; Giannelli et al., 2023). Physiological processes can be altered and aberration of reproductive structures can occur, with negative repercussions on fruiting and flowering (Bhat et al., 2023; A. Kumar et al., 2020). The roots represent the area that is first exposed to stress perception and through mechanisms of altering the position and function of aquaporins can increase its hydraulic conductivity (Chaumont & Tyerman, 2014; Gao et al., 2022; Kaldenhoff et al., 2008).

Salt stress is perceived by plants in a two-phase model, whereby plants are initially affected by osmotic stress, and only later by the build-up of sodium and chlorine ions in plant tissues (Price et al., 2022). Despite numerous studies aimed at elucidating the fundamental mechanisms underlying plant perception, uptake, and response to salt stress, several aspects remain poorly understood. Plants would be able to sense osmotic stress, and documented phenomena of halotropism suggest that there are sodium-specific sensors even if they have not yet been identified (**Figure 1.3**) (Galvan-Ampudia et al., 2013; Sun et al., 2008; H. Zhou et al., 2024).

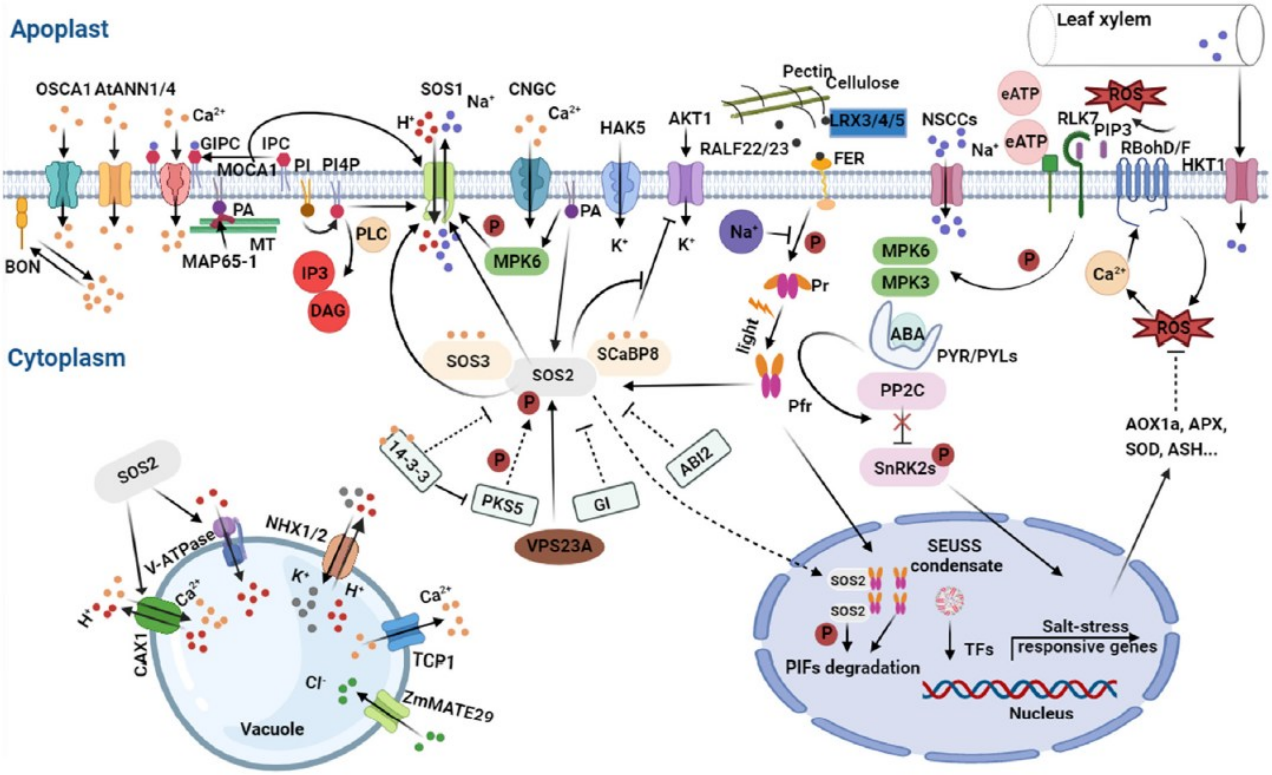


**Figure 1.3.** Plants possibly perceive osmotic stress caused by soil salinization or directly by sodium or chlorine ions. Changes in cell wall composition could actively contribute to the perception of and response to salt stress in plants; in fact, some plasma membrane derivatives may also act as second messengers. For example, known is the role of glycosyl inositol phosphorylceramides (GIPCs), which appear to bind directly to extracellular sodium. Osmotic stress induces excessive accumulation of cytoplasmic calcium ([$Ca^{2+}$]) and overproduction of reactive oxygen species (ROS). $Ca^{2+}$ can be sensed by specific sensors such as SCaBP8

mediating the modulation of the intracellular signaling response to salt stress. Plants can avail themselves of several mechanisms to limit the negative effects imposed by stress conditions. The salt overly sensitive (SOS) system is certainly among the most common for reducing $Na^+$ accumulation in the cytoplasm. Other strategies involve ion homeostasis by importing more potassium ions ($K^+$) or compartmentalization of $Na^+$ in specific organelles. The picture is taken from Zhou et al. (2023).

One of the first consequences induced by salt stress is an increase in cytoplasmic calcium concentration ([$Ca^{2+}$]) that triggers a signaling transduction cascade (Chele et al., 2021; Steinhorst et al., 2022; Xu et al., 2022). The increase in intracellular calcium concentration appears to depend on the opening of specific transport channels induced by the interaction between the $Na^+$ and the glycosyl inositol phosphorylceramides (GIPCs) exposed on the cell surface (Jiang et al., 2019; Steinhorst & Jörg, 2019). There are signaling mechanisms over long root-to-shoot distances that are mediated by calcium, these $Ca^{2+}$ - waves vary in intensity and amplitude in relation to the amount of sodium ions and consequently the severity of stress (Choi et al., 2014; Giannelli et al., 2023). Calcium is a very important signaling molecule for the activation of the Salt Overly Sensitive (SOS) pathway that reduces the accumulation of sodium ion in the cytoplasm of cells (Steinhorst et al., 2022; Yang & Guo, 2018).

The accumulation of sodium ions in the cell cytoplasm is carried by different types of transporters like non-selective cation channels (NSCCs) and the high-affinity $K^+$ transporters (HKTs) (Su et al., 2015). Sodium intake under salt stress conditions leads to a $Na^+/K^+$ ionic imbalance. Given their chemical similarity, sodium accumulated in cells can compete with potassium for cellular functions. However, sodium can't replace potassium as a cofactor in many enzymes, disrupting their activity and causing damage to cell functionality (Almeida et al., 2017). When the cellular concentration of $Na^+$ increases in the cytoplasm, plants may act excluding ions from roots or compartmentalizing into specific organelles. Specialized membrane transporters such as NHX7/SOS1 contribute to the exclusion mechanism (Ji et al., 2013). When the intracellular concentration of $Na^+$ increase, the mechanisms of sodium exclusion in the apoplast and the compartmentalization in vacuoles mediated by $Na^+/H^+$ antiports and vacuolar $Na^+/H^+$ exchanger (NHX) becomes inefficient and accumulating in the cytosol can result in the disruption of cellular functions (Ilangumaran & Smith, 2017; H. Zhou et al., 2024).

To alleviate the ionic imbalance, cells can increase the synthesis of molecules called osmolytes such as proline, glycine, and soluble salts, reducing the cytoplasmic potential. Proline is often used as a marker of salt stress, and its action is not limited to adjustment of redox potential. Proline also provides stability to proteins and membrane structures and acts as a scavenger of reactive oxygen species (ROS) (Per et al., 2017). Overproduction of ROS is one of the early results of salt stress.

Consequently, the detoxification enzyme activity driven by superoxide dismutase (SOD), ascorbate peroxidase (APX), catalase (CAT), guaiacol peroxidase (GPX), dehydroascorbate reductase (DHAR) and others, is overexpressed (Gupta & Huang, 2014; Sharma et al., 2012). Phytohormones play an important regulatory role in stress response, especially abscisic acid (ABA), salicylic acid (SA), and jasmonic acid (JA) which are considered stress hormones. In particular, ABA is one of the hormones that up or down regulate numerous genes related to salt stress tolerance and induces stomatal closure, decreasing transpiration and consequently water loss (Aizaz et al., 2024; H. Zhou et al., 2024).

## 1.4 Microbial-based Biostimulants

During the Green Revolution period, the overuse of chemical fertilizers, pesticides and insecticides in agriculture became widespread to meet the growing demand for food supplies and maximize agricultural yields (Khan et al., 2023). Although there has been an initial increase in production efficiency, their misuse has resulted in a worrying pollution problem of natural ecosystems. Agrochemicals are, in fact, petrochemical derived and not degradable. Therefore, their long-term retention into the soil can reduce its fertility and biodiversity (Datta et al., 2016). The utilization of new generation products, such as plant biostimulants, may reduce the reliance of modern agricultural practices on agrochemicals, while decreasing the pressure exerted on the natural ecosystems, representing a promising and eco-friendly strategy to improve crop growth, productivity and protection (Berg, 2009; Vejan et al., 2016).

The primary sources for the formulation of biostimulants are heterogeneous and comprise among others plant growth-promoting microorganisms (PGPM) (Iosa et al., 2024). The microbial community that colonizes the rhizosphere, the soil layer surrounding the roots, is populous and elaborate and largely includes bacteria, as well as fungi, protozoa, and algae (S. Kumar et al., 2022). Various of these microorganisms, mainly bacteria and fungi, possess plant growth-promoting capabilities (Caldara et al., 2024; Graziano et al., 2022). Specifically, the subgroup of the plant growth promoting rhizobacteria (PGPR) is nowadays frequently employed for agricultural purposes because of their capacity to improve soil fertility, nutrient uptake, and plant resistance to biotic and abiotic stressors (Iosa et al., 2024). In addition to biofertilization and biocontrol functions, in fact, some PGPR strains can exert bioremediation activities in metal contaminated soils or have positive effects on improving soil properties and mitigating GHGs (O'Callaghan et al., 2022).

In recent decades, given their great potential for agricultural improvement, the market for microbial biostimulants is rapidly expanding despite still being very limited compared with that for agrochemicals. Most of the products already available internationally are formulated employing

nitrogen-fixing bacteria for approximately 80% of the total (Basu et al., 2021). To give a few examples, we find Azo-N produced in South Africa and containing *Azospirillum brasilense* and *Azospirillum lipoferum*, Nodulest 10 released in Argentina with *Bradyrhizobium japonicum* and Nitragin Gold® commercialized from USA and composed of *Rhizobia.* Biostimulants based on phosphate and potassium solubilizing bacteria represent only the 14% of the total, including the Indian product K Sol B with *Frateuria aurantia* and the Russian Phosphobac-terin with *Bacillus megaterium* (Basu et al., 2021; Fiodor et al., 2021).

The performance of PGPR can be improved by combining bacteria with arbuscular mycorrizhal fungi (AMF) able to protect crops from salinity, lack of water, phytotoxic elements and ameliorate nutrient uptake (Ganugi et al., 2019; Watts-Williams et al., 2022). Only a small number of all fungal species recorded to date have been molecularly and functionally characterized for use in agricultural applications. Many of the AMF used for formulating microbial biostimulants are generalist symbionts common in almost all soil types around the world, such as *Funneliformis mosseae* (formerly *Glomus mosseae*) and *Rhizoglomus irregulare* (syn. *Rhizophagus irregularis*, formerly *Glomus intraradices*) (Giovannini et al., 2020). There are several studies supporting the role of AMF in improving plant nutrition, with a potential reduction in the use of agrochemicals and in particular phosphorus inputs given their proven ability to increase phosphorus concentrations in shoot and root system (Begum et al., 2019). AMF can also be used to improve plant resistance under abiotic stress conditions, inducing a wide range of effects on plants (Bahadur et al., 2019; Kuila & Ghosh, 2022; Q. Wang et al., 2023).

Farmers are often inadequately informed about the advantages of biostimulants over commonly used agrochemicals and in the dissemination centers there is a shortage of qualified technical staff. In addition, because of the living microorganisms contained, microbial based biostimulants require special transportation services and storage facilities that are often lacking. To curb the limitation to the growth of biofertilizers demand in the global market to which the factors are contributing, it becomes necessary to constantly refine their formulation to achieve more efficient and stable products that can satisfy farmers' quality standards (Bashan et al., 2014; Basu et al., 2021). Either way, whatever formulation is desired, it should be non-hazardous and ecofriendly in nature, be based on low-cost and easy-to-source raw materials and ensure controlled release of the product (Malusá et al., 2012).

### 1.4.1 Plant Growth-Promoting Rhizobacteria (PGPR): Direct Mechanisms

PGPR can enhance plant health in both direct and indirect ways. For instance, PGPR can promote plant growth by favoring plant nutrient uptake, making macronutrients more available through the

processes of nitrogen fixation, phosphorus solubilization and iron sequestration. Nutrients essential for plant development are in fact normally present in the soil in the form of complex organic molecules that must be simplified to be assimilated ( Mahanty et al., 2017; de Andrade et al., 2023).

Nitrogen-fixing bacteria can catalyze the conversion of atmospheric nitrogen ($N_2$) to ammonium ($NH_4^+$) by the action of the multiprotein nitrogenase complex in a biological nitrogen fixation process (BNF) (Mng'ong'o et al., 2023). An interesting example is the *Rhizobiaceae* family whose members colonize the roots of leguminous plants through a symbiotic interaction that results in the formation of specialized root nodules (Andrews & Andrews, 2017).

Although the soil is rich in phosphorus compounds such as apatite, phytates, phosphomonoesters and phosphotriesters, plants cannot take advantage of them because of their insolubility. Phosphate solubilization depends on the ability of certain soil bacterial strains or phosphate-solubilizing bacteria to produce low-molecular-weight organic acids (gluconic or citric acid) endowed with carboxyl and hydroxyl groups capable of chelating the cations that cause their insolubility. An additional strategy is to make phosphorus soluble by the process of mineralization or hydrolysis of phosphate esters. Among the phosphate solubilizers genera are listed *Pseudomonas*, *Bacillus*, *Rhizobium, Burkholderia*, *Achromobacter*, *Agrobacterium*, *Micrococcus*, *Acetobacter*, *Flavobacterium*, and *Erwinia* (Mahanty et al., 2017).

Iron is an important nutrient for plant development and is not available to plants because in an aerobic environment it can form insoluble hydroxides and oxyhydroxides, which are not available for plant uptake (Butler et al., 2021). PGPR also comprehend bacteria secreting siderophores, chelating molecules that bind iron complexes with high affinity. Siderophores can also benefit plant health by acting as decontaminants and relieving stressful conditions in heavy metal-rich soils (Hesse et al., 2018).

PGPR can also directly influence plant physiological and cellular processes, synthetizing and releasing into the rhizospheric environment auxin as a second messenger. Auxin can (i) enhance xylem and root development; (ii) interfere with cell division, extension, and differentiation; (iii) control vegetative growth processes; (iv) mediate responses to light or gravity and (v) affect photosynthesis and pigment formation, biosynthesis of various metabolites, and stress resistance (Mahanty et al., 2017).

### 1.4.2 Plant Growth-Promoting Rhizobacteria (PGPR): Indirect Mechanisms

The most common plant protection strategy implemented by plant growth-promoting bacteria is the production of antimicrobials, many of which have been studied and marketed for their beneficial

properties of preventing/limiting the proliferation of disease-causing pathogens (Santoyo et al., 2021). Many rhizosphere bacteria have been proven to produce metabolites with strong antifungal activity such as hydrogen cyanide, phenazines, pyrrolnitrin, 2-4-diacetylphloroglucinol, pyoluteorin, viscosinamide and tensin (Mahanty et al., 2017). However, PGPR may also trigger plant defense mechanisms against viruses, fungi and bacteria through the Induced Systemic Resistance (ISR) and the System Acquired Resistance (SAR) (Choudhary et al., 2007; Pieterse et al., 2014).

ISR is considered an indirect mechanism because it does not imply contact between PGPR and pathogens and it is instead adducible to the activation of specific signaling pathways. ISR arises from activation of the jasmonic acid and ethylene signaling pathways (Glick 2012). Single bacterial parts or bacterial-derived compounds such as lipopolysaccharides (LPS), flagella, siderophores, cyclic lipopeptides or volatile compounds are also effectors of ISR (Mahanty et al., 2017). Instead, the SAR system confers long-lasting immunity by accumulating salicylic acid in damaged plant tissues. The immune response modulates the expression of pathogenesis-related (PR) genes including NPR1 sequence encoding for a key regulatory protein (Vishwakarma et al., 2020). PGPR can also induce plant resistance against abiotic stressors via Induced Systemic Tolerance (IST). In IST many hormones activate cascade reactions aimed at controlling phytohormone levels, ROS accumulation, exopolysaccharide production, secretion of secondary metabolites, or gene expression, resulting in plant morphological and physiological modification (Hamid et al., 2021).

### 1.4.3 Plant Growth-Promoting Rhizobacteria (PGPR): Salinity Stress Defense

PGPR can act in multiple ways to alleviate the effects of salt stress on plants, as shown in **Figure 1.4**. Certain microorganisms can, for example, support plants in restoring ion balance by reducing the accumulation of $Na^+$ and $Cl^-$ in leaves and regulating $Na^+$ exclusion from roots or the activity of specific transporters to improve the $K^+/ Na^+$ ratio in the shoot (Sunita et al., 2020). Others may instead facilitate nutrient uptake, mitigate sodium-induced toxicity through biofilm formation, and modify root architecture (Bhat et al., 2023).

PGPR can also induce a biosynthesis of osmolytes and antioxidant molecules to lower oxidative damage and osmotic imbalance rate or indirectly promote plant growth and defense by altering plants phytormonal status. Many rhizobacteria, for example, alter plant auxin levels through indole-3-acetic acid (IAA) synthesis from tryptophan present in root exudates (Ilangumaran & Smith, 2017).

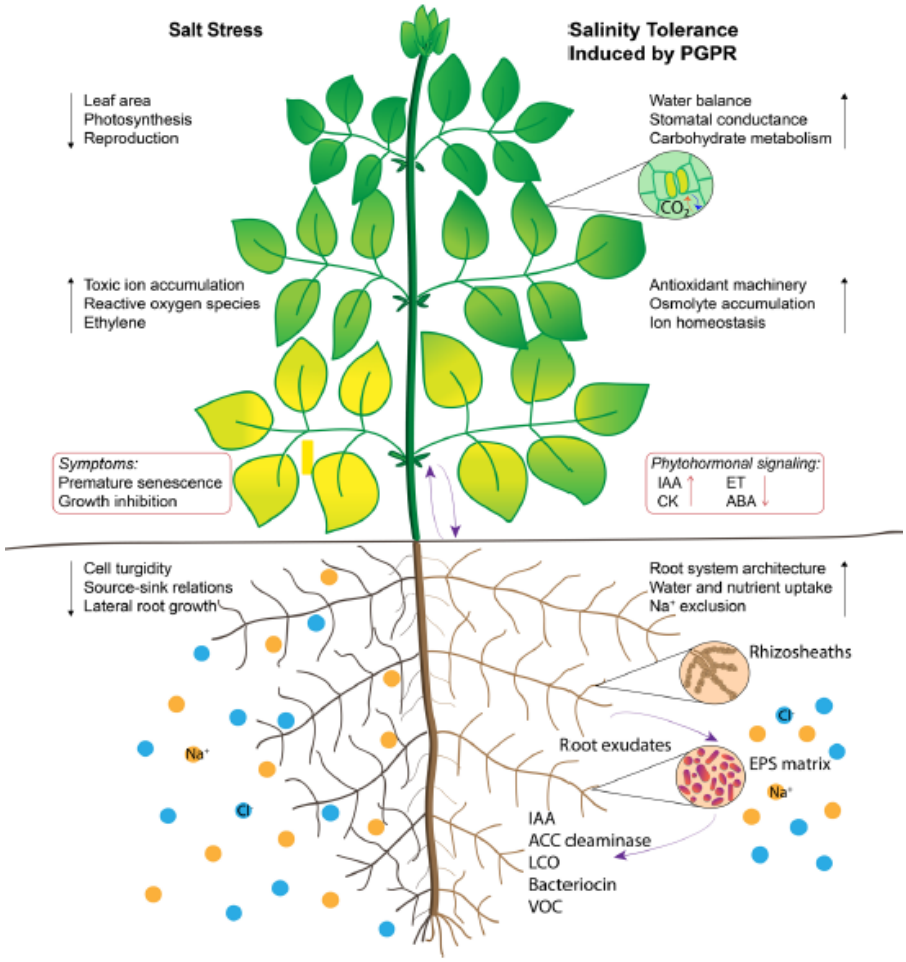


**Figure 1.4.** Graphical representation of the various mechanisms triggered by Plant growth-promoting rhizobacteria (PGPR) to mitigate salt stress-related effects. PGPR can sequestrate ions through exopolysaccharide matrix, influence phytohormone status in plants by releasing signaling molecules and regulating osmolyte biosynthesis, carbohydrate metabolism, and ROS scavenging activities. The picture is taken from llangumaran et al. (2017).

### 1.4.4 Arbuscular Mycorrhizal Fungi (AMF)

Arbuscular mycorrhizal fungi (AMF) are obligate biotrophs that establish a mutualistic symbiotic relationship with relevant agricultural crops such as cereals or fruit trees, medicinal plants and other economically viable plants such as i.e. cotton, sugarcane, cocoa and sunflower (Giovannini et al., 2020). This association triggers a series of complex exchange events that results in improved plant performance of growth and resistance to abiotic and biotic stresses. AMF-host plant communication is mediated by the formation of specialized fungal structures such as hyphae, vesicles and arbuscules in the roots of host plants (Begum et al., 2019; Mahanty et al., 2017). Numerous AMF species can produce spores-storage vesicles containing lipids, while the arbuscules are essential key units for enabling symbiotic exchange (Q. Wang et al., 2023). The hyphae can penetrate cortical cells or extend outside the cellular protoplasm distinguishing endomycorrhizae from ectomycorrhizae (Begum et al.,

2019; Mahanty et al., 2017). In general, AMF retrieves from plants the photosynthates and the lipids they need to complete their life cycle, expanding in return the plant's uptake area in soil through the extraradical mycelium (ERM). The ERM simplifies plant nutrient intake by extending beyond the nutrient depletion zone surrounding the roots, taking up phosphorus, potassium nitrogen, copper, calcium, and zinc in varying amounts depending on its configuration, structure, and extent. The ERM then translocates water and micronutrients to the roots where bidirectional exchanges between the fungi and the plant symbiont take place at the level of arbuscules (Giovannini et al., 2020).

### 1.4.5 Microbial-based Biostimulants: Challenges and Controversies

There are multiple studies confirming the beneficial effects of PGPR on plant growth, especially when subjected to stress conditions (Fiodor et al., 2021; Vejan et al., 2016). Although promising results have been obtained under laboratory or controlled plant growth conditions, it is difficult to express the full potential of PGPR in field agricultural applications with controversial results (Mayer et al., 2010; Fiodor et al., 2021).

Under field conditions, the performance of PGPR and their prevalence in soil can be optimized or reduced by the contribution of multiple factors. Rilling et al. (2019) comprehensively reviewed the environmental variables that can influence the persistence of inoculated microorganisms in soil. Plants exert considerable control over the composition of rhizosphere bacterial communities by regulating the amount and chemical composition of root exudates that serve as attractants and nutrient sources for indigenous microorganisms, in the so called “rhizosphere effect” (Compant et al., 2019). The strength of the rhizosphere effect depends on the proximity to the root system (Backer et al., 2018;). Soil physicochemical properties also help determine the fate of inoculated microorganisms once administered into the medium (Rilling et al., 2019).

The selection of microbial species to formulate a microbial product should ideally consider the desired effects and environmental characteristics, anticipating interaction with the plant species under study and native microbial communities as much as possible (Fiodor et al., 2021). To maximize the chances of PGPR to colonize the rhizosphere and compete with native microbial communities, the ideal concentration of microorganisms to be inoculated must be selected (Iosa et al., 2024). Another strategy is to combine microorganisms with different functions in microbial consortia (MCs). -this association may result in more successful application than using single species. In addition, high genetic diversity within MCs improves resilience and ability to counter adverse environmental conditions. Optimized performance might be attributable to the synergistic interaction among microorganisms, which strengthen their action by supplying nutrients to each other, removing

inhibitory products, stimulating beneficial physiological characteristics, and replacing each other if a specific strain is unable to establish itself in the soil (Vishwakarma et al., 2020).

In general, microorganisms can be inoculated via seed coating, root dipping in bacterial suspension or application of the bacteria through drip-irrigation, direct addition into the soil or carrier-based inoculation and the success of the listed methods strictly depends on the interaction microorganisms-plant species (Lobo et al., 2019). The choice of a proper carrier for microorganisms is also a key factor in the successful application of biofertilizers in agricultural fields. In fact, a suitable delivery system may elongate microbial shelf-life, providing an ideal protective or nutritive environment to ensure maintenance of the concentration and physiological and metabolic characteristics of the microorganisms (Basu et al., 2021; Mahanty et al., 2017). The most common carriers currently used in the biofertilizer industry include peat, charcoal and lignite. One of the main issues is due to the limited availability of materials in some countries of the world, with reference to developing countries (Basu et al., 2021).

## 1.5 Biochar and Soil Microbial Diversity

Biochar is defined from the European Biochar Certificate (EBC) as a porous-structured material rich in carbon, derived from the pyrolysis of biomasses conducted under a strictly controlled regime of conditions. The thermochemical conversion of organic matter occurs at a high temperature, in the range of 350-1000°C, and at low oxygen content. Reaction parameters and feedstocks, usually wood chips, organic waste and agricultural residues or by-products, can both greatly impact on the sustainability of production and the physicochemical and nutritional properties of biochar (Zhen et al., 2010; EBC, 2012-2023).

The EBC collects the European guidelines for sustainable biochar production, ensuring a product with recognized quality standards, result of a meticulous control system that is constantly updated based on the latest analytical techniques and research (EBC, 2012-2023). If not controlled, the decomposition of organic materials may, in fact, originate toxic aromatic molecules such as polycyclic aromatic hydrocarbons (PAH), polychlorinated dibenzodioxins and furans, phenols and phenol derivatives, or other harmful chemicals (Anjum et al., 2014).

Regarding its elemental composition, biochar contains carbon, nitrogen and hydrogen atoms, as well as nutrients such as potassium (K), calcium (Ca), sodium (Na), and magnesium (Mg). In addition, its structure might also comprise variable concentration of humic and fulvic acids. As a rule, the temperature of thermochemical conversion is directly proportional to carbonaceous content and, on the contrary, inversely proportional to nitrogen and hydrogen amount. Another peculiarity is the

presence of polar and nonpolar substances that are affine for inorganic ions (Ding et al., 2016). The temperature and raw materials used to produce biochar also determine its pH and usually wood-based biochar appears to have a higher pH as well as those produced at high temperatures (Huang et al., 2023).

During the last decades, biochar has become increasingly popular for its agricultural applications. It not only enhances soil quality but can also influence abundance, structure and metabolic activity of microbial communities (M. Wang et al., 2020; Ren et al., 2023; Wu et al., 2024).

The influence of biochar on the soil microbial biodiversity is expressed in several ways, making nutrients more available, altering plant-microorganism signaling pathways and protecting microorganisms (Ding et al., 2016). Biochar can have different properties depending on production parameters, and different types of biochar can induce variable environmental and microbial responses (Zhu et al., 2017). In general, the administration of biochar may alter soil physical-chemical properties or composition, triggering events such as shift in pH level, reduction in nutrient leaching and increase in water retention, all factors contributing to shape appropriate moisture conditions to encourage microbial growth (Ding et al., 2016; Huang et al., 2023). According to Sheng & Zhu (2018) under acidic soil conditions, a rise in pH induced by biochar administration was the major driving agent in increasing the percentage of *Bacteroides* and *Gemmatimonadetes* at the expense of *Acidobacteria*. Biochar can also exert a protective role for microorganisms. Due to its pore size (>50 nm), biochar lends itself well to colonization by bacteria, fungi and protozoa, while limiting the access of large arthropods and predation events (Wong & Ogbonagya, 2021). Internal and external colonization phenomena occur by adsorption to its surface through electrostatic or hydrophobic interactions. In addition, its large water-retention capacity can help create a microenvironment with the right degree of moisture to promote microbial proliferation (Ding et al., 2016). As reported by Zheng et al. (2018) biochar can be colonized by actinomycetes and fungi that with their mycelia promote the formation of large soil aggregates, a process that is protective for the microorganisms themselves.

## 1.6 Nanomaterials and their Role in Agriculture

There is evidence of use of nanomaterials (NMs) in some archaeological contexts from Greece, Egypt and Mesopotamia already in the 3$^{rd}$ century BCE. One of the first instances is the use of the first synthetic pigment, known as “Egyptian blue,” which was used for decorative purposes. Such pigment was composed of a sintered mixture of nanometer-sized quartz and glass (Jhonson-McDaniel et al., 2013). One of the oldest and most famous application examples of metal nanoparticles (NPs) can still

be appreciated in the Lycurgus cup, a Roman relic dating back to the 4th century. The peculiarity of the cup is that it appears differently colored, either red or green, depending on the direction of light incidence (Leonhardt, 2007). The reason lies in the dichroic glass, the composition of which is based on Silver-Gold (Ag-Au) nanoparticles alloyed, at a ratio of 7:3, in about 10 percent copper (Cu) (Freestone et al., 2007).

To date, The European Commission defines nanomaterials, whether of natural or synthetic origin, as solid particles with at least 50% of their structure in the size range of 1-100nm. In case these materials possess an elongated shape or are plate-like shaped then at least one of their dimensions should be less than 1nm, while the others can also be greater than 100nm (EU Commission, 2022).

There are several methods of classifying nanomaterials based on their origin, the materials of which they are composed, or their dimensionality. First, there are nanomaterials of natural or synthetic origin, the former can be found in nature because they are produced by biological species or because they are produced from natural materials through anthropogenic activities. Engineered or synthetic nanomaterials, on the other hand, are derived from engine exhaust and fumes, mechanical milling or can be produced through physical, chemical, biological or hybrid methods (Jeevanandam et al., 2018).

Nanomaterials can also be grouped into four categories as 0D, 1D, 2D and 3D based on the number of their dimensions, as shown in **Figure 1.5** (Pokropivny & Skorokhod, 2007). Dimensionality is closely related to electron mobility along with an increase in mobility as the number of dimensions considered increases. The shape and dimensionality of nanomaterials also can define their characteristics.

In terms of their chemical composition, NMs and nanostructured materials can be carbon-based (fullerenes, carbon nanofibers, diamonds carbon nanotubes, and graphene), organic (e.g. micelles, dendrimers, hydrogels, nanoconjugates) or inorganic (e.g., metals, metal oxide, and ceramic nanomaterials) or nanocomposites (Harish et al., 2022; Jeevanandam et al., 2018).

Given the size scale of their structure, nanomaterials exhibit singular characteristics compared with their corresponding bulk materials. They are characterized by a large surface area and a variable degree of porosity, exhibit superior mechanical performance, and offer the possibility of surface functionalization. All these qualities have made them attractive for applications ranging from the biomedical field to the agricultural and food industries (X. He et al., 2019; Mitchell et al., 2021).

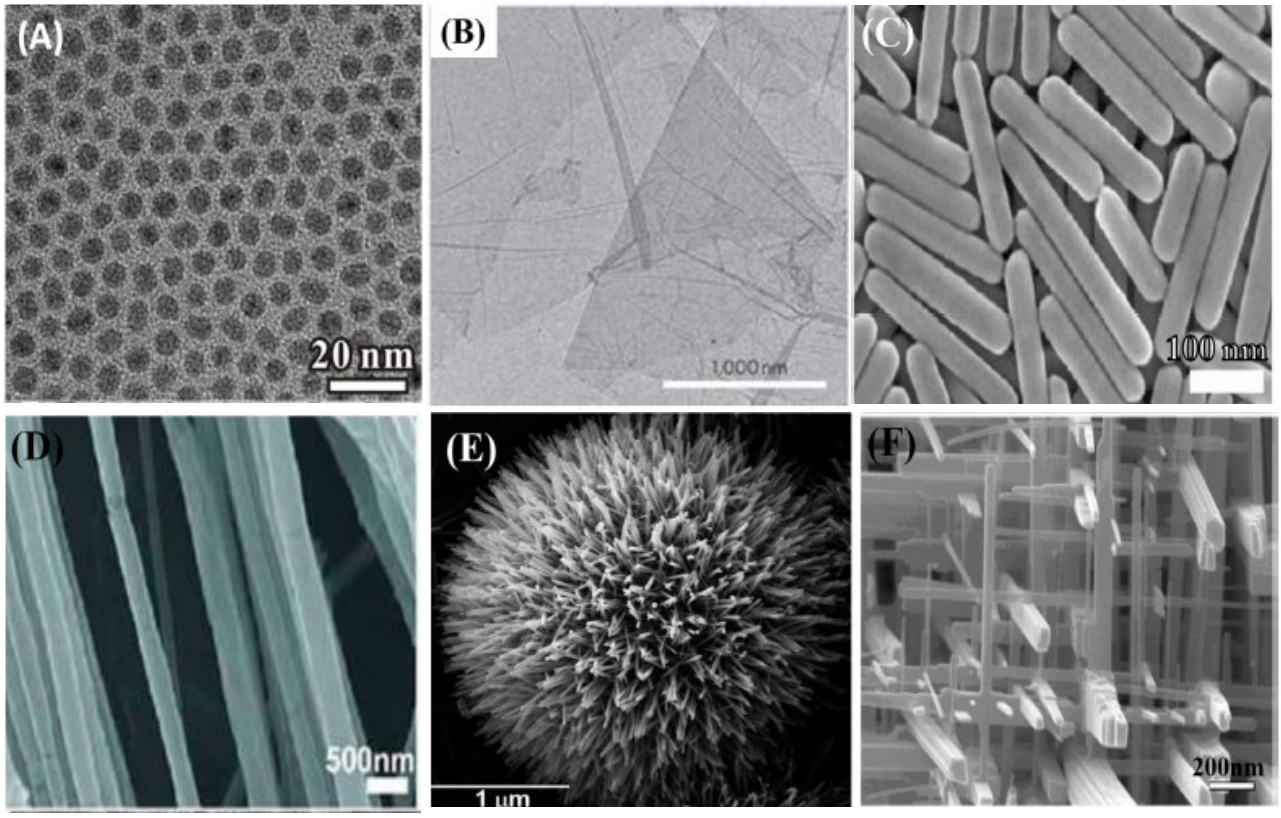


**Figure 1.5.** The pictures are taken from Jeevandam et al. (2018) and report examples of nanomaterials with different morphologies. (A) nonporous Pd NPs (0D) copyright Zhang et al.; licensee Springer, 2012, (B) Graphene nanosheets (2D) copyright 2012, Springer Nature, (C) Ag nanorods (1D) copyright 2011, American Chemical Society, (D) polyethylene oxide nanofibers (1D) copyright 2010, American Chemical Society, (E) urchin-like ZnO nanowires (3D), with permission from The Royal Society of Chemistry, (F) WO3 nanowire network (3D) copyright 2005 Wiley-VCH.

In agriculture, plant biotechnology is assuming an increasingly important role. Nanomaterials can be used for fertilization and for plant protection from biotic and abiotic stresses, as nanosensors to monitor in the long-distance plant health or as nanocarriers for controlled release and delivery of substances (Harish et al., 2022; Pérez-de-Luque, 2017). In addition, several studies have shown that nanoparticles can be used to promote plant growth support (Pavlicevic et al., 2023; Pagano, et al., 2023). To improve the application of nano-biotechnology, a complete understanding of the mechanisms of interaction with plants, including uptake phenomena and accumulation sites in plant tissues, is essential (Pérez-de-Luque, 2017). The chemical composition, morphology and size of nanoparticles, figure among the determinants of uptake in plants, which depends also on plant physiology and thus directly on the plant species (Cifuentes et al., 2010; Zhu et al., 2012; Pérez-de-Luque, 2017). In addition, the stability and bioavailability of nanomaterials can be affected by root exudates and exopolysaccharides (EPs) from microorganisms that can influence their biotransformation in soil (Ma et al., 2018).

Nanoparticles can be applied at the leaf and root level (**Figure 1.6**). The preferred pathways of access to the root are the symplastic pathway, which allows transport through specialized structures called plasmodesmata, and the apoplastic pathway whose solute transport occurs externally to the plasma membrane through extracellular spaces to the central root cylinder and xylem.

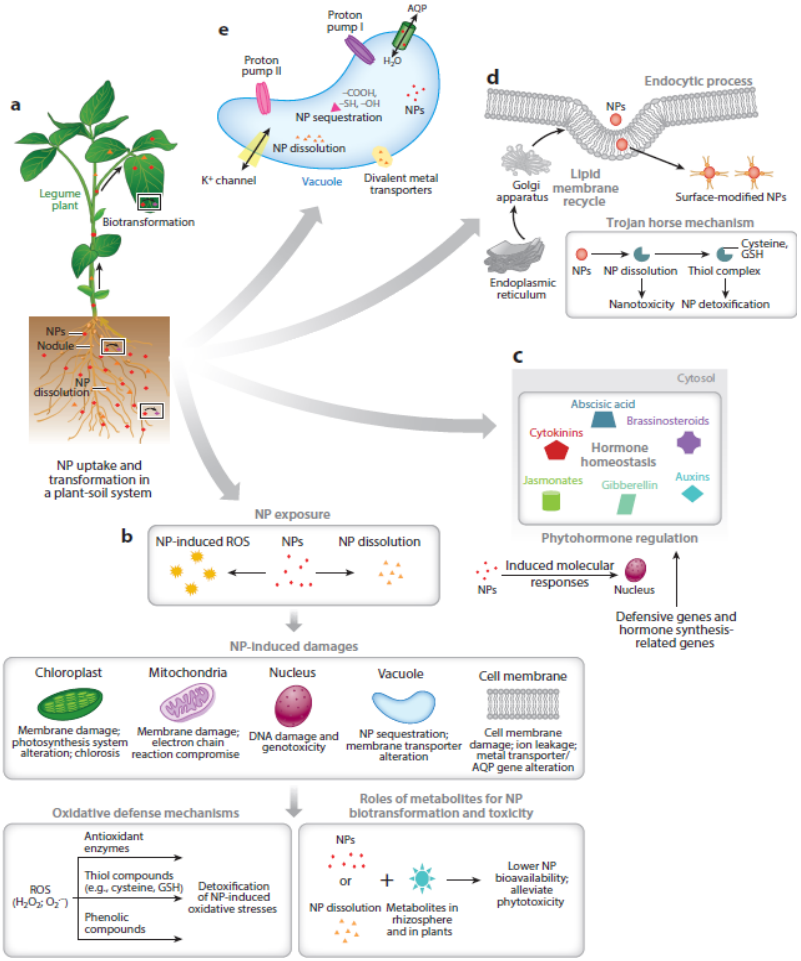


**Figure 1.6.** Graphical representation of potential nanoparticle internalization pathways and plant response to their exposure. Once penetrated the roots, nanoparticles may be subjected or not to biotransformation. Furthermore, they can be compartmentalized in the vacuole or be translocated into the aerial parts. Excessive accumulation can lead to cellular toxicity. However, nanotoxicity at the cellular level can be mitigated by sequestration in the vacuole. Cytotoxicity can be induced by oxidative stress and ROS overproduction that activates antioxidant defense mechanisms and by regulating the plant's hormonal response, both at the biochemical and molecular levels. The image is taken from Ma et al. (2018) with partial elaboration.

For cell penetration during access to the symplastic pathway, nanoparticles must cross the plasma membrane through endocytosis, pore formation or interaction with carrier proteins. Nanoparticles absorbed by plants travel through the vascular system and then deposit in plant tissues and organs such as fruits, grains, or flowers (Pérez-de-Luque, 2017).

When plants encounter nanoparticles, a series of molecular and biochemical responses are triggered, in particular the signaling pathways related to abiotic stress response, such as the over production of ROS. Despite the countless benefits due to nanoparticle applications, it is necessary to have a careful characterization of their structure and especially to assess the risks that could be related to their use. Depending on the type of nanomaterial, dose and duration of exposure, nanotoxicity and potential trophic transfer could in fact occur (Francis et al., 2024; Ma et al., 2018).

## 1.7 *Triticum* L.

Wheat belongs to the monocotyledonous *Poaceae* family and is one of the major cereal crops in the world. It is a global source of energy, macronutrients and micronutrients, especially for developing countries. In addition, consumption of wheat and in particular whole grain products is associated with a reduction in cardiovascular diseases and type 2 diabetes. Despite the health benefits derived from daily consumption of wheat products, its high allergenic power often causes disorders such as celiac disease or non-celiac gluten sensitivity. Cultivated wheat (Triticum) can be classified as diploid (AmAm genome) to which einkorn (*T. monococcum* ssp. monococcum) belongs; tetraploid (AABB) to which emmer (*T. turgidum* ssp. dicoccum) and durum wheat (*T. turgidum* ssp. durum); hexaploid (AABBDD) that is soft wheat (*T. aestivum* ssp. aestivum) and spelt (*T. aestivum* ssp. spelta). Nutritional profile varies slightly depending on wheat variety and growing conditions. Generally, carbohydrates represent the predominant fraction, 71% of which 58% starch and 13% non-starch polysaccharides, proteins cover 11% of the total and lipids and minerals only 2%. The percentage of vitamins and phytochemicals is tiny (<0.1%) but can induce positive effects on humans. Wheat crops resistant to heat, frost, drought, and/or saline soils can increase production yields and contribute to food security (Wieser et al., 2020).

In 2019, the entire genome sequence of durum wheat cv. Svevo was reconstructed. The study of its 14 chromosomes and their coding sequences will have great repercussions in experimental research. The identification of molecular markers associated with the most relevant agronomic traits and coding sequences for gluten proteins will allow, for example, the development of innovative and more effective strategies for improvement or selection of wheat qualities (Maccaferri et al., 2019).

## 1.8 *Glycine max* L.

Soybean (*Glycine max* L.) is an annual crop belonging to the *Fabaceae* family. As reviewed by Sedivy et al. (2017) several theories have been proposed regarding its origin and the history of its domestication. The origin site of modern soybean domestication from the wild soybean (*Glycine soja*, Siebold & Zucc.) can be placed presumably in the Yellow River Basin. About 2.000 years ago soybean cultivation was then exported from China to Korea, Japan, and South and Southeast Asia reaching America at the beginning of 1700. To date, soybean is considered one of the most economically viable legumes, and globally the major soybean producers are the United States, Brazil, and Argentina, followed by China and India (Fang & Kong, 2022). Soy is a valuable source of plant proteins, containing all the nine essential amino acids, that can meet the dietary needs of humans and animals.

Soy-based foods, such as soy milk, soybeans (edamame), tofu and tempeh nowadays present in many diets, represent valid alternatives to meat consumption. The second most important product of soybeans is oil, popular worldwide for its healthful composition, rich in polyunsaturated fatty acids and in particular linoleic acid (omega-6). Soybeans are also a source of fiber in the form of oligosaccharides and non-starch polysaccharides, as well as micronutrients that include calcium, iron and zinc and B vitamins. Consumption of soy foods has beneficial effects on the body that appear to be due to the presence of phytoestrogens. In addition, soy intake might act indirectly by altering the metabolic activity and composition of the gastrointestinal microbiota (Belobrajdic et al., 2023).

Considering the rise in global population and demand for high-protein plant-based products, soybean production is in deficit by 1.2% of annual world needs. Since wild soybean possesses a high level of genetic diversity, that was probably lost from *Glycine max* L. over the process of domestication and crop improvement, its genetic material is a potential source of information and genetic tools to provide greater stress tolerance to the modern crops (Kofsky et al., 2018).

## 1.9 *Solanum lycopersicum* L.

Tomato plant (*Solanum lycopersicum* L.) is a species belonging to the family *Solanaceae* that includes other economically relevant crops such as potatoes and eggplants. Native of South America, particularly the Andean regions, the tomato was presumably domesticated in Mexico before being introduced to Europe in the 16$^{th}$ century (Bai et al. 2007; Bergougnoux et al., 2014). Tomatoes are cultivated worldwide, and consumption of their fruits, either raw or processed in the food industry, supplies a considerable amount of antioxidant compounds that can have a beneficial effect on health. Tomato fruits in fact contain secondary metabolites and bioactive compounds such as vitamins C and E, β-carotene, lycopene, flavonoids, organic acids, phenolics, and chlorophyll (Giri et al. 2025) even if their chemical composition depends on variety, environmental factors (light, temperature, mineral nutrition) and agricultural practices adopted. Antioxidant activity can strengthen the immune system, helping to prevent tumors, atherosclerosis and cardiovascular disease (Raiola et al., 2014).

The tomato is native, as are 12 other related wild species, to western and South America. Since its domestication, although little information is available about it, tomato cultivation has spread to different areas worldwide contributing to its genetic variability. In this process, however, some genetic traits relevant to conferring tolerance to abiotic stressors have been lost (Salava et al., 2021). The Tomato Genome Consortium has released a high-quality reference sequence for tomato plant (Causse et al., 2013). Successful sequencing of the tomato genome has provided valuable information

identifying specific molecular markers related to the regulation of the progression from vegetative to reproductive states, fruit maturation, and defense to abiotic and biotic stresses (Liu et al., 2022).

## 1.10 Aim of the Project

The research work at the basis of my PhD project focused on studying innovative nanobiotechnological approaches that can help mitigate the negative impacts due to global warming on the agri-food system. Nowadays, biotic and abiotic stresses threaten the health of plants and their quality-quantitative agricultural yields. Making plants more resilient to climate change has become an imperative that to be fulfilled requires research and development of effective and eco-friendly alternatives to commonly used agrochemicals. Plants and their associated microorganisms behave as a meta-organism or holobiont. The key lies in investigating this dynamic and complex system of communication and exchange. Therefore, it would be necessary to focus not only on the molecular and physiological mechanisms in plants that allow to elucidate the impact of these new products on plant health, but also on the soil whose fertility and microbial diversity are equally critical in determining a successful application.

Microbial-based biostimulants figure among the most promising solutions. In recent years these products have attracted the attention of researchers for their potential to improve plant nutrition and protection and to enhance the yield and overall quality of the produce. Despite their widespread for agricultural purposes, there are challenges and controversies related to their use. Promising results obtained in the laboratory are not always reproducible under field conditions, which by definition are changeable and uncontrollable. In addition, their efficacy is strictly dependent on the interaction between the selected bacterial species and plant varieties, as well as their ability to survive in the soil, coexisting with native species and creating a stable ecological niche. Deepening knowledge regarding the persistence of microorganisms in agricultural soil after inoculation is essential to improve their performance for a successful application under field conditions. To achieve this goal, a traceability method based on real-time PCR (qtPCR) analyses has been developed in the context of the European innovation project SIMBA “Sustainable Innovation of Microbiome Applications in Food Systems” to be tested in a wheat field trial organized in association with the experimental agricultural farm Podere Stuard (Parma, Italy).

Innovation lies in the usage of different approaches that combined could maximize their potential. From a plant perspective, the combined effects could result in enhanced productivity or resilience to biotic and abiotic stressors, while from a microbial perspective it could be reflected in an increased

persistence into the soil. Therefore, microbial based biostimulants have also been studied in combination with soil improver such as biochar, arbuscular mycorrhizal fungi or nanomaterials.

As extensively described, soil salinization is an issue with very ancient origins that still causes substantial economic and agricultural losses. Nanomaterials of several types are used for agricultural purposes due to their exceptional properties based on their small dimensions that render them able to positively impact plant growth. Some of them have been also proved to sustain plant development under abiotic stress conditions. For this purpose, two experiments were set up, in collaboration with the Connecticut Agricultural Experiment Station (CAES), to explore the interaction between nanomaterials and PGPR in stimulating the response of two plants of agronomic interest, cherry tomato and soybean, to salt stress.

# 2 Materials and Methods

## 2.1 Field Trial: *Triticum durum* L. (cv. Svevo) and *Triticum aestivum* L. (cv. Bramante)

### 2.1.1 Microbial-based Biostimulant and Soil Improver

The MC_C, used for experimental purposes, was developed by Tabacchioni et al. (2021) with a bottom-up approach in the context of the European innovation project SIMBA "Sustainable Innovation of Microbiome Applications in Food Systems," funded through Horizon 2020.

As the result of an exhaustive literature search, microbial species with recognized plant growth-promoting functions were selected and tested in vitro for their compatibility. The most promising combination of microorganisms, all of which competent for at least one among the nitrogen fixation, phosphate solubilization, biocontrol, auxin production and amylolytic activities, have been chosen to assembly new synthetic consortia. In addition, the literature search was extended to the available, most effective and commonly used microorganism delivery systems for agricultural purposes. Although there is no universal carrier, a good quality product should be bio-compatible, available at good cost, easy to sterilize and chemically inert, with good distribution and product storage capacity (Tabacchioni et al., 2021).

The MC_C is comprised of five PGPR strains, as listed in **Table 2.1**. The company CCS Aosta S.r.l (Aosta, Italy) provided the consortium in a lyophilized formulation where each one of the bacterial strains was stabilized using sterile micronized zeolite chosen as a carrier according to the previously mentioned reasons (Hett et al., 2023).

| **MC_C** | |
|---|---|
| *Azotobacter chroococcum* LS132 | N-fixation |
| *Burkholderia ambifaria* MCI7 | Plant growth-promoting |
| *Bacillus spp.* BV84 | Biocontrol/plant growth-promoting |
| *Bacillus amyloliquefaciens* LMG 9814 | α-amylase, α-glucosidase, and iso-amylase production |
| *Pseudomonas fluorescens* DR54 | Biocontrol of pathogen |
| *Rahnella aquatilis* BB23/T4d | Plant growth-promoting |

**Table 2.1.** Bacterial species of MC_C and their specific plant growth promoting functions.

The arbuscular mycorrhizal fungus (AMF) was acquired from the MycAgro lab (Bretenière, France). The granular formulation of the inoculum is based on propagules of *Rhizophagus intraradices* (ex-*Glomus intraradices*) FR121 including spores, hyphae pieces, and mycorrhizal root pieces (10

propagules $g^{-1}$ containing a mix of spores, mycelium, and mycorrhizal root pieces), both homogenized with clay and zeolite mineral particles (Graziano et al., 2022).

The biochar implied as soil improver in this experiment was provided by Iridenergy (Parma, Italy). Char A4 was obtained by pyrolysis of wood pellets conducted at 500 and 700°C for 2h, its extensive characterization is reported by Marmiroli et al. (2018).

### 2.1.2 Experimental Set Up

In the framework of the SIMBA project, an experimental field trial took place during November 2022 in the agricultural experimental farm Podere Stuard (Parma, Italy). The experiment was set up with a split plot design, with three plots per treatment. The three parcels, each one of $3m^2$, were randomly positioned in the experimental field and the scheme was equally repeated for both the wheat cultivars chosen. Seeds of the two wheat cultivars *Triticum durum* (cv. Svevo) and *Triticum aestivum* (cv. Bramante), supplied by Produttori Sementi Bologna PSB s.p.a. (Bologna, Italy), were sown at a density of 400 seeds per square meter ($m^2$).

MC_C has been used alone or differently combined with AMF and/or biochar. The experimental conditions considered in this work to monitor bacterial persistence into the soil were the following: (i) control, without any treatments; (ii) AMF + MC_C; and (iii) AMF + biochar + MC_C. The biochar was omogenized with the soil at 200 $gm^{-2}$ before sowing, while MC_C and AMF were applied in a 2:1 W/W ratio (powder/seeds) for the MC_C and in a 1:1 W/W ratio (granules/seeds) for the AMF. To reinforce their beneficial action, a second dose of MC_C and AMF was administered to the rhizospheric soil 119 days after wheat planting, in the same amount as described above.

For the entire duration of the experiment, in addition, meteorological parameters were collected from the computerized weather station installed near the site of the agricultural experiment, at San Pancrazio (Parma, Italy).

### 2.1.3 Liquid Bacterial Suspension

Single bacterial species from MC_C were provided by the National Agency for New Technologies, Energy and Sustainable Economic Development (ENEA, Rome, Italy). Each was grown in LB (Luria-Bertani) broth (Tryptone 10 g/L; yeast extract 5 g/L; NaCl 10 g/L) overnight at a temperature of 28°C. The liquid bacterial cultures were centrifuged for 5 min at 3000xg, and the recovered pellets were thus collected and stored at -20°C to be used successively for testing primers and preparing the quantification standard curve.

### 2.1.4 Collection of Rhizospheric Soil Samples

To assess the shelf life of the bacterial strains of MC_C into the soil, rhizospheric soil samples were collected overtime for the following conditions: (i) control, without any treatments; (ii) AMF + MC_C; and (iii) AMF + biochar + MC_C. The first soil collection took place in November 2022 at about six days after wheat planting and at the stage of shoot emergence. In spring 2023, following the second addition of MC_C to the seedlings, other samples were collected on the dates: March 30 (T1), April 6 (T2), April 17 (T3) and May 5 (T4). The sampling was randomized to avoid artefacts that could have led to an over/underestimation of the bacterial quantification. Soil was collected from at least three plants of the same parcel and from different parcels over the field, at a depth of about 3cm in the rhizospheric area, as close to the roots as possible. For each one of the three conditions investigated, about 10 g of pooled soil for both *Triticum durum* (cv. Svevo) and *Triticum aestivum* (cv. Bramante) was stored at -80°C for further analyses.

### 2.1.5 DNA Extraction and Quantification

DNA was extracted from (i) bacterial pellets and (ii) 1 g of rhizospheric soil samples utilizing the NucleoSpin Soil kit (Macherey-Nagel, Dueren, Germany), according to the manufacturer's instructions. DNA concentration (ng/µL) was measured spectrophotometrically with a Varian Cary® 50 Bio UV-Visible Spectrophotometer (Agilent Technologies, Santa Clara, CA, USA). The absorbance values of DNA molecules were determined at the two wavelengths of 260nm and 280nm and the ratio 260nm/280nm was used to estimate the purity of the extracted DNA. Soil DNA was kept at -20°C until quantification analysis.

### 2.1.6 Searching Primers Specific for Microbial Species of MC_C

A two-way strategy was adopted to identify specific primer pairs to tag the MC_C bacterial strains. On one hand, research has focused on primers that have already been tested and are therefore available for specific tracking of the bacterial species under consideration. On the other, possible genetic markers were used as template for the design of specific primer pairs. Two software were used compare and align DNA sequences: the Basic Local Alignment Search Tool (BLAST) and the MegaX software vs 11 (Tamura et al., 2021). Primers were instead designed using the Primer3 Plus web tool (vs 3.3.0), available at https://www.primer3plus.com/index.html.

The Raq4 primer pair was designed based on the genomic sequence of Rahnella aquatilis HX2, coding for the F0F1 ATP synthase subunit beta (CP003403.1:4937125-4938507). To estimate the copy number of each target sequence, primer sequences were aligned against those of each bacterial

genome using the BLAST algorithm. Since the pairing sites were unique in at least ten strains of each species, we concluded that one copy of the amplicon corresponded to a single genome equivalent (GE). The GEs were calculated based on the length of the reference genome of each bacterial species according to Trung et al. (2011) using the following equation:

$$Number\ of\ GE\ Copies = \frac{(6.02 \times 10^{23}\ copies\ \cdot mol^{-1}) \times DNA\ amount\ (g)}{Genome\ lenght\ (bp) \times (660g \cdot mol^{-1} \cdot bp^{-1})}$$

### 2.1.7 Electrophoresis on Agarose Gel

Extraction and amplification products were primarily analysed through electrophoresis on agarose gel to verify their purity and integrity. In general, gels were prepared at different agarose percentages, with the running buffer TAE1X (Tris-HCl 40 mM, glacial acetic acid 20mM e EDTA 1mM), the desired amount of agarose (g), finally adding 10µL of Gel Red Biotium 10X a fluorescent nucleic acid dye. The percentage of agarose varied according to the size of the DNA fragments to be visualized, using 0.8% for the genomic DNA and percentages ranging from 1.2% to 1.6% for End-Point PCR products. After a run of about 45 minutes, with a voltage of 80V and 400mA, the results were visualized using the Gel Doc 2000 Imaging System instrument (Bio Rad, Hercules, California, USA).

### 2.1.8 End Point PCR

End Point PCR reactions were performed in a preliminary phase to test the specificity of the selected primer pairs for the microbial strains of the MC_C. Amplification reactions were prepared in a final volume of 20µL using 1ng of DNA as a template, 4µL of Wonder Taq Reaction Buffer 5X (EuroClone SpA®, Milano, Italia), 1.5units (U) of Wonder Taq Polymerase (5U/µL) (EuroClone SpA®, Milano, Italia) and 250 nmol/L of primers forward (FW) and reverse (RV). End Point PCR analyses were carried out with the Veriti™ Dx 96-well Fast Thermal Cycler (Applied Biosystems™, Waltham, Massachusetts, USA) following the thermal protocol described in **Table 2.2** and the denaturation, annealing and extension steps were repeated for 39 cycles.

| Amplification Reaction Step | Time (min) | Temperature (°C) |
|---|---|---|
| Initial denaturation | 5:00 | 95 |
| Denaturation (x39 cycles) | 0:50 | 95 |
| Annealing (x39 cycles) | 0:50 | 58-60 |
| Extension (x39 cycles) | 1:00 | 72 |
| Final extension | 10:00 | 72 |

**Table 2.2.** Thermal protocol of End Point PCR reactions.

### 2.1.9 Real Time PCR

Quantitative Real Time PCR (qtPCR) analyses were conducted using as a template: (i) 1 ng of microbial DNA, corresponding approximately to $10^5$ GEs; (ii) 5 ng of DNA extracted directly from MC_C powder; or (iii) 40 ng of DNA extracted from rhizospheric soil samples. Amplification reactions were prepared in a final volume of 10µL of mix containing 1 X POWRUP SybrGreen Master Mix (Thermofisher, Waltham, MA, USA) and 250nmol/L primers forward (FW) and reverse (RV). Real-time PCR analyses were carried out with the CFX96 apparatus (Biorad, Hercules, CA, USA) following a thermal protocol that includes a first preincubation phase at 95°C for 3min, followed by 40 cycles of denaturation and annealing steps respectively for 10sec at 95°C and for 30sec at 62°C. The amplicon dissociation was performed in a temperature range of 65–95°C, with an increment of 0.1°C/sec. Data were analyzed with CFX Maestro™ Software vs 2.2 (Biorad).

To quantify the bacterial DNA extracted from the soil, a reference standard curve was constructed for all the target strains of the MC_C. Each one of the standard curves was created using five dilutions of the genomic DNA obtained from the bacterial pellets collected as previously described and ranging from 1 to $10^{-4}$ ng and corresponding to $10^5$–$10^1$ GEs. The five dilutions were used as template for the qtPCR reactions made in triplicate for each point of the standard curve.

In a complex matrix like the soil there may be present inhibitory compounds that can reduce the amplification reactions efficiency, consequently causing an underestimation of target bacterial populations. To assess the real occurrence of inhibition's phenomena, different amounts of DNA extracted from the most complex experimental condition AMF+biochar (15-40ng) were added to each dilution of bacterial genomic DNA to build a set of standard curves. The standard curves constructed with and without the addition of AMF+biochar DNA were then compared considering the efficiency (E) and the coefficient of determination ($R^2$). The comparisons indicated that there was no inhibition effect due to compounds released during DNA extraction and derived from the soil, even when mixed with AMF and biochar in the most complex experimental condition. The two examined parameters of the standard curves, E and $R^2$, were in fact not significantly affected, even with the addition of 40 ng of AMF+biochar DNA. Therefore, this amount was used for standardizing all the qtPCR reactions. The resulting standard curves were used to interpolate the quantity of the target DNA in the sample.

### 2.1.10 Data Analysis

ANOVA comparisons were performed by Daniels XL Toolbox for Excel, version 7.3.2, by Daniel Kraus, Würzburg, Germany, available at https://www.xltoolbox.net (URL accessed May 14, 2024). Data were plotted with the R software version 4.3.1, using the ggplot2 package (Wickham 2016).

## 2.2 Greenhouse Experiment: *Solanum lycopersicum* L. and *Glycine max* L.

### 2.2.1 Microbial-based Biostimulant and Nanomaterials

The commercial product Micro-$H_2O$ *Plant Drought Relief* is manufactured by Microbial Applications Inc. (Suwanee, GA 30024) and consists of two species of rhizobacteria as shown in **Table 2.3.**

| **Mikro-$H_2O$** | |
|---|---|
| *Bacillus amyloliquefaciens* | $3.09x10^9$ CFU/g |
| *Bacillus subtilis* | $3.09x10^9$ CFU/g |
| Inert Ingredients | 98.5% |

**Table 2.3.** Bacterial species of Mikro-$H_2O$ *Plant Drought Relief* and their concentration, expressed in CFU/g.

Silicon dioxide nanoparticles ($SiO_2$ NPs) (Silicon dioxide, nanopowder, 10-20 nm, (BET) 99.5% trace metal basis) were purchased from Fisher Scentific (Hempton, NH, USA).

Chitosan tripolyphosphate hybrid nanoparticles (Ch/TPP NPs), on the other hand, were produced in house by the ionic gelation method according to the protocol of Pontes et al. (2021). Briefly, a 0.1% solution of chitosan in acetic acid (0.2%, pH 4.7) was prepared and kept under stirring overnight to promote complete dissolution. An aqueous tripolyphosphate solution 0.1% was also prepared and refrigerated at 4°C. Then, a 5mL volume of TPP solution was added dropwise to 20mL of chitosan solution and maintained under stirring overnight.

### 2.2.2 Experimental Set Up: *Solanum lycopersicum* L.

Seeds of Sun Gold (F1) (*Solanum lycopersicum* L.) purchased by Jhonny's Seeds (Winslow, ME, USA) were germinated in seedlings trays using as substrate Pro-Mix BX soil (Premiere Horticolture Inc., Quakertown, PA, USA). After 20 days, homogeneously germinated plants were transplanted into plastic pots (outside diameter 8.89cm, height 7.62cm) to be grown in controlled greenhouse condition, at 24°C with a 16/8 h photoperiod. At the transplantation, a suspension of $SiO_2$ NPs prepared in Milli-Q water was sonicated to avoid aggregates formation and admixed to the soil at the concentration of 200mg/Kg soil. The Ch/TPP NPs were supplemented to the soil at the concentration of 200mg/Kg soil, in a liquid formulation previously sonicated - Ch/TPP NPs in acetic acid (0.2%, pH 4.7) -. The roots were also drenched with a suspension of Mikro-$H_2O$ powder in tap water, following manufacturer's instructions and recommended doses (2.5g per gallon of water, corresponding to $1.7\times10^6$ CFU/g soil). Ten days after the transplantation the commercial Miracle-Gro all-purpose fertilizer (Marysville, OH, USA) was added to the soil.

For experimental purposes, plants were treated with two different types of nanoparticles ($SiO_2$ NPs and Ch/TPP NPs) and a microbial consortium (Mikro- $H_2O$) diversely combined in six experimental conditions: (i) control, without any treatments; (ii) $SiO_2$ NPs; (iii) Ch/TPP NPs; (iv) Mikro-$H_2O$; (v) $SiO_2$ NPs + Mikro-$H_2O$; (vi) Ch/TPP NPs + Mikro-$H_2O$.

The six experimental conditions described above were analyzed under unstressed and salt stress conditions, with 6 biological replicates for each condition, for a total of 72 plants. Salt stress induction was initiated two weeks after transplanting and treatment by watering the plants twice a week for 4 weeks with a solution of sodium chloride (NaCl) at the concentration of 170mM, while unstressed plants were irrigated with tap water.

### 2.2.3 Experimental Set Up: *Glycine max* L.

KARIKACHI soybean (*Glycine max* L.) seeds (Jhonny's Seeds, Winslow, ME, USA) were germinated in seedlings trays using Pro-Mix BX soil (Premiere Horticolture Inc., Quakertown, PA, USA) as substrate. After 20 days, uniform seedlings were selected for transplanting into plastic pots (outside diameter 10.16cm, height 8.89cm). At the transplanting stage, the soil was omogenized with $SiO_2$ NPs and the roots drenched with the commercial product Mikro-$H_2O$. The $SiO_2$ NPs, previously suspended in Milli-Q water and sonicated to avoid aggregate formation, were added to the soil at the concentration of 200mg/Kg soil. According to the manufacturer's instructions and recommended doses, however, the microbial consortium powder was suspended in tap water for root drench (2.5g per gallon of water, corresponding to $1.7\times10^6$ CFU/g soil).

The plants were grown in the greenhouse, at 24°C with a 16/8 h photoperiod. Four different experimental conditions were considered: (i) control, without any treatments; (ii) $SiO_2$ NPs; (iii) Mikro-$H_2O$; (iv) $SiO_2$ NPs + Mikro-$H_2O$, with the combination of NPs and PGPRs. The listed experimental conditions were studied under non-stress and salt stress conditions, with six biological replicates for each condition, for a total of 48 plants. One week after transplanting, salt stress was induced by watering the plants twice a week for 3 weeks with a sodium chloride (NaCl) solution at a concentration of 170mM, while the unstressed plants were irrigated with tap water.

### 2.2.4 Nanomaterials Characterization

The $SiO_2$ NPs were characterized by determining their tendency to aggregate through the Zeta potential (ζ) and the NPs aggregate size (hydrodynamic diameter) by the Dynamic Light Scattering (DLS). In DLS, a laser light irradiates the sample in a polystyrene cuvette, and light scattered in all directions by the particles is detected. Zeta potential is determined using a combination of electrophoresis and Laser

Doppler Velocimetry. The Zetasizer Nano (Malvern Instruments Ltd., Enigma Business Park, Grovewood Road, Malvern, United Kingdom) instrument was used for the measurements using a volume of 1mL of nanoparticle suspension in dd$H_2O$ at the concentration of 200 mg/L placed in a polystyrene cuvette with the Universal 'Dip' cell (ZEN1002), designed for the application of an electric field to the analyzed sample (Zetasizer Nano Series User Manual).

The same analytical techniques were used to characterize the Ch/TPP hybrid nanoparticles. The Zetasizer Ultra (Malvern, Panalytical Inc.) was used to determine the Zeta potential (ζ) and the hydrodynamic diameter of the Ch/TPP nanoparticle suspension in acetic acid (0.2%, pH 4.7). Images of the Ch/TPP NPs were taken using the transmission electron microscope (TEM) (Hitachi HT7800).

### 2.2.5 Morphological Parameters of Interest

Soybean plants were harvested at the end of the three weeks of salt stress induction, while cherry tomatoes after four weeks since the start of the salt stress-induced period. Upon harvesting, the root system was cut and separated from the shoot, washed gently with tap water to remove soil particles adhering to the root surface and excess of water was removed with tissue paper. The length of the roots and shoots was determined with a tape measure, starting from the collar to the apical leaf or to the lower extremity of the roots. The fresh weight of roots, shoots and pods (in the case of soybean plants) was recorded with a precision scale. A small portion of the roots/shoots was collected to be kept at -80°C for further analyses. All the remaining root, shoot and pod tissues have been oven-dried for 3 days at 70°C and used to derive the dry weight following the water removal through evaporation.

Throughout the induced salt stress period, once a week, morphological parameters of interest such as height, number of leaves, number of nodes, number of flowers/buds and pods of soybean plants were also recorded. The same morphologic parameters were measured for cherry tomatoes to monitor the plant health and the possible influence of the applied treatments. The measurements have been collected at two different times: (i) two and (ii) four weeks after the transplantation.

### 2.2.6 Elemental Analysis

Using a precision balance, about 0.2g of dry homogenized plant tissue (soil, roots, leaves/shoots and pods) were weighed into flat bottom digestion tubes. A volume of 3mL nitric acid ($HNO_3$) with 1mL 30% hydrogen peroxide ($H_2O_2$) was used to digest the leaves/shoots and pods samples while the soil and roots samples were digested with a volume of 5mL nitric acid with 1mL hydrogen peroxide. Acid digestion was performed on a hot block (DigiPREP MS, SCP SCIENCE, Champlain, New York, USA) for 45 min at 115°C. Once cooled to room temperature, samples were diluted with Milli-Q

water to a final volume of 25mL or 50mL for samples digested with 3mL and 5mL nitric acid, respectively.

The micro and macro nutrient content of soil, roots, leaves/shoots and pods was determined through Inductively Coupled Plasma Optical Emission spectroscopy (ICP-OES) (iCAP Pro XP, Thermo Fisher Scientific, Waltham, Massachussetts, USA). A continuing calibration verification (CCV) was run every 20 samples.

### 2.2.7 Total Chlorophyll Content and Carotenoid Determination

Total chlorophyll and carotenoid content of soybean and tomato plants were determined according to *Lichtenthaler*'s method with slight modifications, using leaf samples collected at the harvest. A 5mL volume of a 95% (v/v) ethanol solution was used for pigment extraction from approximately 50mg random fresh leaves. The samples were then incubated for 48h at room temperature in the dark. At the end of the incubation period, the extracts were centrifuged for 5min at room temperature at 4000xg. The collected supernatant was used to measure absorbance at three different wavelengths 665, 649 and 470nm using a microplate reader (SpectraMax M2/M2e, Molecular Devices, California, USA). Measurements were made in triplicate for each biological sample considered).

The amount of chlorophyll and carotenoids was estimated with the equations reported below (J. Zhou et al., 2024):

$$Chla = 13.95A_{665} - 6.8A_{649}$$

$$Chlb = 24.96A_{649} - 7.32A_{665}$$

$$Total\ Chlorophyll = Chla + Chlb$$

$$Carotenoids = (1000A_{470} - 2.05Chla - 114.8Chlb)/248$$

### 2.2.8 Photosynthetic Activity Monitoring

Once a week over the entire salt stress period induced for soybean plants, the MultispeQ V 2.0 device (PhotosynQ, USA) was used to monitor photosynthetic activity by detecting fluorescence-based photosynthetic parameters as reported in **Table 2.4**. Three measurements for one middle leaf were taken for all the biological replicates of each condition under analysis.

| | |
|---|---|
| **LEF** | Linear Electron Flow. The total flow of electrons from antennae complexes (where light is captured) into Photosystem 11, taking the leaf absorptivity into account. Calculated as LEF = Phi2 x PAR x 0.45 |
| **Light lntensity (PAR)** | Photosynthetically active radiation. Fraction of the incoming light (400 nm to 700 nm) which can be utilized to drive photosynthesis; µmol photons * $m^{-2}$ * $s^{-1}$. |
| **NPQT** | Estimate of non-photochemical quenching. The amount of incoming light that is regulated away from photosynthetic processes in order to reduce damage to the plant. |
| **Phi2** | Quantum yield of Photosystem Il. This measurement is essentially the percentage of incoming light (excited electrons) that go into Photosystem Il. Photosystem Il is where most light energy is converted into food. |
| **PhiNO** | Ratio of incoming light that is lost via non-regulated processes. PhiNO is the combination of a number of unregulated processes whose by-products can inhibit photosynthesis or be harmful to the plant. (Kuhlgert et al., 2016) |
| **PhiNPQ** | Ratio of incoming light that goes towards non-photochemical quenching. The plant regulating excess energy in such a way as too reduce damage to the plant. (Kuhlgert et al., 2016) |

**Table 2.4.** Parameters measured with the MultispeQ V 2.0 device.

### 2.2.9 Morphological and Physiological Data Analysis

Statistically significant differences between groups were determined, for both morphological and physiological analyses, with analysis of variance (ANOVA, p-value < 0.05). Combining the microbial-based product in stressed condition with silicon dioxide or chitosan-tripolyphosphate NPs, three-way ANOVA was used to better understand the contribution of each one of the considered variables in determining, if present, the significant differences and their possible interaction. Two-way ANOVA was instead used to analyze the contribution of nanoparticles (silicon dioxide or chitosan-tripolyphosphate NPs) and the microbial product in non-stressed conditions. Pairwise multiple comparisons were also performed using Tukey's HSD test. Micro and macronutrients contents of plant tissues were visualized using principal component analysis (PCA) based on a correlation matrix. Before being displayed with PCA, the data were normalized by dividing all the values in each column of the worksheet by the maximum value of each to obtain values ranging from 0 to 1. The analyses were performed with R software version 4.3.1 using the ggplot2 (Wickham, 2016), car (Fox J., Weisberg S., 2019) and factoextra (Kassambara A., Mundt F., 2020) packages.

# 3 Results

## 3.1 Field Trial: *Triticum durum* L. (cv. Svevo) and *Triticum aestivum* L. (cv. Bramante)

### 3.1.1 Screening of Primers for Specific Amplification of Strains

In the first phase of the work, a literature search and *in silico* sequence analyses were performed to find primer pairs specific for all the designed target bacteria. The specificity of the selected primers has been assessed in a two-phase process. At first End-Point PCR analyses were conducted on DNA extracted from the bacterial pellets of MC_C, collected as previously described, and the amplification products visualized through agarose gel electrophoresis. On a total of about 90 primer pairs tested, 63.3% provided no amplification and about 30% proved to be non-specific giving amplifications for more than one bacterial species. In a second step, the selected primers were tested in real time PCR confirming the preliminary results. Finally, a set of primer pairs was identified to be specific for *B. ambifaria* (Bamb1196, Bamb3350, Bamb4475), (rpsj) and *R. aquatilis* (Raq4) (**Table 3.1**).

### 3.1.2 Qualitative Test on DNA Extracted from Soil

Preliminary tests were carried out to determine the applicability of the traceability method for detecting the MC_C bacterial strains in soil samples. For this purpose, samples were prepared by spiking the MC_C powder into the soil at the percentages of 10%, 5%, and 2.5% (W/W). Real Time PCR analyses with the selected primers, Raq4, rpsj, Bamb1196, Bamb4475, and Bamb3350, provided promising results allowing easy detection of microorganisms with a threshold cycle (CT) $\leq$ 24. Although all three primer pairs specific for *Burkholderia ambifaria* successfully identified their target, Bamb3350 was selected to conduct all subsequent analyses since the recorded CT values were lower than those of the other two. A confirmatory test was performed on DNA extracted from the rhizosphere of seedlings of two varieties of wheat (cv. Svevo and cv. Bramante) from the experimental agricultural field at farm Podere Stuard. Samples, for the conditions (i) AMF + MC_C and (ii) AMF + biochar + MC_C, were collected six days after planting, and qtPCR analyses demonstrated the effectiveness of the detection method. **Figure 3.1** displays the melting curves obtained from the qtPCR analyses performed on the rhizospheric soil samples of the cultivar Svevo. As can be seen, the primers were effective in recognizing their targets in the samples mixed with the powdered MC_C without any amplification in the case of the control, untreated samples. The only exception concerns the rpsj primer pair, indeed, an amplification can be observed in the control sample although after a considerable number of cycles.

| Target Species | Primer Name | Sequence | Tm | Reference | Reference Genome |
|---|---|---|---|---|---|
| *R. aquatilis* | Raq4 | Fw: 5′-CTCCAAACTGGTGCTGGAAG-3′<br>Rev: 5′-CAGCAGTTCCTGGGAGTTTG-3′ | 85.00°C | UNIPR laboratory | ASM24195v1 (strain CIP 7865) |
| *B. amyloliquefaciens* | rpsj | Fw: 5′-ATCTGGTCCGATTCCGTTGCCG-3′<br>Rev: 5′-TGGTGTTGGGTTCACAATGTCG-3′ | 79.00°C | *Ramkumar et al. (2013)* | ASM1939692v1 (strain GKT04) |
| | Bamb 1196 | Fw: 5′-CTGCGTTACACCGTCTTCG-3′<br>Rev: 5′-AAGTGGTCGCAATAGGCATC-3′ | 86.50°C | | |
| *B. ambifaria* | Bamb 3350 | Fw: 5′-ACCCGTATCCAGCAGACCTT-3′<br>Rev: 5′-GTGCATGAACTCGACCGTCT-3′ | 87.00°C | *Chapalain et al. (2013)* | ASM1612775v1 (strain FDAARGOS_1027) |
| | Bamb 4475 | Fw: 5′-CTACGTGAACCAGACGCTTG-3′<br>Rev: 5′-TCGACGAGTACGACGAGTTG-3′ | 87.50°C | | |

**Table 3.1.** List of primer pairs selected for the analysis of bacterial strains of MC_C. Efficiency (E) and $R^2$ were averaged on all standard curves (dilutions ranging from $10^5$ to $10^1$ GEs) used for soil sample quantification. Tm: melting temperature of the amplicon; E: PCR efficiency, calculated as $E = 10^{-1/slope} - 1$; $R^2$: coefficient of determination; Nt: not tested. Reference genome was used to calculate Genome Equivalents (GEs) $ng^{-1}$ DNA.

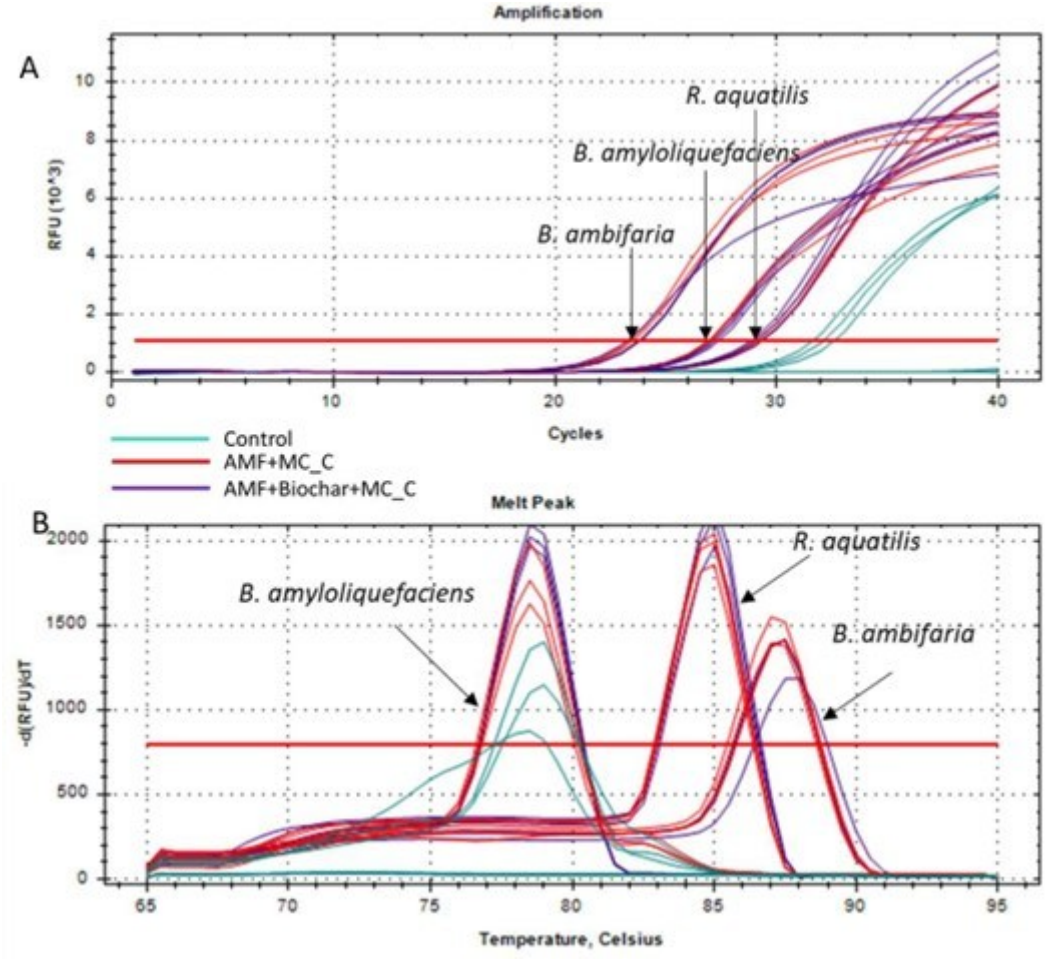


**Figure 3.1.** Test for the detection of *B. ambifaria*, *B. amyloliquefaciens,* and *R. aquatilis* in soil samples collected from the rhizosphere of wheat cv. Svevo six days after the sowing. (A) Amplification chart displays the relative fluorescence units (RFU) at every cycle. (B) Melting curves obtained based on the dissociation of amplicons in a temperature range of 65–95°C. Three replicates were performed for each sample. Horizontal red line represents the fluorescence threshold.

### 3.1.3 Wheat Field Trial: Weather Conditions

For the entire duration of the field trial meteorological parameters were collected from the computerized weather station installed near the site of the agricultural experiment, at San Pancrazio (Parma, Italy). Daily average air temperature (°C), daily average relative air humidity (%) and daily cumulative precipitation (mm) recorded over the collection period of rhizospheric soil samples (22 March 2024 - 5 May 2023) are reported in **Figure 3.2**. The total recorded precipitation was 72.9 mm and the average air temperature value was 12.7°C, the lowest value being 6.1°C and the highest corresponding to 16.6°C.

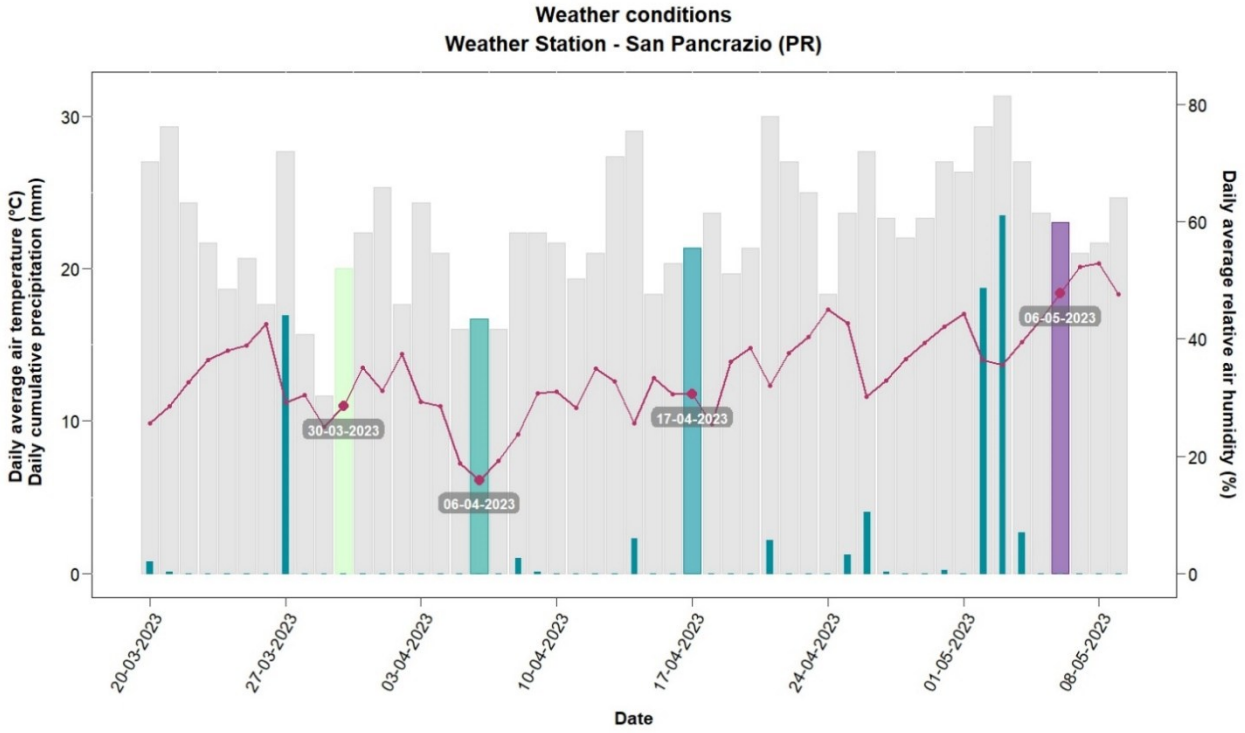


**Figure 3.2.** Graphic representation of the weather parameters daily detected by an automatic computerized weather station installed close to the experimental field (San Pancrazio, Parma) during the sampling period (22 March 2023 – 5 May 2023). The gray-colored histograms indicate the daily average relative humidity (%); the red line represents the daily average air temperature (◦C); and the blue-colored histograms instead the cumulative precipitation (mm). The colored histograms correspond to the sampling days whose dates are indicated by the labels.

### 3.1.4 Wheat Field Trial: Quantification of DNA from Microbial Species in Soil Samples

Real Time PCR analyses were performed on soil samples collected from the rhizosphere of the two wheat cultivars, cv. *Svevo* and cv. *Bramante*, over the spring 2023 at 8 (T1), 15 (T2), 26 (T3) and 44 (T4) days after the second addition of the MC_C. **Figure 3.3** presents boxplots constructed with the quantification values, expressed in GEs, obtained by interpolation with standard curves for all the three targeted bacteria *B. ambifaria*, *B. amyloliquefaciens,* and *R. aquatilis*. The results obtained delineate a common growth trend among the three bacteria, with a small amplification occurring in the untreated soil samples, although at very low levels when compared to the samples fortified with MC_C. However, the statistical differences between the treated and non-treated samples were found to be significant, as reported in **Table 3.2** in which all the statistical comparisons between the samples are reported.

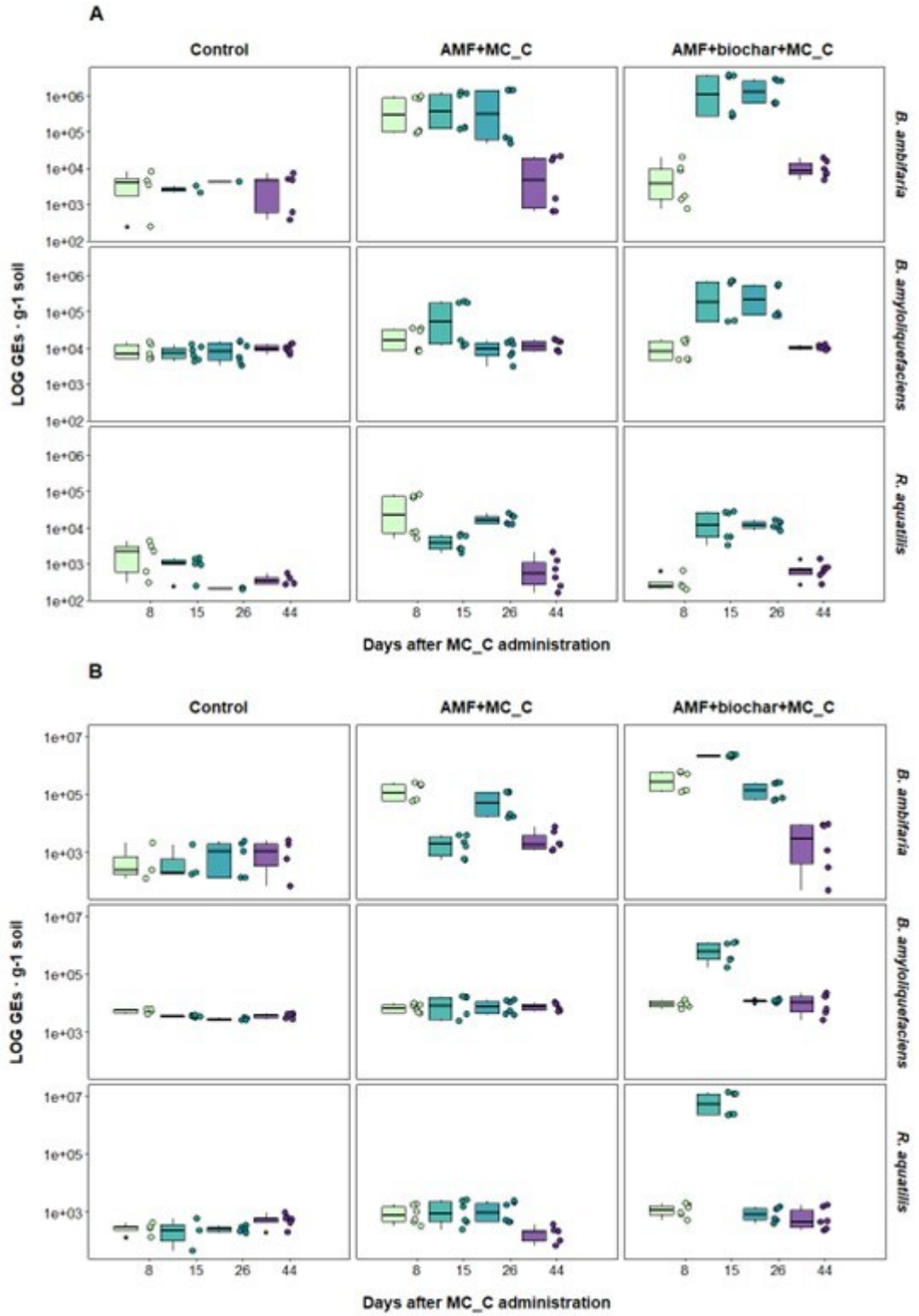


**Figure 3.3.** DNA quantification expressed in GEs of *B. ambifaria*, *B. amyloliquefaciens*, and *R. aquatilis* in rhizospheric soil samples collected over the period 30 March - 5 May. Data are visualized through boxplots elaborated with R Studio software version 4.3.1. Boxplots are based on the quantification data (GEs) of all the Real Time PCR replicates derived by CFX Maestro™ Software (Biorad) via interpolation with standard curves. Comparison of GEs values of *B. ambifaria*, *B. amyloliquefaciens*, and *R. aquatilis* for the three considered conditions: (i) control, without any treatments; (ii) AMF + MC_C; and (iii) AMF + biochar + MC_C for the wheat cv. Bramante (**A**) and cv. Svevo (**B**).

| | AMF + MC_C All Times | AMF + Biochar + MC_C All Times | AMF + MC_C T2, T3, T4 | AMF + Biochar + MC_C T2, T3, T4 |
|---|---|---|---|---|
| | | ***B. ambifaria* – Bramante** | | |
| **CTR All Times** | $2.92 \times 10^{-10}$ **** | $7.81 \times 10^{-9}$ **** | 0.000350 *** | $8.39 \times 10^{-6}$ **** |
| **CTR T2, T3, T4** | | 0.66514 NS | | 0.17311 NS |
| **AMF + MC_C all times** | | | | |
| **AMF + MC_C T2, T3, T4** | | | | |
| | | ***B. ambifaria* - Svevo** | | |
| **CTR All Times** | 0.00367 ** | 0.00010 *** | 0.02886 * | 0.00059 *** |
| **CTR T2, T3, T4** | | 0.00730 ** | | 0.01732 NS |
| **AMF + MC_C all times** | | | | |
| **AMF + MC_C T2, T3, T4** | | | | |
| | | ***B. amyloloquefaciens* - Bramante** | | |
| **CTR All Times** | 0.00998 ** | 0.00029 *** | 0.04268 * | $1.21 \times 10^{-5}$ **** |
| **CTR T2, T3, T4** | | 0.05269 NS | | 0.00502 ** |
| **AMF + MC_C all times** | | | | |
| **AMF + MC_C T2, T3, T4** | | | | |
| | | ***B. amyloloquefaciens* - Svevo** | | |
| **CTR All Times** | 0.00170 ** | $2.70 \times 10^{-5}$ **** | 0.00568 ** | 0.00014 *** |
| **CTR T2, T3, T4** | | 0.00239 ** | | 0.00553 ** |
| **AMF + MC_C all times** | | | | |
| **AMF + MC_C T2, T3, T4** | | | | |

**Table 3.2** *P values* obtained from pairwise comparison conducted by ANOVA. T2, T3, and T4 correspond to the samples collected at 15, 26, and 44 days after MC_C administration. NS = Not Significant ($p > 0.05$), * $p \leq 0.05$, ** $p \leq 0.01$, *** $p \leq 0.001$, **** $p \leq 0.0001$.

| | AMF + MC_C All Times | AMF + Biochar + MC_C All Times | AMF + MC_C T2, T3, T4 | AMF + Biochar + MC_C T2, T3, T4 |
|---|---|---|---|---|
| | | ***R. aquatilis* – Bramante** | | |
| **CTR All Times** | 0.00442 ** | 0.01267 * | 0.00028 ** | 0.00018 *** |
| **CTR T2, T3, T4** | | | | |
| **AMF + MC_C all times** | | 0.62860 NS | | 0.77247 NS |
| **AMF + MC_C T2, T3, T4** | | | | |
| | | ***R. aquatilis* - Svevo** | | |
| **CTR All Times** | 0.04419 * | 0.00042 *** | 0.00226 ** | 0.00018 *** |
| **CTR T2, T3, T4** | | | | |
| **AMF + MC_C all times** | | 0.00247 ** | | 0.00282 ** |
| **AMF + MC_C T2, T3, T4** | | | | |

**Table 3.2.** *P values* obtained from pairwise comparison conducted by ANOVA. T2, T3, and T4 correspond to the samples collected at 15, 26, and 44 days after MC_C administration. NS = Not Significant ($p > 0.05$), * $p \leq 0.05$, ** $p \leq 0.01$, *** $p \leq 0.001$, **** $p \leq 0.0001$.

Despite the general trend, some differences can be highlighted. According to the quantification data of the bacterium *B. ambifaria* in the rhizosphere of the wheat cultivar Bramante, its growth increased up to day 26 (T3) and then decreased rapidly. For the condition AMF + biochar + MC_C, after 15 days since the addition of MC_C to the soil (T2), the maximum average value of GEs correspondent to $1.90 \times 10^6$ was recorded. In the presence of AMF + MC_C, instead, the maximum average value of $7.32 \times 10^{-5}$ GEs was reached at 26 days (T3). The values of $1.90 \times 10^6$ GE$s$ and $1.64 \times 10^6$ GE$s$ were respectively quantified at 15 (T2) and 26 days (T3) for the AMF + biochar + MC_C condition, showing a higher growth rate than in the presence of the AMF + MC_C in the same time interval ($T2 = 6.36 \times 10^{-5}$ GE$s$; $T3 = 7.32 \times 10^{-5}$ GE$s$), although this difference was statistically not significant with a *p value* of 0.66514.

Quantification of *B. ambifaria* DNA in soil samples collected in the rhizosphere of wheat cv. *Svevo* outlined a growth trend similar to that already described with a sudden decrease at T2 that can be considered accidental. In addition, the combination of AMF + biochar + MC_C induced a statistically significant bacterial growth compared to the AMF + MC_C combination ($p\ value\ = 0.00730$).

The growth tendency of *B. amyloliquefaciens* in the rhizosphere of the Bramante wheat variety amended with AMF + biochar + MC_C is comparable to that of *B. ambifaria* under the same condition. Nevertheless, the maximum average value of GEs at T2 $(3.63 \times 10^5)$ and at T3 $(3.09 \times 10^5)$ were lower than those observed for the bacterium *B. ambifaria* (T2 =$1.90 \times 10^6$ GE$s$ and T3 = $1.64 \times 10^6$ GE$s$). Comparing the full data set the differences between the AMF + MC_C and AMF + biochar + MC_C treatments were not statistically significant (p = 0.05269). On the other hand, the differences between the two treatments became significant when considering only the quantification values detected at times T2, T3 and T4 (p = 0.00502).

The growth of *B. amyloliquefaciens* in the rhizosphere of wheat cv. Svevo was rather limited, with a maximum average value of $3.63 \times 10^5$ GEs detected at T2. The quantification values detected in soil fortified with AMF and MC_C and/or biochar were, however, higher than those untreated soil with *p values* of 0.00170 and $2.7 \times 10^5$ respectively. Significant differences were also revealed between the values observed for AMF + MC_C and AMF + biochar + MC_C when comparing the quantification values of the whole data set or only times T2, T3, and T4 (p = 0.00239 and p = 0.00553).

Once MC_C was supplemented to the Bramante wheat variety, *R. aquatilis* reached a maximum growth at T2 in the presence of AMF + MC_C, with an average value of $1.72 \times 10^4$ GEs. Even though the growth was limited, the GEs were significantly higher as compared to the control (p =

0.04419). In this case, the differences between the conditions AMF + MC_C and AMF + biochar + MC_C were not significant (p = 0.62860) when comparing T2, T3, and T4 only (p = 0.77247).

Quantification of the bacterium *R. aquatilis* in the soil of the cultivar Svevo showed a significant increase in GEs following the addition of AMF + biochar + MC_C compared with AMF + MC_C alone, for all the sampling times or only T2, T3 and T4 with *p values* of 0.00247 and 0.00282, respectively. After 15 days (T2), the amount of DNA of the *R. aquatilis* bacterium was found to be more than 100 times as high as other samples, so it was considered an outlier and was excluded from further analyses. GEs in the presence of AMF + biochar + MC_C were slightly higher than those in the presence of AMF + MC_C, as revealed by the mean and median ratio between these two conditions (1.09839 and 1.13917, respectively). Although the evidenced differences, there was no statistical significance (p = 0.08138) (**Table 3.3**).

| | **Average** | **Median** |
|---|---|---|
| | *B. ambifaria* | |
| Bramante All times | 0.97107 | 1.04763 |
| Bramante T2, T3, T4 | 1.10424 | 1.13713 |
| Svevo All times | 1.26138 | 1.34574 |
| Svevo T2, T3, T4 | 1.31697 | 1.40049 |
| | *B. amyloliquefaciens* | |
| Bramante All times | 1.09267 | 1.12214 |
| Bramante T2, T3, T4 | 1.15601 | 1.15881 |
| Svevo All times | 1.12783 | 1.03542 |
| Svevo T2, T3, T4 | 1.15195 | 1.00520 |
| | *R. aquatilis* | |
| Bramante All times | 0.97500 | 0.96419 |
| Bramante T2, T3, T4 | 1.01943 | 1.01178 |
| Svevo All times | 1.43474 | 1.15627 |
| Svevo Excluding T2 | 1.09839 | 1.13917 |
| Svevo T2, T3, T4 | 1.56841 | 1.20323 |

**Table 3.3.** Average and median ratio between bacterial GEs quantified in the soil samples treated with AMF + biochar + MC_C and AMF + MC_C. T2, T3, and T4 correspond to the samples collected at 15, 26, and 44 days after MC_C administration. Average: $\overline{X} = \sum_{i=1}^{n} x_i \cdot n^{-1}$. Median: value that occupies the central position in the data set.

## 3.2 Greenhouse Experiment: *Solanum lycopersicum* L. and *Glycine max* L.

### 3.2.1 Characterization of Silicon Dioxide and Chitosan-Tripolyphosphate Nanoparticles

Through the characterization analyses conducted as described above in section 2.2.4 of *Materials and Methods* chapter, the surface charge and the size of $SiO_2$ NPs aggregates were evaluated using DLS and determination of the Zeta potential in deionized water suspensions (pH 7). **Table 3.4** reports the size of the particles, their purity, the percentage of the element within the molecule, the values of hydrodynamic diameter (DH) and Zeta potential (ζ). Additionally, **Figure 3.4** shows the images obtained via TEM of the two nanoparticles used in this work.

| NPs | Size (nm) | Purity (%) | (ζ)-Z Potential (mV) | (DH) Hydrodynamic Range (nm) |
|---|---|---|---|---|
| *$SiO_2$ NPs* | <20 | 99.5 | -27.0 | 399 |

**Table 3.4.** Characterization of $SiO_2$ NPs used in this work: particle size (nm), purity (%), Zeta potential (ζ) (mV), hydrodynamic range (dh) (nm), percentage of elements in in deionized water suspension at pH=7.

The surface charge and the size of Ch/TPP NPs aggregates were evaluated using DLS and determination of the Zeta potential in suspension in acetic acid (0.2%, pH 4.7), as previously described. The Z Potential (ζ) measured corresponds to 34.51 mV, while the Hydrodynamic diameter (DH) was estimated to be 193.3nm. In **Figure 3.4** are reported images taken via Trasmission Electron Microscope (TEM).

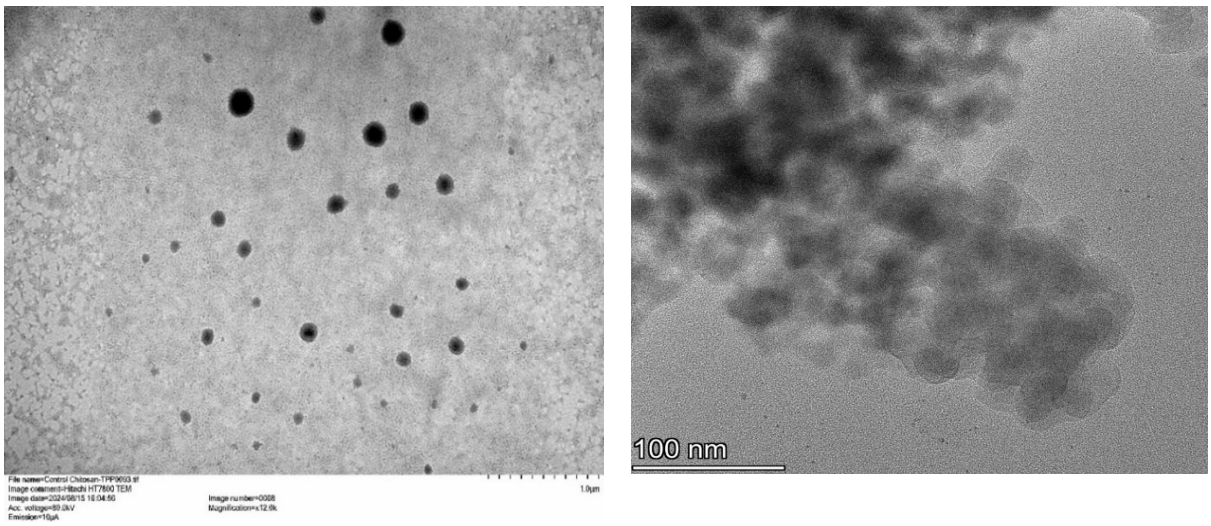


**Figure 3.4.** Trasmission Electron Microscope (TEM) images of Ch/TPP NPs (on the left) and $SiO_2$ NPs (on the right).

### 3.2.2 Morphological Parameters of Interest: *Solanum lycopersicum L.*

As described in detail in the *Materials and Methods* section, upon sampling of cherry tomato plants a set of morphological parameters indicative of their health and agricultural yield were recorded. The use of nanoparticles strongly influenced the fresh weight of roots and shoots of tomato plants. In particular, as can be observed in **Figure 3.5** regarding the fresh weight of the plants, comparing the group comprising the plants untreated and treated only with PGPR with the two groups formed by the treatments based on (i) Ch/TPP NPs and (ii) $SiO_2$ NPs alone or in combination with the microbial consortium, the values seem to be significantly different and lower in the case of nanoparticles addition.

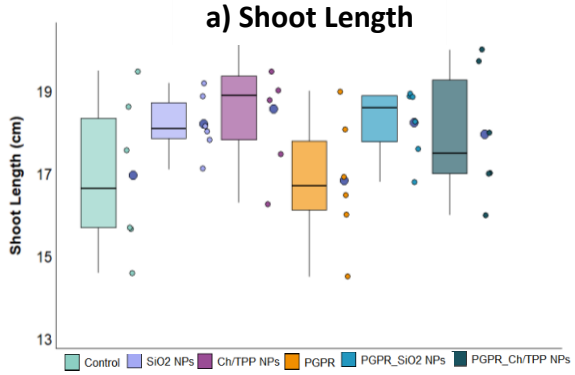


| | F value | *P value* |
|---|---|---|
| ***NPs*** | 8.949 | **0.000989** |
| ***PGPR*** | 2.656 | 0.114379 |
| ***NPs*PGPR*** | 2.213 | 0.128162 |

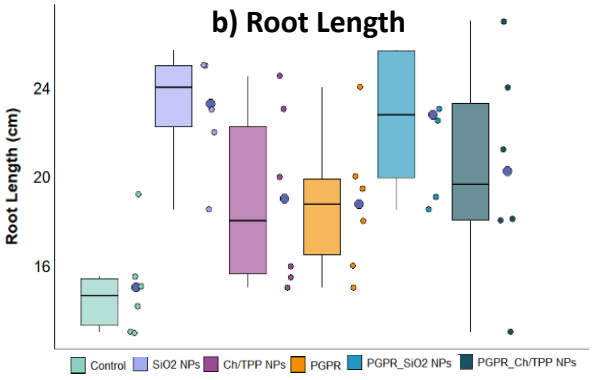


| | F value | *P value* |
|---|---|---|
| ***NPs*** | 3.377 | **0.0497** |
| ***PGPR*** | 0.047 | 0.8298 |
| ***NPs*PGPR*** | 0.028 | 0.9723 |

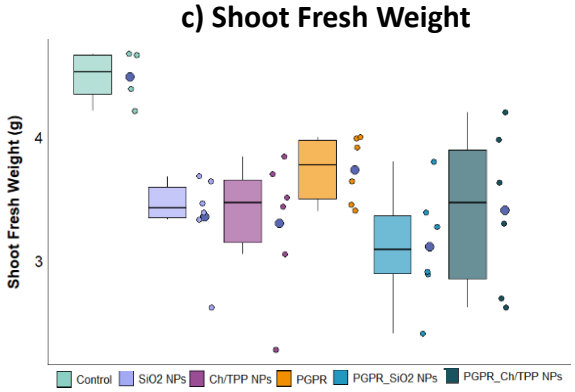


| | F value | *P value* |
|---|---|---|
| ***NPs*** | 3.577 | **0.0404** |
| ***PGPR*** | 0.242 | 0.6265 |
| ***NPs*PGPR*** | 0.171 | 0.8433 |

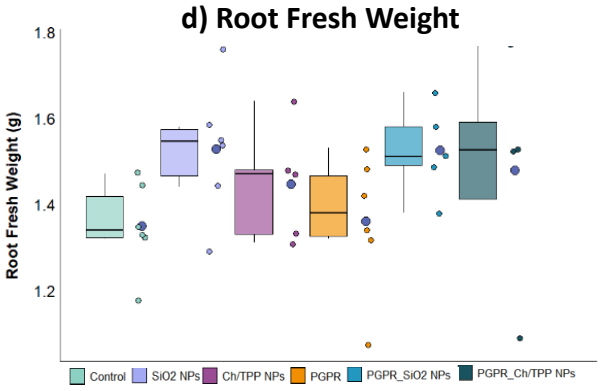


| | F value | *P value* |
|---|---|---|
| ***NPs*** | 8.778 | **0.000997** |
| ***PGPR*** | 1.557 | 0.221701 |
| ***NPs*PGPR*** | 1.055 | 0.360803 |

**Figure 3.5 (on the previous page).** Graphical representation of the parameters measured for tomato plants upon harvesting: Shoot length (**a**), Root length (**b**), Shoot fresh weight (**c**), Root fresh weight (**d**). The boxplots were constructed based on biological replicates subjected to the same treatment with the bigger violet dot indicating the average value of each plant group. In the tables below the charts are reported the *F values* and the *P values* derived from the two-way Analysis of Variance (ANOVA), with values below the significance threshold (*P values* < 0.05) in bold. The significance of the differences was assessed by Tukey's HSD (Honestly Significant Difference).

Conversely, by comparing these same groups, it is apparent that both types of nanoparticles result in a significant increase in the length of plant shoots. The $SiO_2$ NPs treatment was proved to be decisive also in inducing root growth, determining a major length and fresh weight of the radical system with respect to the group consisting of untreated and PGPR-treated plants.

During the greenhouse experiment, some morphological parameters have been recorded at two different times: (i) two weeks and (ii) four weeks after the transplantation. Examining the plant height values reported in **Figure 3.6**, it can be inferred that there is no positive effect due to the action of nanoparticles, whether used alone or in combination with PGPR. The only significant difference is the reduction in height of plants treated only with PGPR compared with the average height of untreated plants. This difference, slightly visible two weeks after transplanting, becomes more pronounced at the second time of data collection.

The treatments exerted no positive action on leaf number, which remains higher in untreated plants for both times considered. Instead, during the fourth week, a decreasing effect on the number of leaves of the nanoparticle-treated plants can be observed. This effect becomes significant when comparing the group of plants untreated or treated only with PGPR with the two groups of plants treated with $SiO_2$ NPs and Ch/TPP alone or in association with the microbial consortium.

In general, after two weeks, untreated plants produced more flowers than treated ones. The difference appears particularly marked when comparing this number with the average number of flowers produced by plants treated with (i) Ch/TPP NPs alone or (ii) in combination with the microorganisms, or even with (iii) plants treated with the microorganisms alone that produced no flowers at the first date of measurements' recording. On the last week, it appears that the addition of PGPR may contribute to reduced flowering of plants treated with the PGPR alone or in combination with $SiO_2$ NPs; however, this effect cannot be considered significant and requires further confirmatory investigation.

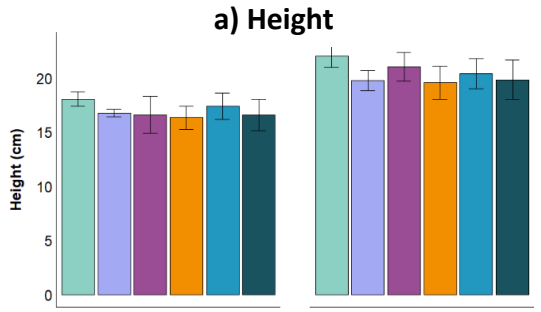


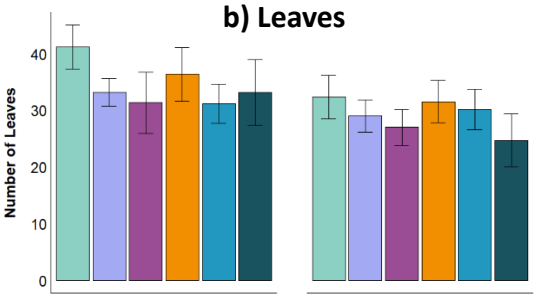


| | Week 2 | | Week 4 | |
|---|---|---|---|---|
| | **F value** | ***P value*** | **F value** | ***P value*** |
| ***NPs*** | 0.338 | 0.7161 | 0.837 | 0.4430 |
| ***PGPR*** | 2.162 | 0.1522 | 4.863 | **0.0352** |
| ***NPs*PGPR*** | 3.649 | **0.0386** | 3.761 | **0.0349** |

| | Week 2 | | Week 4 | |
|---|---|---|---|---|
| | **F value** | ***P value*** | **F value** | ***P value*** |
| ***NPs*** | 8.372 | **0.00129** | 5.361 | **0.011** |
| ***PGPR*** | 0.296 | 0.59024 | 1.318 | 0.261 |
| ***NPs*PGPR*** | 0.685 | 0.51171 | 0.247 | 0.783 |

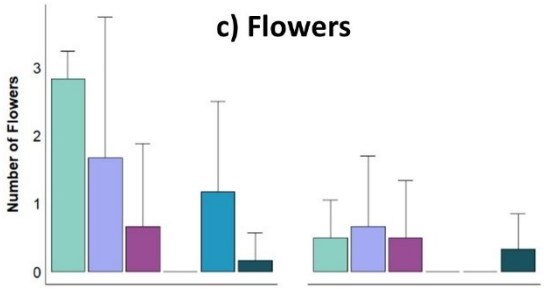


| | Week 2 | | Week 4 | |
|---|---|---|---|---|
| | **F value** | ***P value*** | **F value** | ***P value*** |
| ***NPs*** | 3.064 | 0.06155 | 0.214 | 0.8083 |
| ***PGPR*** | 11.255 | **0.00217** | 4.571 | **0.0408** |
| ***NPs*PGPR*** | 4.170 | **0.02523** | 0.500 | 0.6115 |

**Figure 3.6:** Graphical representation of the morphological parameters recorded for tomato plants (i) two weeks and (ii) four weeks after the transplantation: Height (**a**), Leaves (**b**), Flowers (**c**). The histograms were constructed based on the average values of the biological replicates subjected to the same treatment. The standard deviations are reported for each values group. In the tables below the charts are reported the *F values* and the *P values* derived from the two-way Analysis of Variance (ANOVA), with values below the significance threshold (*P values* < 0.05) in bold. The significance of the differences was assessed by Tukey's HSD (Honestly Significant Difference).

### 3.2.3 Morphological Parameters of Interest: *Glycine max* L.

Looking at **Figure 3.7**, it can be noticed that treatment with $SiO_2$ nanoparticles exerts a positive effect on the fresh weight of the roots, regardless of salt stress application. This effect is confirmed to be statistically significant when comparing the group of data obtained from the plants treated with $SiO_2$ NPs grown under optimal and salt stress conditions with two distinct groups: (i) one comprising the roots' fresh weight of stressed and non-stressed control plants, and (ii) the second one that includes

the values derived from plants supplemented with $SiO_2$ nanoparticles and PGPR for both the growth conditions. When plants are exposed to salt stress, it appears that $SiO_2$ NPs also positively affect the fresh weight of their shoots. Under optimal growth conditions, on the other hand, the shoots of PGPR-treated plants show higher weight values. In either case, however, statistical comparisons have not enlightened relevant differences from other treatments. The same trend of increased fresh weight determined by the microbial consortium is also found when considering pods, but in the case of plants subjected to salt stress. In fact, under salt stress conditions, the cluster of microorganism-based treatments, alone and in combination with $SiO_2$ NPs, results in a statistically higher fresh pod weight than that derived for the cluster formed by the control plants and treated with $SiO_2$ NPs alone.

None of the applied treatments markedly altered plants root length. However, the addition of $SiO_2$ nanoparticles led to contrasting results in terms of shoot length. Under non-stressed conditions, these values increased due to the addition of $SiO_2$ NPs, while a reducing effect occurred when salt stress was applied.

The concomitance of salt stress and treatment with PGPR contributes to higher dry weight values of the pods, independently of the use of nanoparticles. The dry weight of the pods collected from the group of plants treated with the PGPR, either alone or mixed with the $SiO_2$ NPs, is greater than (i) that of the equally treated but unstressed plants, or of the values obtained for the pods of plants untreated or administered with $SiO_2$ NPs and grown under normal conditions (ii) or under the influence of the abiotic stress (iii). In the case of root and shoot dry weight, on the other hand, it is the interaction of $SiO_2$ NPs and PGPR that has the strongest incidence in determining higher weights. The cluster of plants treated with the $SiO_2$ NPs alone and together with the microorganisms exhibits higher values of root dry weight if compared to the cluster of plants untreated or treated with the microbial consortium alone. In the case of shoots, on the other hand, it seems that control and PGPR-treated plants tend to have considerably lower dry weight values subjected to abiotic stress and not treated with the nanoparticles.

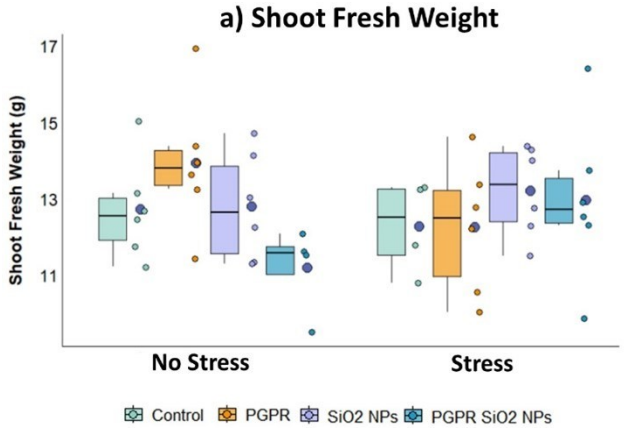


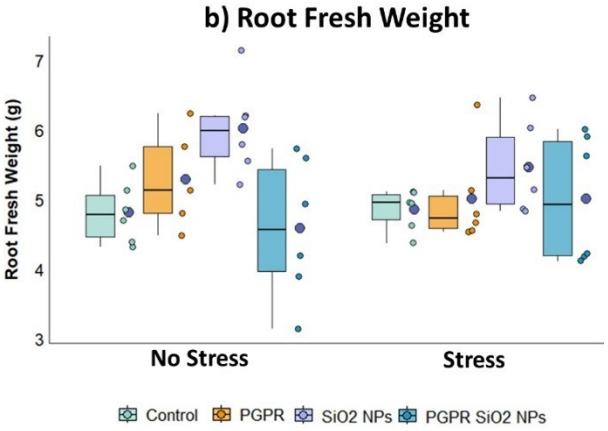


| | F value | *P value* |
|---|---|---|
| ***Stress*** | 0.027 | 0.8699 |
| ***NPs*** | 0.139 | 0.7112 |
| ***PGPR*** | 0.036 | 0.8513 |
| ***Stress* NPs*** | 4.361 | **0.0439** |
| ***Stress* PGPR*** | 0.012 | 0.9126 |
| ***NPs*PGPR*** | 2.535 | 0.1201 |
| ***Stress* NPs* PGPR*** | 1.846 | 0.1827 |

| | F value | *P value* |
|---|---|---|
| ***Stress*** | 0.163 | 0.68819 |
| ***NPs*** | 1.959 | 0.16950 |
| ***PGPR*** | 2.598 | 0.11509 |
| ***Stress* NPs*** | 0.003 | 0.96024 |
| ***Stress* PGPR*** | 0.812 | 0.37314 |
| ***NPs*PGPR*** | 8.918 | **0.00486** |
| ***Stress* NPs* PGPR*** | 0.163 | 0.68819 |

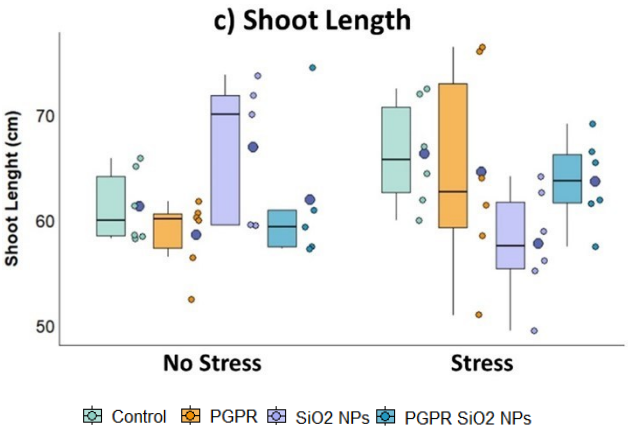


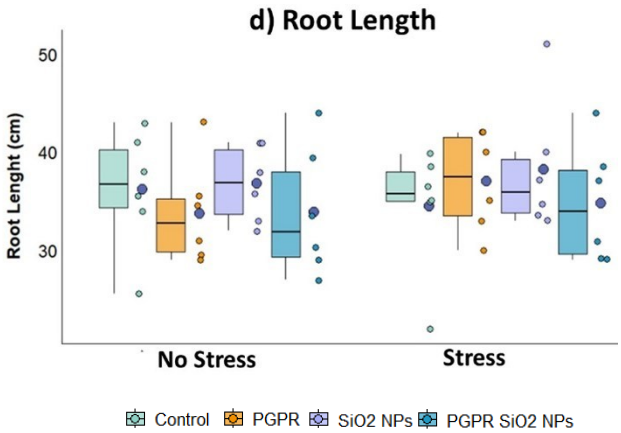


| | F value | *P value* |
|---|---|---|
| ***Stress*** | 0.383 | 0.539 |
| ***NPs*** | 0.034 | 0.856 |
| ***PGPR*** | 0.155 | 0.696 |
| ***Stress* NPs*** | 6.637 | **0.014** |
| ***Stress* PGPR*** | 2.682 | 0.110 |
| ***NPs*PGPR*** | 0.650 | 0.425 |
| ***Stress* NPs* PGPR*** | 1.969 | 0.169 |

| | F value | *P value* |
|---|---|---|
| ***Stress*** | 0.331 | 0.568 |
| ***NPs*** | 0.115 | 0.737 |
| ***PGPR*** | 0.858 | 0.360 |
| ***Stress* NPs*** | 0.015 | 0.904 |
| ***Stress* PGPR*** | 0.428 | 0.517 |
| ***NPs*PGPR*** | 0.914 | 0.345 |
| ***Stress* NPs* PGPR*** | 0.668 | 0.418 |

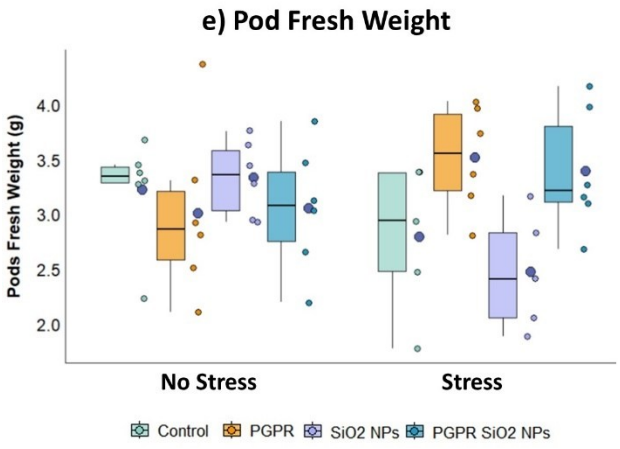


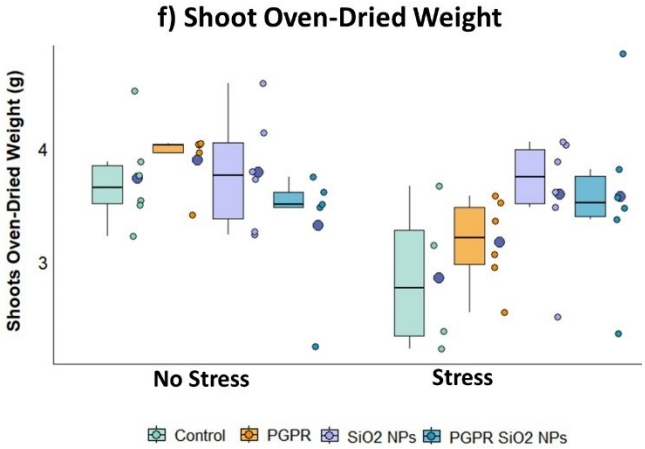


| | F value | *P value* |
|---|---|---|
| ***Stress*** | 0.192 | 0.664 |
| ***NPs*** | 0.126 | 0.725 |
| ***PGPR*** | 2.428 | 0.127 |
| ***Stress* NPs*** | 0.753 | 0.391 |
| ***Stress* PGPR*** | 10.055 | **0.003** |
| ***NPs*PGPR*** | 0.037 | 0.848 |
| ***Stress* NPs* PGPR*** | 0.143 | 0.707 |

| | F value | *P value* |
|---|---|---|
| ***Stress*** | 4.485 | **0.0412** |
| ***NPs*** | 0.816 | 0.3723 |
| ***PGPR*** | 0.042 | 0.8386 |
| ***Stress* NPs*** | 5.303 | **0.0272** |
| ***Stress* PGPR*** | 0.702 | 0.4076 |
| ***NPs*PGPR*** | 2.084 | 0.1575 |
| ***Stress* NPs* PGPR*** | 0.184 | 0.6702 |

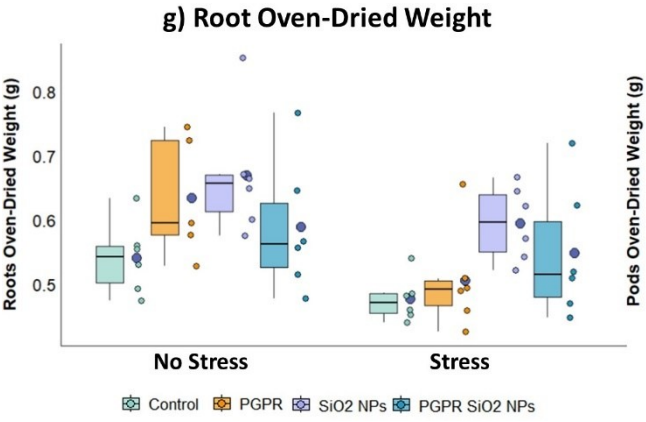


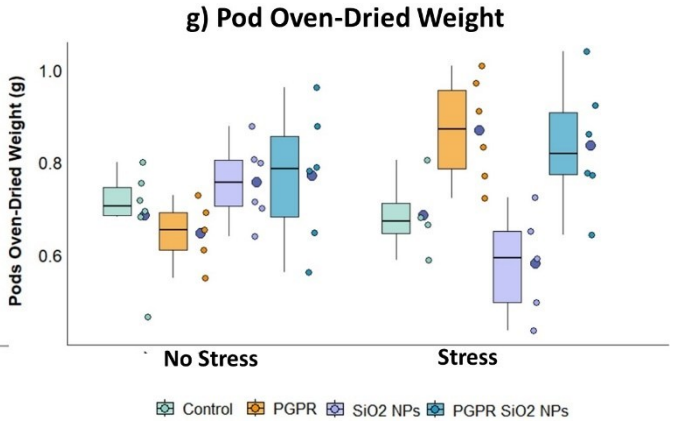


| | F value | *P value* |
|---|---|---|
| ***Stress*** | 9.946 | **0.0031** |
| ***NPs*** | 7.008 | **0.0116** |
| ***PGPR*** | 0.028 | 0.8690 |
| ***Stress* NPs*** | 0.523 | 0.4741 |
| ***Stress* PGPR*** | 0.051 | 0.8219 |
| ***NPs*PGPR*** | 6.603 | **0.0141** |
| ***Stress* NPs* PGPR*** | 1.065 | 0.3084 |

| | F value | *P value* |
|---|---|---|
| ***Stress*** | 1.238 | 0.27329 |
| ***NPs*** | 0.163 | 0.68887 |
| ***PGPR*** | 8.919 | **0.00505** |
| ***Stress* NPs*** | 5.443 | **0.02535** |
| ***Stress* PGPR*** | 11.429 | **0.00175** |
| ***NPs*PGPR*** | 0.795 | 0.37837 |
| ***Stress* NPs* PGPR*** | 0.018 | 0.89406 |

**Figure 3.7 (on the previous page).** Graphical representation of the parameters measured for soybean plants upon harvesting: Shoot fresh weight (**a**), Root fresh weight (**b**), Shoot length (**c**), Root length (**d**), Pod fresh weight (**e**), Shoot oven-dried weight (**f**), Root oven-dried weight (**g**), Pod oven-dried weight (**h**). The boxplots were constructed based on biological replicates subjected to the same treatment with the bigger violet dot indicating the average value of each plant group. In the tables below the charts are reported the *F values* and the *P values* derived from the three-way Analysis of Variance (ANOVA), with values below the significance threshold (*P values* < 0.05) in bold. The significance of the differences was assessed by Tukey's HSD (Honestly Significant Difference).

Once a week for the entire period of salt stress induction, some morphological parameters were recorded to monitor plants' salt stress perception and response. The graphical representation of these parameters is reported in **Figure 3.8.** Under optimal growth conditions, a higher average height value can be observed in the case of plants subjected to treatment with $SiO_2$ NPs, regardless of association with PGPR, than in untreated plants or plants treated with the microbial consortium alone, even if these differences cannot be considered significant. This trend remains constant over the three weeks of salt stress treatment. Under stress conditions, on the other hand, it appears that $SiO_2$ NPs does not exert the same effect; in fact, for all three times considered, the average heights of plants treated with $SiO_2$ NPs turn out to be lower, although not statistically, than the other average heights recorded.

During the first week, salt stress did not significantly alter the number of leaves, which remained constant for all treated and untreated plants. Similarly, it can be inferred that there is still no evidence of the effect of the applied treatments. At the end of the second week, conversely, the number of leaves is clearly and significantly reduced for the cluster of untreated and PGPR-only treated plants grown under optimal conditions if compared to the same cluster of stressed plants. Under salt stress conditions, the beneficial effect of $SiO_2$ NPs also emerges, which, independently of the combination with PGPR, are responsible for a significant increase in the number of leaves, compared to the cluster of untreated and PGPR-only treated plants grown under the same stress situation. At the third and final week, on the other hand, the variable that seems to have a greater incidence in influencing the number of leaves is precisely the induced salt stress that acts negatively by reducing the number of leaves for all treated and untreated plants.

Examining the number of buds counted during the first week, we can detect differences in plant behavior that could be due to the use of $SiO_2$ NPs, which under salt stress conditions would appear to increase bud production. However, this hypothesis has not been confirmed by statistics, probably because of the large dispersion of the data collected for the different biological replicates, which do not enable us to eliminate with certainty the effects of random variability.

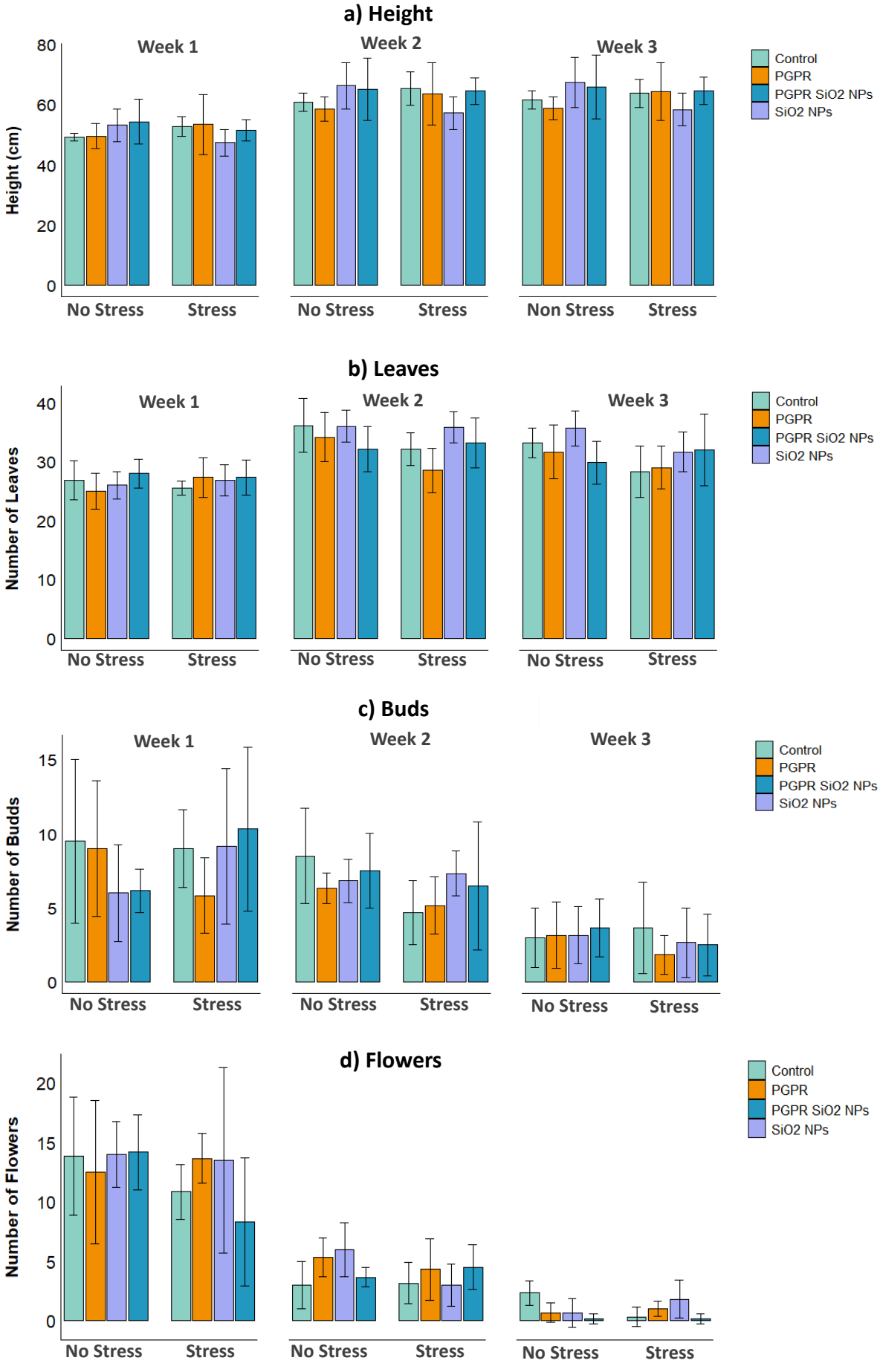
a) Height
Week 1
Week 2
Week 3
Height (cm)
0
20
40
60
80
No Stress
Stress
Non Stress
Control
PGPR
PGPR SiO2 NPs
SiO2 NPs
b) Leaves
Number of Leaves
0
10
20
30
40
c) Buds
Number of Budds
0
5
10
15
d) Flowers
Number of Flowers
0
5
10
15
20

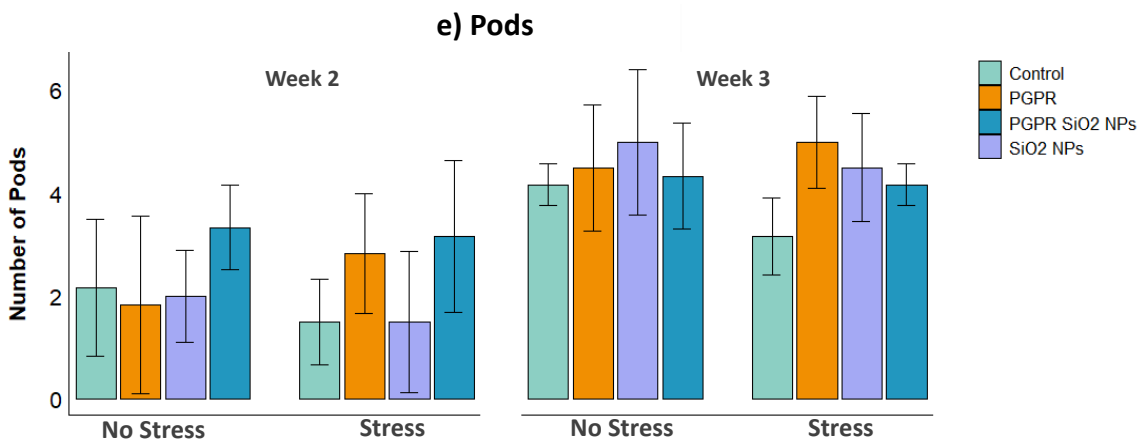


**Figure 3.8.** Graphical representation of the morphological parameters recorded once a week for soybean plants over the entire duration of the salt stress induction: Height (**a**), Leaves (**b**), Buds (**c**), Flowers (**d**), Pods (**e**). The histograms were constructed based on the average values of the biological replicates subjected to the same treatment. The standard deviations are reported for each values group. In the tables below the charts are reported the *F values* and the *P values* derived from the three-way Analysis of Variance (ANOVA), with values below the significance threshold (*P values* < 0.05) in bold. The significance of the differences was assessed by Tukey's HSD (Honestly Significant Difference).

Instead, the tendency of data collected during the second week proves the direct contribution of salt stress in reducing the average number of buds produced by all treated and untreated plants compared with normal budding conditions. At the third and final week, the number of buds appears constant for all plants with no significant difference.

During the first week, the number of flowers does not fluctuate significantly under optimal growth conditions. Under salt stress conditions, a certain degree of variability can be observed even if it does not support the assumption that there is a direct influence due to treatments rather than random fluctuations. During the second week, on the other hand, the number of flowers of untreated plants decreases slightly compared to treated plants although not statistically significantly. When the plants are subjected to salt stress, however, it appears that the addition of the PGPR in a manner independent of their association with nanomaterials induces the production of a higher average number of flowers. At the last recording of the measurements, the influence of salt stress seems to drastically reduce the number of flowers produced by untreated plants or by plants treated with the combination of $SiO_2$ NPs and PGPR with respect to normal flowering production.

Under optimal growth conditions, an increase in the number of pods produced by plants treated with the PGPR and $SiO_2$ NPs combination can be detected although this difference does not appear to be statistically significant. Regardless of the state of stress induced and perceived by plants, there seems in fact to be a direct influence of the PGPR in bringing an increment of observed values. The result of the comparison between (i) the group comprising the microorganism-based treatments, including

their association with nanoparticles, and (i) formed by the untreated plants or treated only with nanoparticles is considered significant, can confirm this assertion.

### 3.2.4 Photosynthetic Activity Monitoring: *Solanum lycopersicum L.*

Chlorophyll and carotenoid contents were measured at the end of the experiment, at the time of sampling, for all treatments considered. Visually, by examining **Figure 3.9**, it can be observed that the chlorophyll content is higher in plants treated with nanoparticles, whether Ch/TPP or $SiO_2$ NPs. This difference is confirmed by statistical analysis when comparing the two groups formed by (i) the untreated and PGPR-treated plants alone or combined with both types of nanoparticles and (ii) the nanoparticle-treated plants. Despite plants subjected to $SiO_2$ NPs treatment exhibit the maximum average value of chlorophyll content with respect to data obtained from plants treated with Ch/TPP NPs, the difference was proved to be not statistically significant.

Regarding carotenoid content, the trend remains almost unchanged, with the nanoparticle-treated plants showing higher values. Statistical analysis confirmed that the difference is significant when comparing the group of untreated plants and treated with PGPR alone with the group of plants treated with $SiO_2$ NPs with and without PGPR. Therefore, it can be inferred that, regardless of the association with PGPR, $SiO_2$ NPs treatment has an effect of increasing the average carotenoid content.

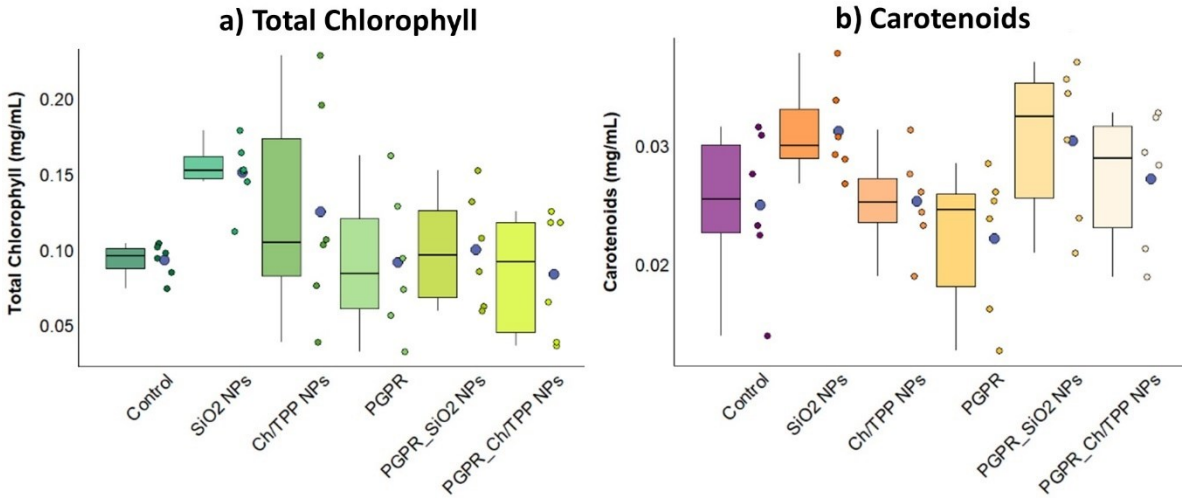


| | F value | *P value* |
|---|---|---|
| ***NPs*** | 1.800 | 0.1826 |
| ***PGPR*** | 4.631 | **0.0396** |
| ***NPs*PGPR*** | 1.088 | 0.3499 |

| | F value | *P value* |
|---|---|---|
| ***NPs*** | 5.051 | **0.0129** |
| ***PGPR*** | 0.097 | 0.7580 |
| ***NPs*PGPR*** | 0.534 | 0.5916 |

**Figure 3.9:** Graphical representation of the total chlorophyll and carotenoid content of tomato plants measured upon harvesting: Total Chlorophyll (**a**), Carotenoids (**b**). The boxplots were constructed based on biological

replicates subjected to the same treatment with the bigger violet dot indicating the average value of each plant group. In the tables below the charts are reported the *F values* and the *P values* derived from the three-way Analysis of Variance (ANOVA), with values below the significance threshold (*P values* < 0.05) in bold. The significance of the differences was assessed by Tukey's HSD (Honestly Significant Difference).

### 3.2.5 Photosynthetic Activity Monitoring: *Glycine max* L.

Photosynthetic activity of soybean plants was monitored throughout the experiment. Measurements collected in the first week of induced salt stress, as shown in **Figure 3.10**, highlighted some significant differences due to the treatments applied. Under stress conditions for example, Phi2, which represents the percentage of incoming light reaching Photosystem II, has shown to be significantly higher in plants treated with PGPR and $SiO_2$ NPs than in all other plants grown under the same conditions. The data obtained for stressed plants subjected to $SiO_2$ NPs treatment are also significantly lower than the values obtained for plants grown under optimal conditions to which PGPR, $SiO_2$ NPs or the combination of the two were administered. Even in the case of Light Intensity (PAR) there is a significant difference between stressed plants treated with PGPR and $SiO_2$ NPs and those administered only with PGPR whose values are significantly lower. A similar trend can also be observed for Linear Electron Flow (LEF) whose values, under stress conditions, are very low when comparing the group of untreated and PGPR-treated plants with that formed by plants treated with PGPR alone or in combination with $SiO_2$ NPs. In addition, PhiNPQ, that measures an excess of energy that could be devolved to reparation processes in plants, seems to reach maximum value for stressed plants treated with the $SiO_2$ NPs. The average of these values has been proved to be greater than those obtained from plants treated with (i) $SiO_2$ NPs alone or (ii) combined with PGPR in normal or (iii) stressed growth conditions. Finally, PhiNO, the rate of the incoming light lost via non-regulated processes, appears to be influenced directly by salt stress. The other parameters, such as NPQt and the SPAD, did not show significant differences due to the experimental treatments.

During the second and third week of salt stress induction only a few of the registered parameters displayed significant differences, the other trends remain constant with minor changes. The SPAD values collected in the second week, however, evidenced the positive effect of the addition of PGPR alone or in combination with the $SiO_2$ NPs exerted on stressed plants. The only significant difference can be found by comparing the group of untreated or $SiO_2$ NPs -treated plants grown under normal (i) or stressed conditions (ii). In the third week only PhiNO, similarly to the previous measurements, seems to respond to the applied salt stress with a maximum average value registered for stressed plants treated with PGPR.

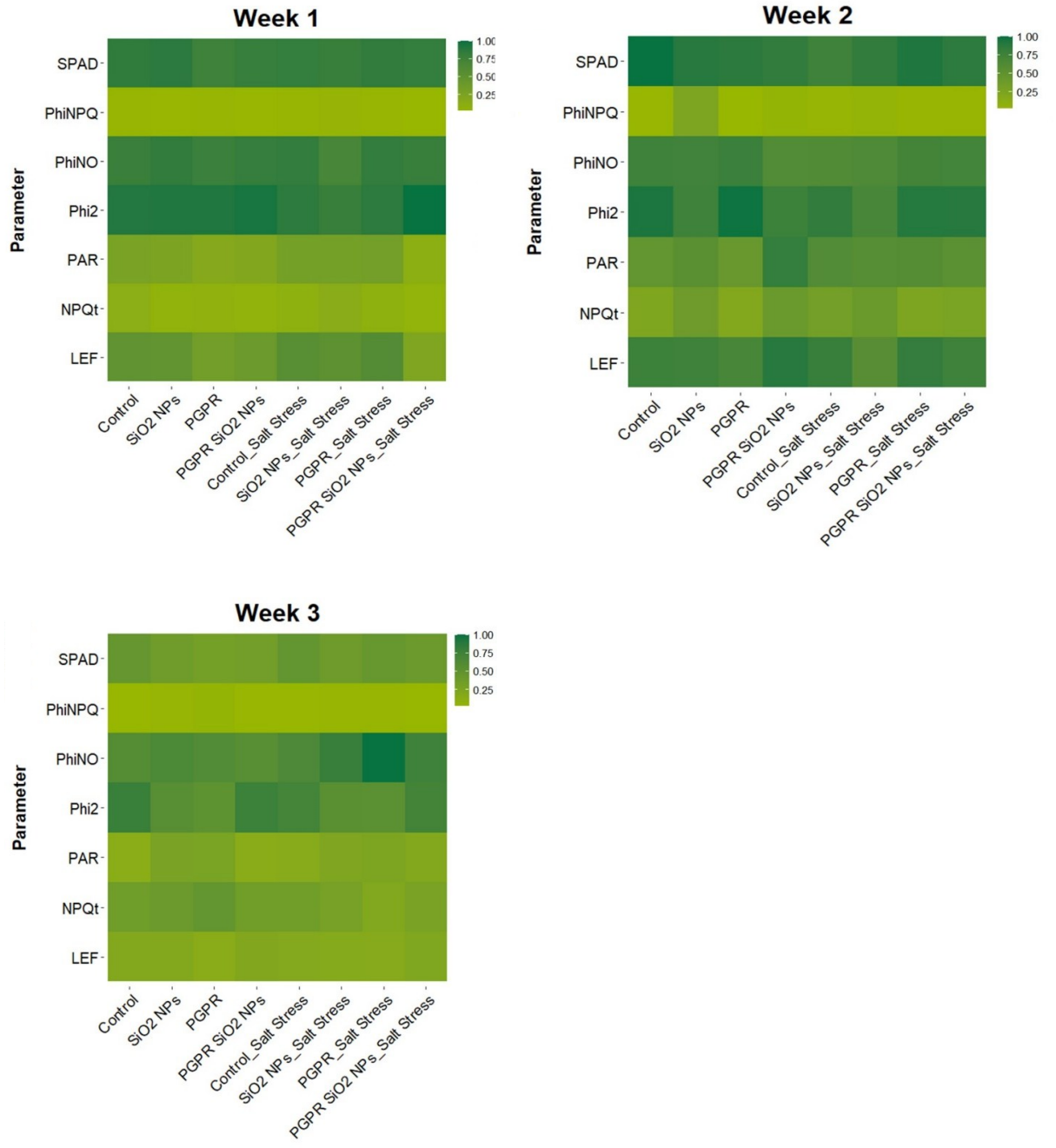


**Figure 3.10.** Graphical representation of the data measured with the SPAD device, collected once a week for the entire period of salt stress induction. Parameters displayed by heatmaps are listed below: SPAD, PhiNPQ, PhiNO, Phi2, Light Intensity (PAR), NPQt and Linear Electron Flow (LEF).

From the data collected upon harvesting (**Figure 3.11**), under induced salt stress conditions, the group formed by the control plants and treated by the silicon nanoparticles exhibited significantly less chlorophyll when compared with that of the same group of plants grown under optimal conditions. The combined supplementation of nanoparticles and PGPR exerted a positive effect on the amount of chlorophyll. While higher than that of the other stressed plants, no other significant differences could be revealed.

Conversely, the estimation of carotenoids has suggested that the interaction between PGPR and silicon nanoparticles may have a positive effect on carotenoid content under normal or stressful growth conditions. Statistical analysis confirmed the significance of the difference recorded among the means of observations for the group of untreated and PGPR-only treated plants grown under normal growth and stress conditions.

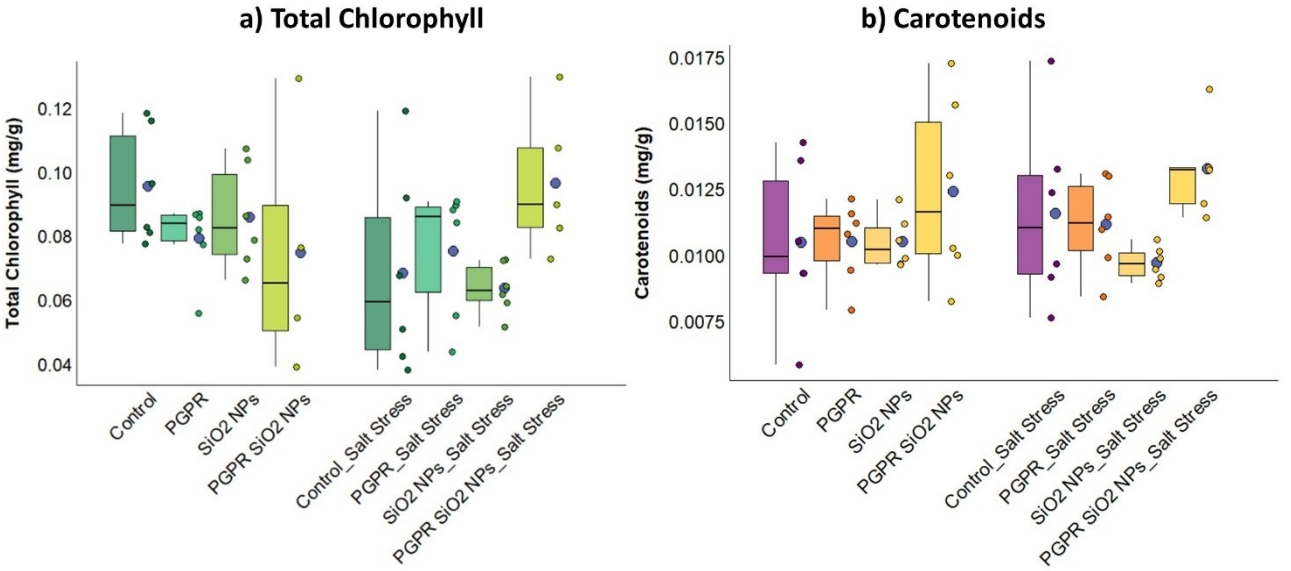


| | *F value* | *P value* |
|---|---|---|
| ***Stress*** | 2.128 | 0.153 |
| ***NPs*** | 0.009 | 0.926 |
| ***PGPR*** | 0.254 | 0.617 |
| ***Stress* NPs*** | 0.886 | 0.353 |
| ***Stress* PGPR*** | 6.378 | **0.016** |
| ***NPs*PGPR*** | 1.455 | 0.235 |
| ***Stress* NPs* PGPR*** | 0.621 | 0.436 |

| *F value* | *P value* |
|---|---|
| 0.270 | 0.6063 |
| 0.453 | 0.5050 |
| 3.091 | 0.0866 · |
| 0.469 | 0.4974 |
| 0.121 | 0.7298 |
| 4.314 | **0.0444** |
| 0.570 | 0.4547 |

**Figure 3.11.** Graphical representation of the parameters measured for soybean plants upon harvesting: Total Chlorophyll (**a**), Carotenoids (**b**). The boxplots were constructed based on biological replicates subjected to the same treatment with the bigger violet dot indicating the average value of each plant group. In the tables below the charts are reported the *F values* and the *P values* derived from the three-way Analysis of Variance (ANOVA), with values below the significance threshold (*P values* < 0.05) in bold. The significance of the differences was assessed by Tukey's HSD (Honestly Significant Difference).

### 3.2.6 Elemental Analysis of Plant Tissues: *Solanum lycopersicum* L.

**Figure 3.12 (a)** displays the results of the elemental analysis performed on the roots of tomato plants. The first dimension explains 89.4% of the total variance of the dataset and is functional to divide the plants treated with or without PGPR, regardless of the association with silicon and chitosan

nanoparticles. The group of untreated plants and those treated with $SiO_2$ NPS are in the left quadrants at the bottom and top, respectively, and although with slight differences, the profiles that emerged are similar. Looking at the heatmap in **Figure 3.12 (c)** it is evident that the content of the detected elements is significantly lower in the roots of these plants when compared with that of the roots of plants treated with the PGPR alone or in combination with both types of nanoparticles and with Ch/TPP NPs alone.

In the right quadrants, however, two clusters are easily identifiable. The first one consists of the plants treated with PGPR alone and is in the lower quadrant where the large contribution of calcium, manganese, copper and phosphorus in determining this clustering can be noted. The maximum amount of calcium was measured in the roots of plants treated with PGPR alone, which was found to be statistically higher than in the roots of control plants (i), of plants treated with Ch/TPP (ii) and $SiO_2$ (iii) nanoparticles. In addition, the association of the nanoparticles with the microorganisms promoted calcium accumulation in the root system at statistically different and higher levels than those due to the use of nanoparticles alone. Comparing the average of the manganese values quantified in the roots of plants administered with Ch/TPP based treatments with the average value found in the group of plants treated with $SiO_2$ NPs, the difference was statistically significantly higher.

The second cluster, positioned in the upper right side, is that of the plants treated with the combination of $SiO_2$ NPs and PGPR, the clustering of which seems instead to have been driven by elements such as silicon, potassium, sulfur and boron. Potassium accumulation occurred at a higher level in the roots of plants treated with the combination of PGPR and $SiO_2$ NPs than in untreated plants (i) and those treated with silica (ii) and chitosan (iii) nanoparticles alone and PGPR (iv).

Silicon uptake was also enhanced by the simultaneous use of microorganisms and nanoparticles. The recorded measurements were found to be significantly different and higher than the amounts of the roots of plants treated with PGPR alone (i), with silica nanoparticles (i) and with the combination of chitosan nanoparticles and PGPR (iii).

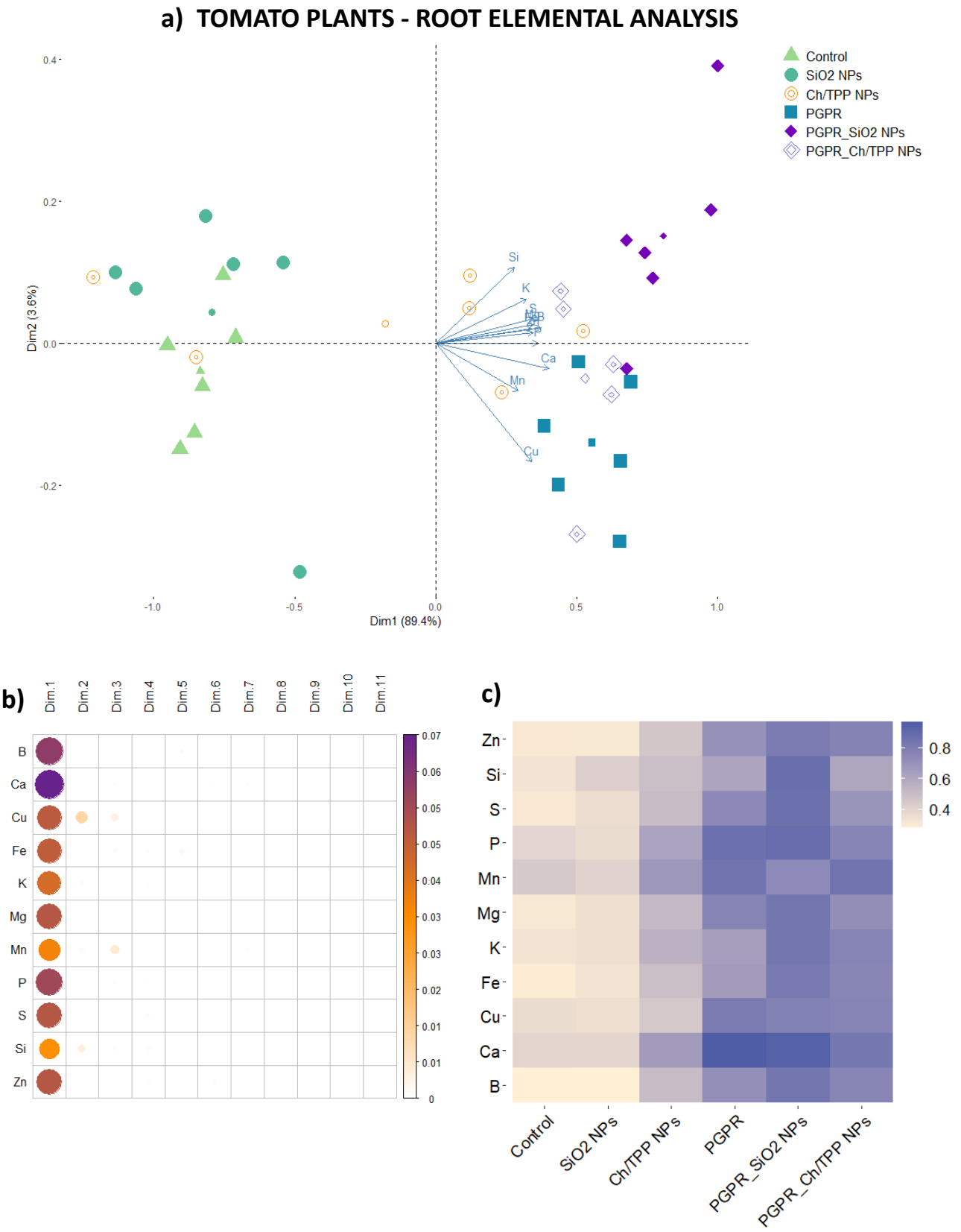


**Figure 3.12.** Graphical visualization via Principal Component Analysis (PCA) of the quantification data obtained for the elemental composition of roots of tomato plants **(a)**. Corrplot or correlation matrix chart of the Cos2 of each variable that underline their single contribution in explaining the new dimensions **(b).** Heatmap of elements detected in the roots. As reported in detail in the *Materials and Methods* section, quantification data of the same element were normalized based on the maximum value of each column **(c)**.

Also, in the case of the elemental composition of the leaves of tomato plants, as shown in **Figure 3.13 (a)**, the group of untreated plants is located close to the group of plants treated with silica nanoparticles, indicating the sharing of a similar profile although with some differences. The uptake of some of the elements considered were directly affected using PGPR. In fact, the mean values quantified for boron, manganese, calcium, magnesium, iron, sulfur and zinc in the PGPR-based treatment groups, regardless of the combination with nanoparticles, was statistically different from their content detected in the untreated or nanoparticle-only treated plants. The collected data seem to suggest that the use of PGPR may have a positive effect on zinc and silicon amounts. In contrast, differences in phosphorus levels were not significant, even if it was noticed a higher level in plants treated with Ch/TPP NPs and PGPR. On the other hand, the results suggest that copper uptake was affected by the interaction between the nanoparticles and PGPR. Where both solutions were administered, for example, the amount of copper was statistically greater than that measured for plants under chitosan treatment. Plants administered with chitosan nanoparticles showed an accumulation of potassium in the leaves of tomato plants, and this difference becomes significant when this amount is compared with that of plants treated with silicon nanoparticles.

Two other clusters can be identified in the lower quadrants, along the axis of the biplot indicating the silicon contribution, and they are the two groups of plants treated with Ch/TPP NPs and PGPR. Their grouping was guided by the high silicon contents that were tracked in both groups. Statistical analysis confirmed that the plants treated with the silicon nanoparticles showed significantly lower silicon values than the average of observations collected for the other plants.

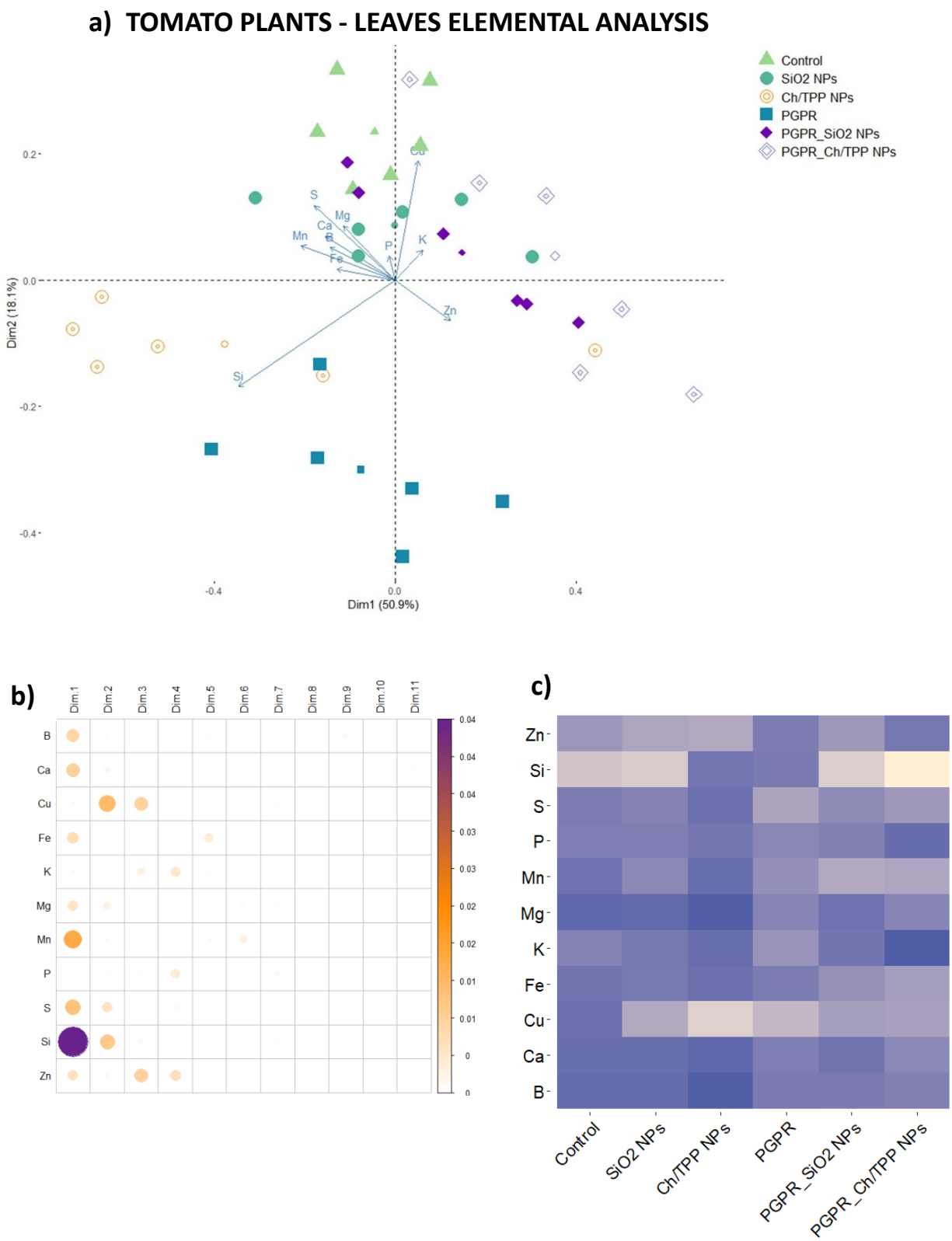


**Figure 3.13.** Graphical visualization via Principal Component Analysis (PCA) of the quantification data obtained for the elemental composition of leaves of tomato plants **(a)**. Corrplot or correlation matrix chart of the Cos2 of each variable that underline their single contribution in explaining the new dimensions **(b).** Heatmap of elements detected in the roots. As report in detail in the *Materials and Methods* section, quantification data of the same element were normalized based on the maximum value of each column **(c)**.

### 3.2.7 Elemental Analysis of Plant Tissues: *Glycine max* L.

Data derived from the elemental analysis of plant tissues of soybean (roots, leaves and pods) were visualized by Principal Component Analysis (PCA) to better understand the specific behavior of differently treated groups of plants with respect to the variables considered. Examining the root system, for example, in **Figure 3.14 (a)** it can be observed that the first component (PCA1), which explains 41.9% of the total variance, can separate stressed and non-stressed plants from each other, regardless of the treatment applied. The second main component (PCA2) that explains 21.5% of the total variance appears to separate PGPR-based treatments from others, although some overlaps are visible.

The first easily identifiable cluster in the upper right quadrant is that of untreated plants subjected to salt stress that are clustered at the apex of the biplot axis indicating the major contribution of sodium. This arrangement confirms the occurrence of stress perception with a consequent and significant sodium accumulation in the roots of soybean plants as shown in **Figure 3.14 (c)**. The quantity of sodium internalized into the radical roots appears to be reduced, however, by using silica nanoparticles regardless of their combination with PGPR. In fact, the amount of sodium accumulated in the roots of plants untreated or treated with PGPR alone was found to be significantly higher compared with that found instead in the group of plants subjected to salt stress but treated with $SiO_2$ NPs alone or in combination with PGPR. The level of potassium is directly influenced by the salt stress that reduces its content in stressed plants compared to those grown under optimal conditions. Despite in response to the abiotic stress plants untreated or treated with PGPR seem to accumulate more potassium than the others, none of these differences was found to be significant statistically.

The stressed plants treated with the combination of the $SiO_2$ NPs and PGPR, located in the lower right quadrant, form a second cluster. These plants are poorly dispersed and evidence a different elemental composition of their roots with respect to the other stressed plants. In particular, calcium seems to be present in significantly higher amounts, especially when comparing the group formed by plants treated with the PGPR-$SiO_2$ NPs combination grown under optimal and stress conditions, with the group of plants treated only with PGPR grown under stressed and unstressed conditions. Two other elements that characterize the elemental profile of the roots of these plants are magnesium and sulfur whose quantified values were found to be significantly lower than those detected in the roots of the other plants.

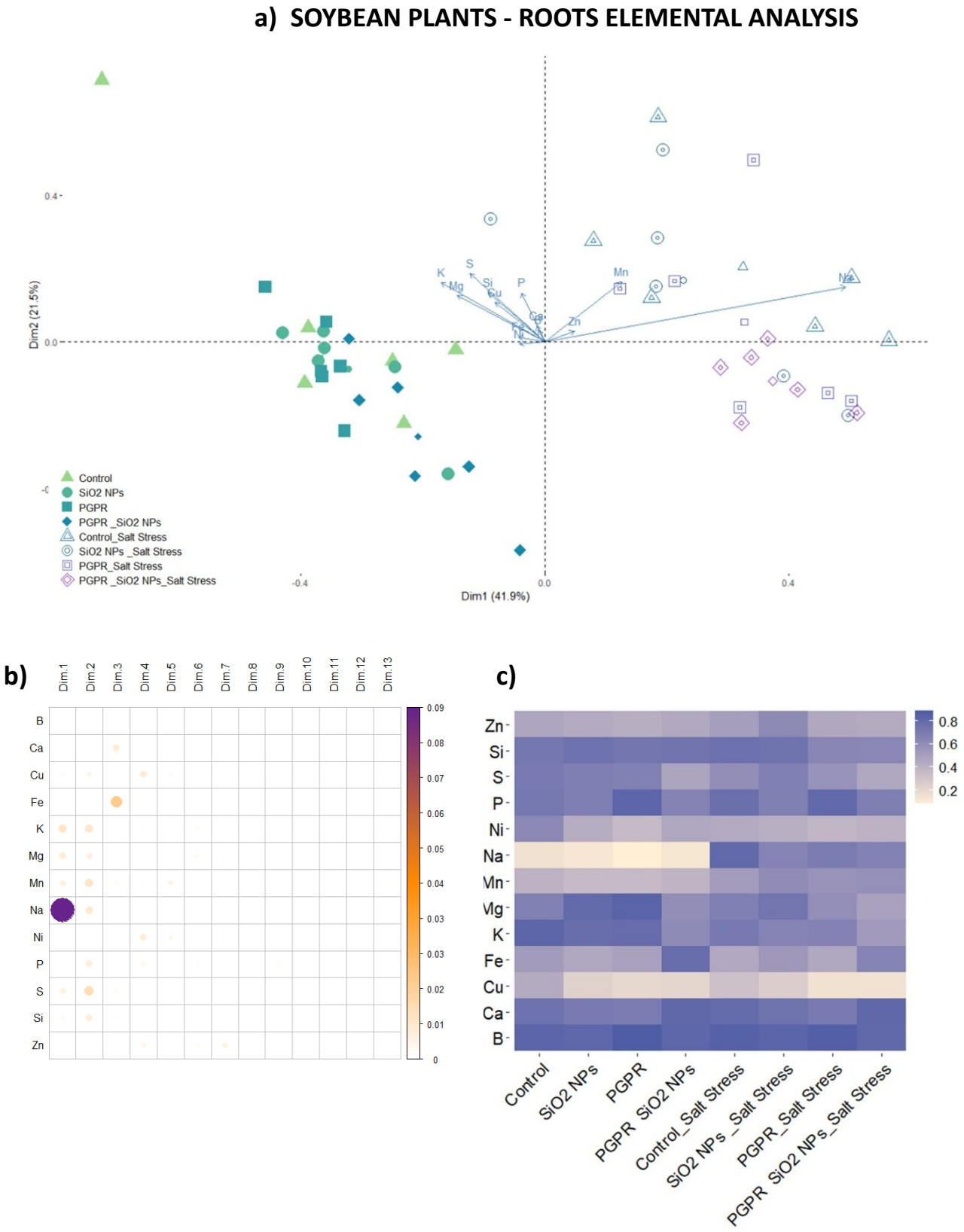


**Figure 3.14:** Graphical visualization via Principal Component Analysis (PCA) of the quantification data obtained for the elemental composition of roots of soybean plants **(a)**. Corrplot or correlation matrix chart of the Cos2 of each variable that underline their single contribution in explaining the new dimensions **(b).** Heatmap of elements detected in the roots. As report in detail in the *Materials and Methods* section, quantification data of the same element were normalized based on the maximum value of each column **(c)**.

The quantification values of both the elements for the group of stressed and unstressed plants treated with PGPR and $SiO_2$ NPs together proved to be significantly lower if compared with three different groups: untreated plants (i), plans treated with only PGPR (ii), or $SiO_2$ NPs (iii), considered under optimal growth and abiotic stress conditions. On the other hand, for stressed plants treated only with PGPR or $SiO_2$ NPs, no defined clusters can be identified due to a greater dispersion of the biological replicates. These plants tend to cluster with the other two described groups, underling similarities in the elemental composition of their roots. More biological replications could in the future potentially help to better define their response to salt stress by reducing individual plant variability.

Analyzing the group of unstressed plants, on the other hand, there are not such obvious subdivisions between treatments. The elemental profile of the root system of plants treated with PGPR or $SiO_2$ NPs is maintained. The only ones that are distanced by locating in the lower left quadrant are the plants treated with the combination PGPR-$SiO_2$ NPs.

The Principal Component Analysis (PCA) in **Figure 3.15 (a)** depicts the elemental composition of soybean leaves. The first dimension explains 60.7% of the total variance and separates, although less clearly, stressed plants from those grown under optimal conditions. The untreated stressed plants and almost all the stressed plants administered with PGPR are localized in the upper right quadrant. The profiling of the elements of their leaves is characterized by higher amounts of manganese, boron, zinc, potassium, magnesium and calcium than the other salt-stressed plants. Even under optimal growth conditions, treatment with PGPR showed a similar trend if compared with untreated plants. Plants treated by silica nanoparticles alone, instead, clustered in the lower left quadrant indicating instead a slightly greater accumulation of silicon, calcium, phosphorus and sulfur.

Induced salt stress appears to be the major contributing variable to the rising levels of some of these elements including sodium, calcium, iron and magnesium and comparing the two macrogroups of stressed and non-stressed plants, the differences are apparent. Potassium accumulation is favored under salt stress conditions in the leaves of untreated or PGPR-treated plants. The average value of potassium detected for this group of plants is significantly higher than for all other groups of plants grown under optimal and stress conditions. In contrast, $SiO_2$ NPs alone or in combination with PGPR apparently caused potassium accumulation in leaves of plants grown under optimal conditions although there were no differences between the treatments that could be considered significant. The administration of PGPR, regardless of their combination with $SiO_2$ NPs, has led to a rise in the level of manganese retained by the leaves of plants grown under optimal conditions.

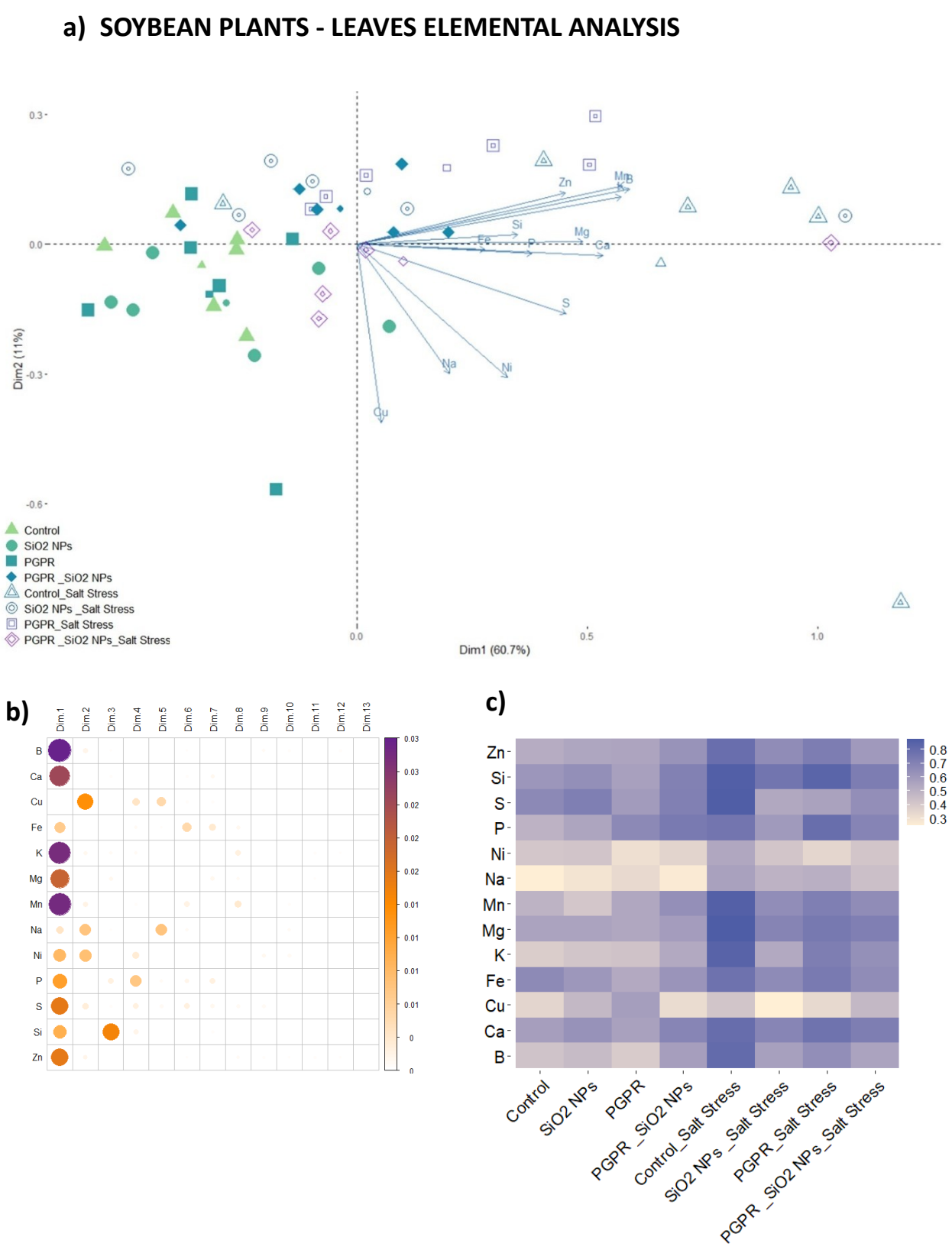


**Figure 3.15.** Graphical visualization via Principal Component Analysis (PCA) of the quantification data obtained for the elemental composition of leaves of soybean plants **(a)**. Corrplot or correlation matrix chart of the Cos2 of each variable that underline their single contribution in explaining the new dimensions **(b).** Heatmap of elements detected in the roots. As report in detail in the *Materials and Methods* section, quantification data of the same element were normalized based on the maximum value of each column **(c)**.

Conversely, significantly lower amounts were detected in the leaves of stressed plants treated with $SiO_2$ NPs, with or without PGPR, than in the group formed by control plants and plants treated with PGPR alone. There seems to be a strong influence of salt stress and use of PGPR in determining the phosphorus and silicon content of the leaves, which were both significantly higher in the roots of the stressed plants of the control group and treated with PGPR than the average values measured in the same group but grown under optimal conditions.

# 4 Discussion

## 4.1 Enlightening The Fate of Plant Growth-Promoting Rhizobacteria in Agricultural soils

To date, there are several analytical techniques for tracking and quantifying microorganisms in environmental samples. The traditional culturing-based methods are laborious and time-consuming. In addition, the presence in agricultural soils of indigenous microorganisms with similar morphology to those targeted may hinder their identification (Zhang et al., 2020). On the other hand, qtPCR is a reproducible, environmentally safe and sensitive method with a detection limit of up to $10^2$ CFU/g soil (Rilling et al., 2019). This technology overcomes the limitations imposed by traditional culturing-based methods by lowering time and costs of large-scale analyses and ensuring specific detection based on DNA sequences (Stets et al., 2015; Xiang et al., 2010). The development of portable and inexpensive qtPCR systems could also enable in situ detection outside of laboratories (L. He et al., 2020). Several reports have demonstrated successful utilization of qtPCR on plant tissues and soil for tracking and enumerating single or multiple PGPR species (Blaya et al., 2016; Couillerot et al., 2010; Mavrodi et al., 2007; Mendis et al., 2018; Stets et al., 2015; Timmusk et al., 2009; Zhang et al., 2020). The purpose of this research work was to develop a qtPCR-based protocol based on species-specific traceability for the quantification of MC_C consortium microorganisms supplied to the soil of two wheat cultivars (Svevo and Bramante). The development of specific probes and a reproducible procedure requires a deep genetic knowledge of the identified target (Manfredini et al., 2023). In our case the search for specific primers resulted in a challenging task because of the lack of sequencing data for the strains used in the field trial. Specific primers for the bacteria *R. aquatilis*, *B. ambifaria* and *B. amyloliquefaciens* were retrieved after a screening of about one hundred experimentally designed or found in literature. The developed method was proved to be effective in determining the shelf-life of PGPR species from the MC_C consortium administered to agricultural soil of the two wheat varieties. Replicate reproducibility can be perturbed by dispersal phenomena of microorganisms, climatic factors, or the uneven distribution of inoculated bacteria in the soil, as

shown by the wide distribution of data for some of the samples and by the presence of outliers. Furthermore, it is recognized that the rhizospheric soil collection is the most critical phase in the entire traceability process, which can ensure data quality and robustness (Manfredini et al., 2021). Furthermore, the presence of soil indigenous microorganisms closely related to the target can render the detection difficult, leading to cross amplification (Stets et al., 2015).

The results showed that the traced bacteria colonized the rhizosphere of wheat, growing for about three weeks after inoculation. Although the general growth trend recorded is similar for the microorganisms, the differences noted for the colonization and persistence in soil could be attributable to genetic and physiological characteristics (Xiang et al., 2010). The administration of the MC_C consortium occurred in winter with temperatures below 20°C and therefore not optimal for these mesophilic bacteria. *Burkolderia* species are endowed with high tolerance to extreme environments and temperature changes, as well as great phenotypic plasticity (Tavares et al., 2020). For example, the *Burkolderia cepacia* group that includes *B. ambifaria* can survive in environments such as distilled water at 10°C (Carson et al., 1973). This might explain why the quantified values of GEs for *Burkolderia ambifaria* were higher compared to those of the other two bacterial strains, regardless of the addition of biochar and/or the mycorrhizal fungus *Rhizophagus intraradices* (AMF). Probably the other two bacteria are less able to adapt to environmental changes and non-optimal growth conditions.

The two wheat cultivars Svevo and Bramante do not seem to clearly influence the growth and colonization of inoculated PGPR. In order to investigate the plant-microorganisms interaction further analyses are required.

The beneficial effect of biochar on the persistence of microorganisms in soil was confirmed by GEs quantified for all three bacterial species monitored. It is reported that biochar can reduce nutrient leaching, alter the plant-microorganism signaling pathways or be used as a growth habitat for microorganisms, consequently affecting the structure and composition of the soil microbiota (Bolan et al., 2023; Caldara et al., 2024; Huang et al., 2023; Marmiroli et al., 2018). The biochar structure is porous and can be colonized externally, when microorganisms absorb to its surface through electrostatic or hydrophobic interactions, or internally offering them shelter from predators and species competing for survival in the soil (Bolan et al., 2023; Ding et al., 2016; Huang et al., 2023). The synergistic action between bacteria and biochar has been also confirmed by the effect on the quality and production yield of the two wheat cultivars Svevo and Bramante treated with the combination biochar and Micosat F1, a commercial product containing both bacteria and fungi (CCS Aosta, Italy) (Caldara et al., 2024). Effects on marketable production of tomatoes were also obtained with the combination of biochar with MC_B, AMF or Micosat F1 (Tabacchioni et al., 2021; Vassura

et al., 2023). However, it must be considered that the properties of biochar are strictly dependent on pyrolysis parameters including temperature range and starting raw material (Huang et al., 2023).

The present work showed that the developed qtPCR-based method enabled the microorganisms of MC_C to be traced in agricultural soils, demonstrating that the three bacterial species were able to colonize and grow in the rhizosphere of the two wheat cultivars. The protocol can certainly be improved with the help of genetic information that can be used to design specific primers. One of the main limitations of qtPCR is the inability to discriminate viable bacteria to dead ones (Zhang et al., 2020). However, this limitation can be overcome by combining qtPCR analyses and staining with reagents such as Propidium Monoazide (Àlvarez et al., 2013). In conclusion, there is evidence that inoculation of the MC_C microbial consortium in agricultural soils resulted in a growth period of about one month. After this time the persistence remains more awkward.

## 4.2 Nanobiotechnological Approaches to Stimulate Plant Resilience

Nanomaterials and plant biostimulants can be considered next-generation products that have the potential to promote plant growth and enhance the resilience to biotic and abiotic stressors in an eco-friendly way (Rouphael & Colla, 2020; Verma et al., 2022). Chitosan-based nanoparticles are eco-compatible and possess important antimicrobial and growth promotion properties (Ingle et al., 2022). Conversely, silicon is termed as a “quasi-essential” element, it is involved in various physiological and metabolic processes and plays a role in the structural integrity of cells (Du et al., 2022; Naidu et al., 2023). Based on their properties in alleviating symptoms of abiotic stresses (Ingle et al., 2022; Luyckx et al., 2017), silica and chitosan nanoparticles have been chosen to be tested alone and combined with the selected microbial-based product comprised of two *Bacillus* strains (*Bacillus subtilis* and *Bacillus amyloliquefaciens*). These bacteria belong to the genus *Bacillus* renewed for the plant growth promotion capabilities of its microorganisms (phytohormones and siderophores production; phosphorus and nutrients solubilization) (Nunes et al., 2023).

The interaction between plants and nanomaterials should be considered because it may result in controversial effects, depending on plant variety, administration modes and doses. While appropriate doses can support plant development, overly high doses may, on the other hand, led to oxidation of biomolecules and in extreme cases to cell toxicity and death (Dilnawaz et al., 2023). Based on previous experiments conducted on tomato plants, both the nanomaterials have been administered to the soil at the concentration of 200mg/Kg of soil. In this study, Ch-TPP NPs did not significantly influence plant development, the only visible effect was the increase in shoot lenght. However, the morphological data collected underlined a positive contribution of $SiO_2$ NPs in stimulating growth of

cherry tomato and soybean plants, even with slight differences in shoot and root weight/length, as previously described. Several studies reported an increment of vegetal biomass attributable to the use of silica nanoparticles. Mahmoud et al. (2022) demonstrated that the application of silicon nanoparticles mitigated negative impacts of salt stress in the Valencia Sweet Orange (*Citrus* × *sinensis* L.). Similar effects have also been proved for cucumber and rice plants in counteracting water deficit and salt stress (Alsaeedi et al., 2019; Jin et al., 2024). In general, saline environments force plants into a state of osmotic and oxidative stress that can impair their development by inhibiting cell division and elongation (Rahman et al., 2021). Silicon, inducing proliferation of secondary and tertiary endodermis cells, may instead favor the adaptation of the plants by modulating the architecture of their root system. The resulted improvement of water and nutrients uptake **(**Hattori et al., 2005; Jin et al., 2024) induces development of roots, leaves and stems of plants (Roohizadeh et al., 2015) explaining the higher number of leaves found for soybean plants supplemented with $SiO_2$ NPs.

Silica can relieve the stress sensed by plants also limiting sodium uptake into the roots and increasing potassium content to maintain the ratio $Na^+/K^+$ and preserve ion homeostasis (Coskun et al., 2016). In addition, intracellular cytoplasmatic concentration of $Ca^{2+}$ rises in response to abiotic stimuli and acts as a second messenger to activate a signal transduction cascade for regulating various plant processes (Xu et al., 2022). In accordance with the scientific literature, under salt stress conditions, the amount of sodium detected in soybean roots has been significantly reduced in the presence of silicon dioxide nanoparticles while calcium has increased. The potassium intake was not comparable to that internalized by untreated plants, but the $Na^+/K^+$ ratio remained higher. The major quantity of potassium was instead found in the roots of soybean plants treated with the PGPR, while sodium content resulted lower but not significantly respect to the untreated plants. Accumulation of calcium in the roots was evident in the case of the combined $SiO_2$ NPs-PGPR treatment. Similarly to silicon, *Bacillus* spp. can also restore ion balance (Nunes et al., 2023). Siddika et al. (2024) reported that two *Bacillus* strains enhanced the stress defense in rice plants subjected to high salinity by hindering sodium accumulation into the roots, favoring on the other hand the uptake of potassium. A proposed mechanism for sodium exclusion from roots by bacteria of the genus *Bacillus* may depend on biofilm production that could retain ions in its exopolysaccharide matrix (Giannelli et al., 2023).

At high salinity levels, the closure of stomata and limitation of leaf surface area can inhibit photosynthetic activity (Ali & Ayaz, 2022). As a consequence of the lack of carbon dioxide fixation, there is an overproduction of ROS that can damage various cellular structures through lipid peroxidation (da Fonseca et al., 2022). Determination of chlorophyll and carotenoids has revealed

that under optimal growth conditions nanoparticles can slightly increase their average values compared with untreated plants or plants administered with PGPR only. In contrast, the combined nanobiotechnological approach seems to have greater effect under conditions of induced salt stress in as previously reported by Alharbi et al. (2022). In several studies the separate application of silica and PGPR has resulted effective in augmenting chlorophyll and carotenoids content, particularly by intensifying the ROS scavenging activity, altering stomatal conductance and improving nutrient and water use efficiency (da Fonseca et al., 2022; Hasanuzzaman & Fujita, 2023; Kumari et al., 2024; Mukarram et al., 2023). Cherry tomato plants treated with Ch-TPP NPs also showed an increase in chlorophyll content, while the association with PGPR resulted more effective in inducing a higher level of carotenoids if compared to the untreated plants.

Adequate supply of micro- and macronutrient minerals is also essential to support plant development and increase productive yield, as well as to recover and maintain proper physiological functioning (Cai et al., 2020). The elemental profiles of leaves and roots of soybean and tomato plants evidenced some differences driven by the treatments. In cherry tomato plants, PGPR administration favored the accumulation of phosphorus in the roots, while Ch/TPP NPs seemed to determine higher contents of phosphorus, magnesium and boron in the leaves. Potassium and zinc levels appeared to rise in the leaves of plants treated with the combination of Ch/TPP NPs and PGPR. Soybean plants treated with microbial-based product appear to absorb higher quantity of micro/macro nutrients such as boron, calcium, magnesium and phosphorus. This observation may depend on *Bacillus spp.* ability to solubilize phosphorus and other elements, rendering them bioavailable for plants in the soil layer surrounding the roots. Another explanation could be the alleviation of the perceived osmotic and oxidative stress (Nunes et al., 2023). Boron may enhance the concentration of proline, proteins, and soluble sugar. It is a structural element in cell walls and is involved in protein synthesis and seed and flower production (Galeriani et al., 2022). Calcium is also a structural component of cell walls and mediated auxins-induced abscission processes of leaves, flowers, and fruits (Cai et al., 2020; Galeriani et al., 2022). *Leguminosae* such as *Brassicaceae* have a high tolerance to boron and require large amounts for their normal functioning (Schon & Blevins, 1987). Microbial activity appears to regulate its uptake, and can be probably ascribed to the higher number of pods and grains per plant observed.

# 5 Conclusions

Despite the large number of studies focusing on plant response to microbial biostimulants, still very little is known about the fate of PGPR strains inoculated in agricultural soils. The ability to adapt to a changing environment and interact with the indigenous soil microbiota is critical to prolong their persistence into the soil. Compared to the use of single species, the synergistic interactions among bacteria of a microbial consortium can also result in an inoculant more resilient and versatile. The present work demonstrated the efficacy of the qtPCR in assessing the shelf life of PGPR supplied as a microbial consortium in a field trial. The developed method proved the successful colonization of three out five bacteria of the microbial consortium MC_C (*B. ambifaria*, *B. amyloliquefaciens* and *R. aquatilis*) administered to wheat plants with biochar and the mycorrhizal fungus *Rhizophagus intraradices.* In the period between 15 and 20 days after the bacterial inoculation, a maximum growth was reached for all the bacteria. The analyses also evidenced that biochar positively influenced PGPR colonization. The research work also focused on investigating the interaction between microbial-based products and nanomaterials in counteracting abiotic stresses. Analyses have shown that under optimal growth conditions, silicon dioxide nanoparticles are most effective in inducing development and enhancing photosynthetic activity of the cherry tomatoes (*Solanum lycopersicum* L.). Although it has not yet been possible to make inferences regarding the effectiveness of silicon oxide and chitosan nanoparticles under salt stress conditions because the data collected require further investigation, it will be very important to evaluate their potential in alleviating the symptoms of perceived salt stress in plants. The greenhouse experiment on soybean plants confirmed the role of $SiO_2$ NP in modulating the architecture of the root system under salt stress conditions to improve water and nutrients uptake. Silica nanoparticles were also found to reduce sodium internalization into the roots, favoring on the other hand the rise of calcium content. PGPR favored instead the accumulation of potassium and regulated the uptake of other nutrients such as the boron that is involved in seeds and flowers production. Finally, the combination of the nano-biotechnological approaches resulted in an increase of the total chlorophyll and carotenoids content, enhancing photosynthetic efficiency of stressed plants.

# 6 Future Perspectives

Despite the positive results so far, confirmatory analyses will be needed to expand knowledge regarding the plant-rhizosphere system. Traceability of PGPR inoculated into the soil is critical for improving the performance of microbial biostimulants. In the future, the method based on real time

PCR (qtPCR) could be implemented with staining approaches, such as the one based on the use of Propidium Monoazide, to allow the recognition of live bacteria from dead ones. In addition, the completion of the Whole Genome Sequencing of the microbial strains within the MC-C consortium, carried out as part of the SIMBA project and reported by Cangioli et al. (2024) will enable expanding the panel of specific and usable primers for the identification and monitoring of these PGPR strains into the soil and the rhizosphere. In the future, it would also be relevant to study the microbial variability associated with the use of nanoparticles in the soil, either using single-microorganism-targeted approaches as the developed qtPCR method or metagenomic to analyze overall bacterial and fungal populations. It would also be interesting to further investigate the communication between plants and rhizobacteria by monitoring the quantitative and qualitative changes in root exudation in response to saline irrigation and treatments.

# Acknowledgements

A heartfelt thanks goes to my supervisor, Professor Nelson Marmiroli, point of reference and guide throughout the research program. I would also like to express my gratitude to Prof. Maestri, Dr. Caterina Agrimonti and Dr. Luca Pagano for their support at various stages of my experimental research. My thanks also go to all the colleagues of the Unit of Biotechnology of the Department of Chemistry, Life Science, and Environmental Sustainability (University of Parma) that have supported me along the path, contributing to my personal and professional growth.

I am grateful for the opportunity I was given by Professor Jason C. White to work at the Connecticut Agricultural Experiment Station (CAES, New Haven, CT, USA) with a group of competent and experienced researchers under his careful supervision. A heartful appreciation goes to my supervisor, Dr. Nubia Zuverza-Mena, point of reference that made my work experience abroad exceptional.

I would also like to thank Dr. Milica Pavlicevic and Dr. Raja Muthuramalingam for their assistance in characterizing the nanoparticles produced at the CAES (New Haven, CT, USA).

Lastly, my deepest gratitude goes to the people I love, my family and close friends, always understanding and supportive.

# References


Aizaz, M., Lubna, Jan, R., Asaf, S., Bilal, S., Kim, K.-M., & AL-Harrasi, A. (2024). Regulatory Dynamics of Plant Hormones and Transcription Factors under Salt Stress. *Biology*, *13*(9), 673. https://doi.org/10.3390/biology13090673

Alharbi, K., Hafez, E., Omara, A. E., & Awadalla, A. (2022). *Plant Growth Promoting Rhizobacteria and Silica Nanoparticles Stimulate Sugar Beet Resilience to Irrigation with Saline Water in Salt-Affected Soils*. 1–17.

Ali, Q., & Ayaz, M. (2022). *Revealing plant growth-promoting mechanisms of Bacillus strains in elevating rice growth and its interaction with salt stress*. *September*, 1–17. https://doi.org/10.3389/fpls.2022.994902

Almeida, D. M., Margarida Oliveira, M., & Saibo, N. J. M. (2017). Regulation of Na+ and K+ homeostasis in plants: Towards improved salt stress tolerance in crop plants. *Genetics and Molecular Biology*, *40*(1), 326–345. https://doi.org/10.1590/1678-4685-gmb-2016-0106

Àlvarez, G., González, M., Isabal, S., Blanc, V., & León, R. (2013). Method to quantify live and dead cells in multi-species oral biofilm by real-time PCR with propidium monoazide. *AMB Express*, *3*, 1–8. https://doi.org/10.1186/2191-0855-3-1

Andrews, M., & Andrews, M. E. (2017). Specificity in legume-rhizobia symbioses. *International Journal of Molecular Sciences*, *18*(4). https://doi.org/10.3390/ijms18040705

Ayaz, M., Ali, Q., Jiang, Q., Wang, R., Wang, Z., Mu, G., Khan, S. A., Khan, A. R., Manghwar, H., Wu, H., Gao, X., & Gu, Q. (2022). *Salt Tolerant Bacillus Strains Improve Plant Growth Traits and Regulation of Phytohormones in Wheat under Salinity Stress*.

Backer, R., Rokem, J. S., Ilangumaran, G., Lamont, J., Praslickova, D., Ricci, E., Subramanian, S., & Smith, D. L. (2018). Plant growth-promoting rhizobacteria: Context, mechanisms of action, and roadmap to commercialization of biostimulants for sustainable agriculture. *Frontiers in Plant Science*, *871*(October), 1–17. https://doi.org/10.3389/fpls.2018.01473

Bahadur, A., Batool, A., Nasir, F., Jiang, S., Mingsen, Q., Zhang, Q., Pan, J., Liu, Y., & Feng, H. (2019). Mechanistic insights into arbuscular mycorrhizal fungi-mediated drought stress tolerance in plants. *International Journal of Molecular Sciences*, *20*(17), 1–18. https://doi.org/10.3390/ijms20174199

Bashan, Y., de-Bashan, L. E., Prabhu, S. R., & Hernandez, J. P. (2014). Advances in plant growth-promoting bacterial inoculant technology: Formulations and practical perspectives (1998-2013). *Plant and Soil*, *378*(1–2), 1–33. https://doi.org/10.1007/s11104-013-1956-x

Basu, A., Prasad, P., Das, S. N., Kalam, S., Sayyed, R. Z., Reddy, M. S., & Enshasy, H. El. (2021). Plant growth promoting rhizobacteria (Pgpr) as green bioinoculants: Recent developments, constraints, and prospects. *Sustainability (Switzerland)*, *13*(3), 1–20. https://doi.org/10.3390/su13031140

Begum, N., Qin, C., Ahanger, M. A., Raza, S., Khan, M. I., Ashraf, M., Ahmed, N., & Zhang, L. (2019). Role of Arbuscular Mycorrhizal Fungi in Plant Growth Regulation: Implications in Abiotic Stress Tolerance. *Frontiers in Plant Science*, *10*(September), 1–15. https://doi.org/10.3389/fpls.2019.01068

Belobrajdic, D. P., James-Martin, G., Jones, D., & Tran, C. D. (2023). Soy and Gastrointestinal Health: A Review. *Nutrients*, *15*(8). https://doi.org/10.3390/nu15081959

Benitez-Alfonso, Y., Soanes, B. K., Zimba, S., Sinanaj, B., German, L., Sharma, V., Bohra, A., Kolesnikova, A., Dunn, J. A., Martin, A. C., Khashi u Rahman, M., Saati-Santamaría, Z., García-Fraile, P., Ferreira, E. A., Frazão, L. A., Cowling, W. A., Siddique, K. H. M., Pandey, M. K., Farooq, M., … Foyer, C. H. (2023). Enhancing climate change resilience in agricultural crops. *Current Biology*, *33*(23), R1246–R1261. https://doi.org/10.1016/j.cub.2023.10.028

Berg, G. (2009). Plant-microbe interactions promoting plant growth and health: Perspectives for controlled use of microorganisms in agriculture. *Applied Microbiology and Biotechnology*, *84*(1), 11–18. https://doi.org/10.1007/s00253-009-2092-7

Bhat, M. A., Mishra, A. K., Jan, S., Bhat, M. A., Kamal, M. A., Rahman, S., Shah, A. A., & Jan, A. T. (2023). *Plant Growth Promoting Rhizobacteria in Plant Health : A Perspective Study of the Underground Interaction*. 1–21.

Blaya, J., Lloret, E., Santísima-Trinidad, A. B., Ros, M., & Pascual, J. A. (2016). Molecular methods (digital PCR and real-time PCR) for the quantification of low copy DNA of Phytophthora nicotianae in environmental samples. *Pest Management Science*, *72*(4), 747–753. https://doi.org/10.1002/ps.4048

Bolan, S., Sharma, S., Mukherjee, S., Kumar, M., Rao, C. S., Nataraj, K. C., Singh, G., Vinu, A., Bhowmik, A., Sharma, H., El-Naggar, A., Chang, S. X., Hou, D., Rinklebe, J., Wang, H.,

Siddique, K. H. M., Abbott, L. K., Kirkham, M. B., & Bolan, N. (2023). Biochar modulating soil biological health: A review. *Science of The Total Environment*, *914*(December 2023), 169585. https://doi.org/10.1016/j.scitotenv.2023.169585

Bose, J., Munns, R., Shabala, S., Gilliham, M., Pogson, B., & Tyerman, S. D. (2017). Chloroplast function and ion regulation in plants growing on saline soils: Lessons from halophytes. *Journal of Experimental Botany*, *68*(12), 3129–3143. https://doi.org/10.1093/jxb/erx142

Butler, A., Harder, T., Ostrowski, A. D., & Carrano, C. J. (2021). Photoactive siderophores: Structure, function and biology. *Journal of Inorganic Biochemistry*, *221*, 111457. https://doi.org/10.1016/j.jinorgbio.2021.111457

Cai, H., Tao, N., & Guo, C. (2020). Systematic investigation of the effects of macro-elements and iron on soybean plant response to fusarium oxysporum infection. *Plant Pathology Journal*, *36*(5), 398–405. https://doi.org/10.5423/PPJ.OA.04.2020.0069

Caldara, M., Gullì, M., Graziano, S., Riboni, N., Maestri, E., Mattarozzi, M., Bianchi, F., Careri, M., & Marmiroli, N. (2024). Microbial consortia and biochar as sustainable biofertilisers: Analysis of their impact on wheat growth and production. *Science of the Total Environment*, *917*(January). https://doi.org/10.1016/j.scitotenv.2024.170168

Cangioli, L., Tabacchioni, S., Visca, A., Fiore, A., Aprea, G., Ambrosino, P., Ercole, E., Sørensen, S., Mengoni, A., & Bevivino, A. (2024). Genome Insights into Beneficial Microbial Strains Composing SIMBA Microbial Consortia Applied as Biofertilizers for Maize, Wheat and Tomato. *Microorganisms*, *12*(12), 1–13. https://doi.org/10.3390/microorganisms12122562

Carson, L. A., Favero, M. S., Bond, W. W., & Petersen, N. J. (1973). Morphological, biochemical, and growth characteristics of pseudomonas cepacia from distilled water. *Applied Microbiology*, *25*(3), 476–483. https://doi.org/10.1128/aem.25.3.476-483.1973

Causse, M., Desplat, N., Pascual, L., Paslier, M. Le, Sauvage, C., Bauchet, G., Bérard, A., Bounon, R., Tchoumakov, M., & Brunel, D. (2013). *Whole genome resequencing in tomato reveals variation associated with introgression and breeding events*.

Chaumont, F., & Tyerman, S. D. (2014). Aquaporins: Highly regulated channels controlling plant water relations. *Plant Physiology*, *164*(4), 1600–1618. https://doi.org/10.1104/pp.113.233791

Chaves, M. M., Flexas, J., & Pinheiro, C. (2009). Photosynthesis under drought and salt stress: Regulation mechanisms from whole plant to cell. *Annals of Botany*, *103*(4), 551–560.

https://doi.org/10.1093/aob/mcn125

Chele, K. H., Tinte, M. M., Piater, L. A., Dubery, I. A., & Tugizimana, F. (2021). Soil salinity, a serious environmental issue and plant responses: A metabolomics perspective. *Metabolites*, *11*(11). https://doi.org/10.3390/metabo11110724

Choi, W. G., Toyota, M., Kim, S. H., Hilleary, R., & Gilroy, S. (2014). Salt stress-induced Ca2+ waves are associated with rapid, long-distance root-to-shoot signaling in plants. *Proceedings of the National Academy of Sciences of the United States of America*, *111*(17), 6497–6502. https://doi.org/10.1073/pnas.1319955111

Choudhary, D. K., Prakash, A., & Johri, B. N. (2007). Induced systemic resistance (ISR) in plants: Mechanism of action. *Indian Journal of Microbiology*, *47*(4), 289–297. https://doi.org/10.1007/s12088-007-0054-2

Chun, J. A., Lim, C., Kim, D., & Kim, J. S. (2018). Assessing impacts of climate change and sea-level rise on seawater intrusion in a coastal aquifer. *Water (Switzerland)*, *10*(4), 1–11. https://doi.org/10.3390/w10040357

Cifuentes, Z., Custardoy, L., de la Fuente, J. M., Marquina, C., Ibarra, M. R., Rubiales, D., & Pérez-de-Luque, A. (2010). Absorption and translocation to the aerial part of magnetic carbon-coated nanoparticles through the root of different crop plants. *Journal of Nanobiotechnology*, *8*(1), 26. https://doi.org/10.1186/1477-3155-8-26

Compant, S., Samad, A., Faist, H., & Sessitsch, A. (2019). A review on the plant microbiome: Ecology, functions, and emerging trends in microbial application. *Journal of Advanced Research*, *19*, 29–37. https://doi.org/10.1016/j.jare.2019.03.004

Coskun, D., Britto, D. T., Huynh, W. Q., & Kronzucker, H. J. (2016). The role of silicon in higher plants under salinity and drought stress. *Frontiers in Plant Science*, *7*(2016JULY), 1–7. https://doi.org/10.3389/fpls.2016.01072

Couillerot, O., Poirier, M. A., Prigent-Combaret, C., Mavingui, P., Caballero-Mellado, J., & Moënne-Loccoz, Y. (2010). Assessment of SCAR markers to design real-time PCR primers for rhizosphere quantification of Azospirillum brasilense phytostimulatory inoculants of maize. *Journal of Applied Microbiology*, *109*(2), 528–538. https://doi.org/10.1111/j.1365-2672.2010.04673.x

da Fonseca, M. de C., Bossolani, J. W., de Oliveira, S. L., Moretti, L. G., Portugal, J. R., Scudeletti,

D., de Oliveira, E. F., & Crusciol, C. A. C. (2022). Bacillus subtilis Inoculation Improves Nutrient Uptake and Physiological Activity in Sugarcane under Drought Stress. *Microorganisms*, *10*(4). https://doi.org/10.3390/microorganisms10040809

Datta, S., Singh, J., Singh, S., & Singh, J. (2016). Earthworms, pesticides and sustainable agriculture: a review. *Environmental Science and Pollution Research*, *23*(9), 8227–8243. https://doi.org/10.1007/s11356-016-6375-0

de Andrade, L. A., Santos, C. H. B., Frezarin, E. T., Sales, L. R., & Rigobelo, E. C. (2023). Plant Growth-Promoting Rhizobacteria for Sustainable Agricultural Production. *Microorganisms*, *11*(4). https://doi.org/10.3390/microorganisms11041088

Diffenbaugh, N. S., Singh, D., Mankin, J. S., Horton, D. E., Swain, D. L., Touma, D., Charland, A., Liu, Y., Haugen, M., Tsiang, M., & Rajaratnam, B. (2017). Quantifying the influence of global warming on unprecedented extreme climate events. *Proceedings of the National Academy of Sciences of the United States of America*, *114*(19), 4881–4886. https://doi.org/10.1073/pnas.1618082114

Dilnawaz, F., Misra, A. N., & Apostolova, E. (2023). Plant Stress Involvement of nanoparticles in mitigating plant ' s abiotic stress. *Plant Stress*, *10*(October), 100280. https://doi.org/10.1016/j.stress.2023.100280

Ding, Y., Liu, Y., Liu, S., Li, Z., Tan, X., Huang, X., Zeng, G., Zhou, L., & Zheng, B. (2016). Biochar to improve soil fertility. A review. *Agronomy for Sustainable Development*, *36*(2). https://doi.org/10.1007/s13593-016-0372-z

Du, J., Liu, B., Zhao, T., Xu, X., Lin, H., Ji, Y., Li, Y., Li, Z., Lu, C., Li, P., Zhao, H., Li, Y., Yin, Z., & Ding, X. (2022). Silica nanoparticles protect rice against biotic and abiotic stresses. *Journal of Nanobiotechnology*, *20*(1), 1–18. https://doi.org/10.1186/s12951-022-01420-x

Duchenne-Moutien, R. A., & Neetoo, H. (2021). Climate change and emerging food safety issues: A review. *Journal of Food Protection*, *84*(11), 1884–1897. https://doi.org/10.4315/JFP-21-141

Ebi, K. L., Vanos, J., Baldwin, J. W., Bell, J. E., Hondula, D. M., Errett, N. A., Hayes, K., Reid, C. E., Saha, S., Spector, J., & Berry, P. (2020). Extreme Weather and Climate Change: Population Health and Health System Implications. *Annual Review of Public Health*, *42*, 293–315. https://doi.org/10.1146/annurev-publhealth-012420-105026

Eswar, D., Karuppusamy, R., & Chellamuthu, S. (2021). Drivers of soil salinity and their

correlation with climate change. *Current Opinion in Environmental Sustainability*, *50*(October 2020), 310–318. https://doi.org/10.1016/j.cosust.2020.10.015

Fang, C., & Kong, F. (2022). Soybean. *Current Biology*, *32*(17), R902–R904. https://doi.org/10.1016/j.cub.2022.06.054

Fiodor, A., Singh, S., & Pranaw, K. (2021). The contrivance of plant growth promoting microbes to mitigate climate change impact in agriculture. *Microorganisms*, *9*(9), 1–36. https://doi.org/10.3390/microorganisms9091841

Fox J., Weisberg S. (2019). _An R Companion to Applied Regression_, Third edition. Sage, Thousand Oaks CA.

Francis, D. V., Abdalla, A. K., Mahakham, W., Sarmah, A. K., & Ahmed, Z. F. R. (2024). Interaction of plants and metal nanoparticles: Exploring its molecular mechanisms for sustainable agriculture and crop improvement. *Environment International*, *190*(June), 108859. https://doi.org/10.1016/j.envint.2024.108859

Fu, H., & Yang, Y. (2023). How Plants Tolerate Salt Stress. *Current Issues in Molecular Biology*, *45*(7), 5914–5934. https://doi.org/10.3390/cimb45070374

Galeriani, T. M., Neves, G. O., Santos Ferreira, J. H., Oliveira, R. N., Oliveira, S. L., Calonego, J. C., & Crusciol, C. A. C. (2022). Calcium and Boron Fertilization Improves Soybean Photosynthetic Efficiency and Grain Yield. *Plants*, *11*(21). https://doi.org/10.3390/plants11212937

Galvan-Ampudia, C. S., Julkowska, M. M., Darwish, E., Gandullo, J., Korver, R. A., Brunoud, G., Haring, M. A., Munnik, T., Vernoux, T., & Testerink, C. (2013). Halotropism is a response of plant roots to avoid a saline environment. *Current Biology*, *23*(20), 2044–2050. https://doi.org/10.1016/j.cub.2013.08.042

Ganugi, P., Masoni, A., Pietramellara, G., & Benedettelli, S. (2019). A review of studies from the last twenty years on plant–arbuscular mycorrhizal fungi associations and their uses for wheat crops. *Agronomy*, *9*(12). https://doi.org/10.3390/agronomy9120840

Gao, Y., Zou, H., Wang, B., & Yuan, F. (2022). *Progress and Applications of Plant Growth-Promoting Bacteria in Salt Tolerance of Crops*.

Giannelli, G., Potestio, S., & Visioli, G. (2023). *The Contribution of PGPR in Salt Stress Tolerance in Crops : Unravelling the Molecular Mechanisms of Cross-Talk between Plant and Bacteria*.

Giovannini, L., Palla, M., Agnolucci, M., Avio, L., Sbrana, C., Turrini, A., & Giovannetti, M. (2020). Arbuscular mycorrhizal fungi and associated microbiota as plant biostimulants: Research strategies for the selection of the best performing inocula. *Agronomy*, *10*(1). https://doi.org/10.3390/agronomy10010108

Graziano, S., Caldara, M., Gullì, M., Bevivino, A., Maestri, E., & Marmiroli, N. (2022). A Metagenomic and Gene Expression Analysis in Wheat (T. durum) and Maize (Z. mays) Biofertilized with PGPM and Biochar. *International Journal of Molecular Sciences*, *23*(18). https://doi.org/10.3390/ijms231810376

Gupta, B., & Huang, B. (2014). Mechanism of salinity tolerance in plants: Physiological, biochemical, and molecular characterization. *International Journal of Genomics*, *2014*. https://doi.org/10.1155/2014/701596

Hamid, B., Zaman, M., Farooq, S., Fatima, S., Sayyed, R. Z., Baba, Z. A., Sheikh, T. A., Reddy, M. S., Enshasy, H. El, Gafur, A., & Suriani, N. L. (2021). Bacterial plant biostimulants: A sustainable way towards improving growth, productivity, and health of crops. *Sustainability (Switzerland)*, *13*(5), 1–24. https://doi.org/10.3390/su13052856

Harish, V., Tewari, D., Gaur, M., Yadav, A. B., Swaroop, S., Bechelany, M., & Barhoum, A. (2022). Review on Nanoparticles and Nanostructured Materials: Bioimaging, Biosensing, Drug Delivery, Tissue Engineering, Antimicrobial, and Agro-Food Applications. *Nanomaterials*, *12*(3). https://doi.org/10.3390/nano12030457

Hasanuzzaman, M., & Fujita, M. (2023). Plant Responses and Tolerance to Salt Stress: Physiological and Molecular Interventions 2.0. *International Journal of Molecular Sciences*, *24*(21), 1–6. https://doi.org/10.3390/ijms242115740

Hassani, A., Azapagic, A., & Shokri, N. (2021). Global predictions of primary soil salinization under changing climate in the 21st century. *Nature Communications*, *12*(1), 1–17. https://doi.org/10.1038/s41467-021-26907-3

He, L., Sang, B., & Wu, W. (2020). Battery-powered portable rotary real-time fluorescent qPCR with low energy consumption, low cost, and high throughput. *Biosensors*, *10*(5). https://doi.org/10.3390/BIOS10050049

He, X., Deng, H., & Hwang, H. min. (2019). The current application of nanotechnology in food and agriculture. *Journal of Food and Drug Analysis*, *27*(1), 1–21.

https://doi.org/10.1016/j.jfda.2018.12.002

Heino, M., Kinnunen, P., Anderson, W., Ray, D. K., Puma, M. J., Varis, O., Siebert, S., & Kummu, M. (2023). Increased probability of hot and dry weather extremes during the growing season threatens global crop yields. *Scientific Reports*, *13*(1). https://doi.org/10.1038/s41598-023-29378-2

Hesse, E., O'Brien, S., Tromas, N., Bayer, F., Luján, A. M., van Veen, E. M., Hodgson, D. J., & Buckling, A. (2018). Ecological selection of siderophore-producing microbial taxa in response to heavy metal contamination. *Ecology Letters*, *21*(1), 117–127. https://doi.org/10.1111/ele.12878

Hett, J., Döring, T. F., Bevivino, A., & Neuhoff, D. (2023). Impact of microbial consortia on organic maize in a temperate climate varies with environment but not with fertilization. *European Journal of Agronomy*, *144*(August 2022). https://doi.org/10.1016/j.eja.2023.126743

Huang, K., Zhang, J., Tang, G., Bao, D., Wang, T., & Kong, D. (2023). Impacts and mechanisms of biochar on soil microorganisms. *Plant, Soil and Environment*, *69*(2), 45–54. https://doi.org/10.17221/348/2022-PSE

Huber, D. G., Gulledge, J., & Ph, D. (2011). SCIENCE EXTREME WEATHER & CLIMATE CHANGE : UNDERSTANDING THE LINK AND by. *Solutions*, *December*(1), 1–13.

Ilangumaran, G., & Smith, D. L. (2017). *Plant Growth Promoting Rhizobacteria in Amelioration of Salinity Stress : A Systems Biology Perspective*. *8*(October), 1–14. https://doi.org/10.3389/fpls.2017.01768

Ingle, P. U., Shende, S. S., Shingote, P. R., Mishra, S. S., Sarda, V., Wasule, D. L., Rajput, V. D., Minkina, T., Rai, M., Sushkova, S., Mandzhieva, S., & Gade, A. (2022). Chitosan nanoparticles (ChNPs): A versatile growth promoter in modern agricultural production. *Heliyon*, *8*(11), e11893. https://doi.org/10.1016/j.heliyon.2022.e11893

Iosa, I., Agrimonti, C., & Marmiroli, N. (2024). Real-Time PCR (qtPCR) to Discover the Fate of Plant Growth-Promoting Rhizobacteria (PGPR) in Agricultural Soils. *Microorganisms*, *12*(5). https://doi.org/10.3390/microorganisms12051002

Jeevanandam, J., Barhoum, A., Chan, Y. S., Dufresne, A., & Danquah, M. K. (2018). Review on nanoparticles and nanostructured materials: History, sources, toxicity and regulations. *Beilstein Journal of Nanotechnology*, *9*(1), 1050–1074. https://doi.org/10.3762/bjnano.9.98

Ji, H., Pardo, J. M., Batelli, G., Van Oosten, M. J., Bressan, R. A., & Li, X. (2013). The salt overly sensitive (SOS) pathway: Established and emerging roles. *Molecular Plant*, *6*(2), 275–286. https://doi.org/10.1093/mp/sst017

Jiang, Z., Zhou, X., Tao, M., Yuan, F., Liu, L., Wu, F., Wu, X., Xiang, Y., Niu, Y., Liu, F., Li, C., Ye, R., Byeon, B., Xue, Y., Zhao, H., Wang, H. N., Crawford, B. M., Johnson, D. M., Hu, C., … Pei, Z. M. (2019). Plant cell-surface GIPC sphingolipids sense salt to trigger Ca2+ influx. *Nature*, *572*(7769), 341–346. https://doi.org/10.1038/s41586-019-1449-z

Kaldenhoff, R., Ribas-Carbo, M., Sans, J. F., Lovisolo, C., Heckwolf, M., & Uehlein, N. (2008). Aquaporins and plant water balance. *Plant, Cell and Environment*, *31*(5), 658–666. https://doi.org/10.1111/j.1365-3040.2008.01792.x

Kassambara A., Mundt F. (2020). _factoextra: Extract and Visualize the Results of Multivariate Data Analyses_. R package version 1.0.7.

Khalid, M. F., Iqbal Khan, R., Jawaid, M. Z., Shafqat, W., Hussain, S., Ahmed, T., Rizwan, M., Ercisli, S., Pop, O. L., & Alina Marc, R. (2022). Nanoparticles: The Plant Saviour under Abiotic Stresses. *Nanomaterials*, *12*(21). https://doi.org/10.3390/nano12213915

Khan, A., Singh, A. V., Gautam, S. S., Agarwal, A., Punetha, A., Upadhayay, V. K., Kukreti, B., Bundela, V., Jugran, A. K., & Goel, R. (2023). Microbial bioformulation: a microbial assisted biostimulating fertilization technique for sustainable agriculture. *Frontiers in Plant Science*, *14*(December), 1–22. https://doi.org/10.3389/fpls.2023.1270039

Kofsky, J., Zhang, H., & Song, B. (2018). *The Untapped Genetic Reservoir : The Past , Current , and Future Applications of the Wild Soybean ( Glycine soja )*. *9*(July). https://doi.org/10.3389/fpls.2018.00949

Kuhlgert, S., Austic, G., Zegarac, R., Osei-Bonsu, I., Hoh, D., Chilvers, M. I., Roth, M. G., Bi, K., TerAvest, D., Weebadde, P., & Kramer, D. M. (2016). MultispeQ Beta: A tool for large-scale plant phenotyping connected to the open photosynQ network. *Royal Society Open Science*, *3*(10). https://doi.org/10.1098/rsos.160592

Kuila, D., & Ghosh, S. (2022). Aspects, problems and utilization of Arbuscular Mycorrhizal (AM) application as bio-fertilizer in sustainable agriculture. *Current Research in Microbial Sciences*, *3*, 100107. https://doi.org/10.1016/j.crmicr.2022.100107

Kumar, A., Singh, S., Gaurav, A. K., Srivastava, S., & Verma, J. P. (2020). Plant Growth-

Promoting Bacteria: Biological Tools for the Mitigation of Salinity Stress in Plants. *Frontiers in Microbiology*, *11*(July), 1–15. https://doi.org/10.3389/fmicb.2020.01216

Kumar, S., Diksha, Sindhu, S. S., & Kumar, R. (2022). Biofertilizers: An ecofriendly technology for nutrient recycling and environmental sustainability. *Current Research in Microbial Sciences*, *3*. https://doi.org/10.1016/j.crmicr.2021.100094

Kumari, K., Rani, N., & Hooda, V. (2024). Unravelling the effects of nano SiO2, nano TiO2 and their nanocomposites on Zea mays L. growth and soil health. *Scientific Reports*, *14*(1), 1–15. https://doi.org/10.1038/s41598-024-61456-x

Lobo, C. B., Juárez Tomás, M. S., Viruel, E., Ferrero, M. A., & Lucca, M. E. (2019). Development of low-cost formulations of plant growth-promoting bacteria to be used as inoculants in beneficial agricultural technologies. *Microbiological Research*, *219*(October 2018), 12–25. https://doi.org/10.1016/j.micres.2018.10.012

Luyckx, M., Hausman, J. F., Lutts, S., & Guerriero, G. (2017). Silicon and plants: Current knowledge and technological perspectives. *Frontiers in Plant Science*, *8*(March), 1–8. https://doi.org/10.3389/fpls.2017.00411

Ma, C., White, J. C., Zhao, J., Zhao, Q., & Xing, B. (2018). Uptake of Engineered Nanoparticles by Food Crops: Characterization, Mechanisms, and Implications. *Annual Review of Food Science and Technology*, *9*, 129–153. https://doi.org/10.1146/annurev-food-030117-012657

Maccaferri, M., Harris, N. S., Twardziok, S. O., Pasam, R. K., Gundlach, H., Spannagl, M., Ormanbekova, D., Lux, T., Prade, V. M., Milner, S. G., Himmelbach, A., Mascher, M., Bagnaresi, P., Faccioli, P., Cozzi, P., Lauria, M., Lazzari, B., Stella, A., Manconi, A., … Cattivelli, L. (2019). Durum wheat genome highlights past domestication signatures and future improvement targets. *Nature Genetics*, *51*(5), 885–895. https://doi.org/10.1038/s41588-019-0381-3

Maggiore, A., Afonso, A., Barrucci, F., & Sanctis, G. De. (2020). Climate change as a driver of emerging risks for food and feed safety, plant, animal health and nutritional quality. *EFSA Supporting Publications*, *17*(6). https://doi.org/10.2903/sp.efsa.2020.en-1881

Mahanty, T., Bhattacharjee, S., Goswami, M., Bhattacharyya, P., Das, B., Ghosh, A., & Tribedi, P. (2017). Biofertilizers: a potential approach for sustainable agriculture development. *Environmental Science and Pollution Research*, *24*(4), 3315–3335.

https://doi.org/10.1007/s11356-016-8104-0

Mahmoud, L. M., Shalan, A. M., El-Boray, M. S., Vincent, C. I., El-Kady, M. E., Grosser, J. W., & Dutt, M. (2022). Application of silicon nanoparticles enhances oxidative stress tolerance in salt stressed 'Valencia' sweet orange plants. *Scientia Horticulturae*, *295*(November 2021), 110856. https://doi.org/10.1016/j.scienta.2021.110856

Malusá, E., Sas-Paszt, L., & Ciesielska, J. (2012). Technologies for beneficial microorganisms inocula used as biofertilizers. *The Scientific World Journal*, *2012*. https://doi.org/10.1100/2012/491206

Manfredini, A., Malusà, E., & Canfora, L. (2023). Aptamer-based technology for detecting Bacillus subtilis in soil. *Applied Microbiology and Biotechnology*, *107*(22), 6963–6972. https://doi.org/10.1007/s00253-023-12765-0

Manfredini, A., Malusà, E., Costa, C., Pallottino, F., Mocali, S., Pinzari, F., & Canfora, L. (2021). Current Methods, Common Practices, and Perspectives in Tracking and Monitoring Bioinoculants in Soil. *Frontiers in Microbiology*, *12*(August), 1–22. https://doi.org/10.3389/fmicb.2021.698491

Marmiroli, M., Bonas, U., Imperiale, D., Lencioni, G., Mussi, F., Marmiroli, N., & Maestri, E. (2018). Structural and functional features of chars from different biomasses as potential plant amendments. *Frontiers in Plant Science*, *9*(August), 1–13. https://doi.org/10.3389/fpls.2018.01119

Mavrodi, O. V., Mavrodi, D. V., Thomashow, L. S., & Weller, D. M. (2007). Quantification of 2,4-diacetylphloroglucinol-producing Pseudomonas fluorescens strains in the plant rhizosphere by real-time PCR. *Applied and Environmental Microbiology*, *73*(17), 5531–5538. https://doi.org/10.1128/AEM.00925-07

Mendis, H. C., Thomas, V. P., Schwientek, P., Salamzade, R., Chien, J. T., Waidyarathne, P., Kloepper, J., & De La Fuente, L. (2018). Strain-specific quantification of root colonization by plant growth promoting rhizobacteria Bacillus firmus I-1582 and Bacillus amyloliquefaciens QST713 in non-sterile soil and field conditions. *PLoS ONE*, *13*(2). https://doi.org/10.1371/journal.pone.0193119

Mitchell, M. J., Billingsley, M. M., Haley, R. M., Wechsler, M. E., Peppas, N. A., & Langer, R. (2021). Engineering precision nanoparticles for drug delivery. *Nature Reviews Drug*

*Discovery*, *20*(2), 101–124. https://doi.org/10.1038/s41573-020-0090-8

Mng'ong'o, M. E., Ojija, F., & Aloo, B. N. (2023). The role of Rhizobia toward food production, food and soil security through microbial agro-input utilization in developing countries. *Case Studies in Chemical and Environmental Engineering*, *8*(May), 100404. https://doi.org/10.1016/j.cscee.2023.100404

Mukarram, M., Khan, M. M. A., Kurjak, D., Lux, A., & Corpas, F. J. (2023). Silicon nanoparticles (SiNPs) restore photosynthesis and essential oil content by upgrading enzymatic antioxidant metabolism in lemongrass (Cymbopogon flexuosus) under salt stress. *Frontiers in Plant Science*, *14*(February), 1–18. https://doi.org/10.3389/fpls.2023.1116769

Naidu, S., Pandey, J., Mishra, L. C., Chakraborty, A., Roy, A., Singh, I. K., & Singh, A. (2023). Silicon nanoparticles: Synthesis, uptake and their role in mitigation of biotic stress. *Ecotoxicology and Environmental Safety*, *255*(January), 114783. https://doi.org/10.1016/j.ecoenv.2023.114783

Naseri, S., Beheshti, A., Agha, A., Sharifi, R., & Bahraminejad, S. (2022). Rhizobacteria modify soil biological indices and induce tolerance to osmotic stress in tomato depending on the salinity level and bacteria species. *Brazilian Journal of Microbiology*, 1473–1481. https://doi.org/10.1007/s42770-022-00781-7

O'Callaghan, M., Ballard, R. A., & Wright, D. (2022). Soil microbial inoculants for sustainable agriculture: Limitations and opportunities. *Soil Use and Management*, *38*(3), 1340–1369. https://doi.org/10.1111/sum.12811

Omuto, C. ., Vargas, R. ., El Mobarak, A. ., Mohammed, N., Viarkin, K., & Yigini, Y. (2020). *Mapping of Salt-Affected of Salt-Affected*.

Pérez-de-Luque, A. (2017). Interaction of nanomaterials with plants: What do we need for real applications in agriculture? *Frontiers in Environmental Science*, *5*(APR), 1–7. https://doi.org/10.3389/fenvs.2017.00012

Peterson, P. S., de Medeiros, F. H. V., de Oliveira, T. S., de Almeida Zago, J. R., & Bettiol, W. (2023). Bacillus subtilis and Bacillus licheniformis promote tomato growth. *Brazilian Journal of Microbiology*, *54*(1), 397–406. https://doi.org/10.1007/s42770-022-00874-3

Pokropivny, V. V., & Skorokhod, V. V. (2007). Classification of nanostructures by dimensionality and concept of surface forms engineering in nanomaterial science. *Materials Science and*

*Engineering C*, *27*(5-8 SPEC. ISS.), 990–993. https://doi.org/10.1016/j.msec.2006.09.023

Pontes, M. S., Antunes, D. R., Oliveira, I. P., Forini, M. M. L., Santos, J. S., Arruda, G. J., Caires, A. R. L., Santiago, E. F., & Grillo, R. (2021). Chitosan/tripolyphosphate nanoformulation carrying paraquat: Insights on its enhanced herbicidal activity. *Environmental Science: Nano*, *8*(5), 1336–1351. https://doi.org/10.1039/d0en01128b

Price, L., Han, Y., Angessa, T., & Li, C. (2022). Molecular Pathways of WRKY Genes in Regulating Plant Salinity Tolerance. *International Journal of Molecular Sciences*, *23*(18). https://doi.org/10.3390/ijms231810947

Rahman, M., Rahman, K., Sathi, K. S., Alam, M. M., Nahar, K., Fujita, M., & Hasanuzzaman, M. (2021). Supplemental selenium and boron mitigate salt-induced oxidative damages in glycine max l. *Plants*, *10*(10), 1–16. https://doi.org/10.3390/plants10102224

Raiola, A., Rigano, M. M., Calafiore, R., Frusciante, L., & Barone, A. (2014). *Enhancing the Health-Promoting Effects of Tomato Fruit for Biofortified Food*. *2014*. https://doi.org/10.1155/2014/139873

Ren, H., Guo, H., Shafiqul Islam, M., Zaki, H. E. M., Wang, Z., Wang, H., Qi, X., Guo, J., Sun, L., Wang, Q., Li, B., Li, G., & Radwan, K. S. A. (2023). Improvement effect of biochar on soil microbial community structure and metabolites of decline disease bayberry. *Frontiers in Microbiology*, *14*(May), 1–13. https://doi.org/10.3389/fmicb.2023.1154886

Rilling, J. I., Acuña, J. J., Nannipieri, P., Cassan, F., Maruyama, F., & Jorquera, M. A. (2019). Current opinion and perspectives on the methods for tracking and monitoring plant growth–promoting bacteria. *Soil Biology and Biochemistry*, *130*(January 2018), 205–219. https://doi.org/10.1016/j.soilbio.2018.12.012

Rockström, J., Williams, J., Daily, G., Noble, A., Matthews, N., Gordon, L., Wetterstrand, H., DeClerck, F., Shah, M., Steduto, P., de Fraiture, C., Hatibu, N., Unver, O., Bird, J., Sibanda, L., & Smith, J. (2017). Sustainable intensification of agriculture for human prosperity and global sustainability. *Ambio*, *46*(1), 4–17. https://doi.org/10.1007/s13280-016-0793-6

Rouphael, Y., & Colla, G. (2020). Editorial: Biostimulants in Agriculture. *Frontiers in Plant Science*, *11*(February), 1–7. https://doi.org/10.3389/fpls.2020.00040

Salava, H., Thula, S., Mohan, V., & Kumar, R. (2021). *Application of Genome Editing in Tomato Breeding : Mechanisms , Advances , and Prospects*.

Schon, M. K., & Blevins, D. G. (1987). Boron Stem Infusions Stimulate Soybean Yield by Increasing Pods on Lateral Branches. *Plant Physiology*, *84*(4), 969–971. https://doi.org/10.1104/pp.84.4.969

Sedivy, E. J., Wu, F., & Hanzawa, Y. (2017). *Soybean domestication : the origin , genetic architecture and molecular bases*. 539–553. https://doi.org/10.1111/nph.14418

Sharma, P., Jha, A. B., Dubey, R. S., & Pessarakli, M. (2012). Reactive Oxygen Species, Oxidative Damage, and Antioxidative Defense Mechanism in Plants under Stressful Conditions. *Journal of Botany*, *2012*, 1–26. https://doi.org/10.1155/2012/217037

Sheng, Y., & Zhu, L. (2018). Biochar alters microbial community and carbon sequestration potential across different soil pH. *Science of the Total Environment*, *622–623*, 1391–1399. https://doi.org/10.1016/j.scitotenv.2017.11.337

Shrivastava, P., & Kumar, R. (2015). Soil salinity : A serious environmental issue and plant growth promoting bacteria as one of the tools for its alleviation. *Saudi Journal of Biological Sciences*, *22*(2), 123–131. https://doi.org/10.1016/j.sjbs.2014.12.001

Siddika, A., Rashid, A., Khan, S. N., Prasad, P. V. V., & Hasanuzzaman, M. (2024). *Harnessing plant growth- promoting rhizobacteria , Bacillus subtilis and B . aryabhattai to combat salt stress in rice : a study on the regulation of antioxidant defense , ion homeostasis , and photosynthetic parameters*. *June*, 1–14. https://doi.org/10.3389/fpls.2024.1419764

Steinhorst, L., He, G., Moore, L. K., Schültke, S., Schmitz-Thom, I., Cao, Y., Hashimoto, K., Andrés, Z., Piepenburg, K., Ragel, P., Behera, S., Almutairi, B. O., Batistič, O., Wyganowski, T., Köster, P., Edel, K. H., Zhang, C., Krebs, M., Jiang, C., … Kudla, J. (2022). A Ca2+-sensor switch for tolerance to elevated salt stress in Arabidopsis. *Developmental Cell*, *57*(17), 2081-2094.e7. https://doi.org/10.1016/j.devcel.2022.08.001

Steinhorst, L., & Jörg, K. (2019). How plant perceive salt. *Nature*, 8–10.

Stets, M. I., Campbell Alqueres, S. M., Souza, E. M., Pedrosa, F. de O., Schmid, M., Hartmann, A., & Cruz, L. M. (2015). Quantification of Azospirillum brasilense FP2 bacteria in wheat roots by strain-specific quantitative PCR. *Applied and Environmental Microbiology*, *81*(19), 6700–6709. https://doi.org/10.1128/AEM.01351-15

Straffelini, E., & Tarolli, P. (2023). Climate change-induced aridity is affecting agriculture in Northeast Italy. *Agricultural Systems*, *208*(December 2022), 103647.

https://doi.org/10.1016/j.agsy.2023.103647

Su, Y., Luo, W., Lin, W., Ma, L., & Kabir, M. H. (2015). Model of cation transportation mediated by high-affinity potassium transporters (HKTs) in higher plants. *Biological Procedures Online*, *17*(1), 1–13. https://doi.org/10.1186/s12575-014-0013-3

Sun, F., Zhang, W., Hu, H., Li, B., Wang, Y., Zhao, Y., Li, K., Liu, M., & Li, X. (2008). Salt modulates gravity signaling pathway to regulate growth direction of primary roots in arabidopsis. *Plant Physiology*, *146*(1), 178–188. https://doi.org/10.1104/pp.107.109413

Sunita, K., Mishra, I., Mishra, J., Prakash, J., & Arora, N. K. (2020). Secondary Metabolites From Halotolerant Plant Growth Promoting Rhizobacteria for Ameliorating Salinity Stress in Plants. *Frontiers in Microbiology*, *11*(October), 1–12. https://doi.org/10.3389/fmicb.2020.567768

Tabacchioni, S., Passato, S., Ambrosino, P., Huang, L., Caldara, M., Cantale, C., Hett, J., Del Fiore, A., Fiore, A., Schlüter, A., Sczyrba, A., Maestri, E., Marmiroli, N., Neuhoff, D., Nesme, J., Sørensen, S. J., Aprea, G., Nobili, C., Presenti, O., … Bevivino, A. (2021). Identification of beneficial microbial consortia and bioactive compounds with potential as plant biostimulants for a sustainable agriculture. *Microorganisms*, *9*(2), 1–23. https://doi.org/10.3390/microorganisms9020426

Tang, H., Du, L., Xia, C., & Luo, J. (2024). Bridging gaps and seeding futures: A synthesis of soil salinization and the role of plant-soil interactions under climate change. *IScience*, *27*(9), 110804. https://doi.org/10.1016/j.isci.2024.110804

Tavares, M., Kozak, M., Balola, A., & Sá-Correia, I. (2020). Burkholderia cepacia complex bacteria: A feared contamination risk in water-based pharmaceutical products. *Clinical Microbiology Reviews*, *33*(3), 1–25. https://doi.org/10.1128/CMR.00139-19

Timmusk, S., Paalme, V., Lagercrantz, U., & Nevo, E. (2009). Detection and quantification of Paenibacillus polymyxa in the rhizosphere of wild barley (Hordeum spontaneum) with real-time PCR. *Journal of Applied Microbiology*, *107*(3), 736–745. https://doi.org/10.1111/j.1365-2672.2009.04265.x

Trung, T. T., Hetzer, A., Göhler, A., Topfstedt, E., Wuthiekanun, V., Limmathurotsakul, D., Peacock, S. J., & Steinmetz, I. (2011). Highly sensitive direct detection and quantification of Burkholderia pseudomallei bacteria in environmental soil samples by using real-time PCR. *Applied and Environmental Microbiology*, *77*(18), 6486–6494.

https://doi.org/10.1128/AEM.00735-11

Van Zelm, E., Zhang, Y., & Testerink, C. (2020). Salt Tolerance Mechanisms of Plants. *Annual Review of Plant Biology*, *71*, 403–433. https://doi.org/10.1146/annurev-arplant-050718-100005

Vassura, I., Fabbri, D., Rombolà, A. G., Rizzi, B., Menichetti, A., Cornali, S., Pagano, L., Reggiani, R., Vecchi, M. R., & Marmiroli, N. (2023). Multi-analytical techniques to study changes in carbon and nitrogen forms in a tomato-cultivated soil treated with biochar and biostimulants. *Soil and Environmental Health*, *1*(4), 0–7. https://doi.org/10.1016/j.seh.2023.100050

Vejan, P., Abdullah, R., Khadiran, T., Ismail, S., & Nasrulhaq Boyce, A. (2016). Role of plant growth promoting rhizobacteria in agricultural sustainability-A review. *Molecules*, *21*(5), 1–17. https://doi.org/10.3390/molecules21050573

Verma, K. K., Zeng, Y., Song, X. P., Singh, M., Wu, K. C., Rajput, V. D., & Li, Y. R. (2022). Nanosilicon: An approach for abiotic stress mitigation and sustainable agriculture. *Frontiers in Plant Science*, *13*(December), 1–9. https://doi.org/10.3389/fpls.2022.1025974

Vishwakarma, K., Kumar, N., Shandilya, C., Mohapatra, S., Bhayana, S., & Varma, A. (2020). Revisiting Plant–Microbe Interactions and Microbial Consortia Application for Enhancing Sustainable Agriculture: A Review. *Frontiers in Microbiology*, *11*(December), 1–21. https://doi.org/10.3389/fmicb.2020.560406

Wang, M., Lan, X., Xu, X., Fang, Y., Singh, B. P., Sardans, J., Romero, E., Peñuelas, J., & Wang, W. (2020). Steel slag and biochar amendments decreased CO2 emissions by altering soil chemical properties and bacterial community structure over two-year in a subtropical paddy field. *Science of the Total Environment*, *740*, 140403. https://doi.org/10.1016/j.scitotenv.2020.140403

Wang, Q., Liu, M., Wang, Z., Li, J., Liu, K., & Huang, D. (2023). The role of arbuscular mycorrhizal symbiosis in plant abiotic stress. *Frontiers in Microbiology*, *14*(January), 1–14. https://doi.org/10.3389/fmicb.2023.1323881

Watts-Williams, S. J., Gill, A. R., Jewell, N., Brien, C. J., Berger, B., Tran, B. T. T., Mace, E., Cruickshank, A. W., Jordan, D. R., Garnett, T., & Cavagnaro, T. R. (2022). Enhancement of sorghum grain yield and nutrition: A role for arbuscular mycorrhizal fungi regardless of soil phosphorus availability. *Plants People Planet*, *4*(2), 143–156. https://doi.org/10.1002/ppp3.10224

Wieser, H., Koehler, P., & Scherf, K. A. (2020). The Two Faces of Wheat. *Frontiers in Nutrition*, *7*(October). https://doi.org/10.3389/fnut.2020.517313

Wickham H. (2016). ggplot2: Elegant Graphics for Data Analysis. Springer-Verlag New York.

Wu, Q., Zhou, W., Chen, D., Tian, J., & Ao, J. (2024). Biochar Mitigates the Negative Effects of Microplastics on Sugarcane Growth by Altering Soil Nutrients and Microbial Community Structure and Function. *Plants*, *13*(1). https://doi.org/10.3390/plants13010083

Xiang, S. R., Cook, M., Saucier, S., Gillespie, P., Socha, R., Scroggins, R., & Beaudette, L. A. (2010). Development of amplified fragment length polymorphism-derived functional strain-specific markers to assess the persistence of 10 bacterial strains in soil microcosms. *Applied and Environmental Microbiology*, *76*(21), 7126–7135. https://doi.org/10.1128/AEM.00574-10

Xu, T., Niu, J., & Jiang, Z. (2022). Sensing Mechanisms: Calcium Signaling Mediated Abiotic Stress in Plants. *Frontiers in Plant Science*, *13*(June). https://doi.org/10.3389/fpls.2022.925863

Yang, Y., & Guo, Y. (2018). Elucidating the molecular mechanisms mediating plant salt-stress responses. *New Phytologist*, *217*(2), 523–539. https://doi.org/10.1111/nph.14920

Zhang, S., Ma, Y., Jiang, W., Meng, L., Cao, X., Hu, J., Chen, J., & Li, J. (2020). Development of a Strain-Specific Quantification Method for Monitoring Bacillus amyloliquefaciens TF28 in the Rhizospheric Soil of Soybean. *Molecular Biotechnology*, *62*(10), 521–533. https://doi.org/10.1007/s12033-020-00268-6

Zheng, H., Wang, X., Luo, X., Wang, Z., & Xing, B. (2018). Biochar-induced negative carbon mineralization priming effects in a coastal wetland soil: Roles of soil aggregation and microbial modulation. *Science of the Total Environment*, *610–611*, 951–960. https://doi.org/10.1016/j.scitotenv.2017.08.166

Zhou, H., Shi, H., Yang, Y., Feng, X., Chen, X., Xiao, F., Lin, H., & Guo, Y. (2024). Insights into plant salt stress signaling and tolerance. *Journal of Genetics and Genomics*, *51*(1), 16–34. https://doi.org/10.1016/j.jgg.2023.08.007

Zhou, J., Wang, Y., Zuverza-Mena, N., Dimkpa, C. O., & White, J. C. (2024). Copper-Based Materials as an Effective Strategy for Improving Drought Resistance in Soybean (Glycine max) at the Reproductive Stage. *ACS Agricultural Science and Technology*, *4*(7), 735–746. https://doi.org/10.1021/acsagscitech.4c00193

UNIONE EUROPEA
Fondo Sociale Europeo
Ministero dell'Università e della Ricerca
PON RICERCA E INNOVAZIONE
REACT EU
UNIVERSITÀ DI PARMA

La borsa di dottorato è stata cofinanziata con risorse del
Programma Operativo Nazionale Ricerca e Innovazione 2014-2020, risorse FSE REACT-EU
Azione IV.4 "Dottorati e contratti di ricerca su tematiche dell'innovazione"
e Azione IV.5 "Dottorati su tematiche Green"